Harnessing the potential of the medicinal fungus *Innonotus obliquus* to induce tumoricidal macrophages

Deborah Elikplim Dzovor

Thesis submitted for the degree of Master of Science in
Biochemistry & Molecular Biology
60 credits

Department of Biosciences
Faculty of Mathematics & Natural Sciences
UNIVERSITY OF OSLO
February 2021

ACKNOWLEDGEMENTS

This research was conducted with the Tumor Immunology group at the Department of Pathology, Oslo University Hospital (Rikshospitalet), in the period between January 2019 and January 2021. Alexandre Corthay and Inger Øynebråten supervised the project, with Gareth Wyn Griffith as my internal supervisor.

My first and foremost gratitude is to God Almighty, for the strength and wisdom He granted me to successfully complete this degree.

I would like to express my greatest appreciation to my main supervisor, Alexandre Corthay, for the unique opportunity to work on this project. His expertise and meticulous attention to detail propelled me to improve my writing skill, which brought my work up to standard. I would like to specifically single out Inger Øynebråten, for her extreme patience and great sacrifice in critically reading my thesis. Without her generous assistance and valuable feedback, this thesis would not have materialized.

I wish to express my profound gratitude to all members of the Tumor Immunology group, especially to Asha and Angie. I would not have survived the challenging times without you girls, thank you for sharing in my frustration and fun moments in the lab. I cannot forget to thank Brian, for keeping me company and providing technical support through all the failed experiments and numerous Buffy coat isolations, which we lost count of – not to mention the petty disagreements we always had. Words will not be enough to convey my sincere appreciation to Christian Wold at the School of Pharmacy, many thanks indeed for accepting to collaborate with me. You were an inspiration, and it was truly exciting teaming up with you.

An enormous appreciation goes to my family in Ghana for their emotional, financial, and moral support. My parents and siblings, especially my lovely brother Enoch and pal, Edem, what will I do without you guys? I love you! Special thanks to my mentor, Mr. Frank Nartey, you have been such an amazing person, I genuinely appreciate every support you gave me. Finally, my heartfelt thanks to my significant other, Martin, lots of love, thank you for being there for me.

Table of Contents

ABSTRACT

Macrophages are essential innate immune cells which have increasingly become attractive manipulable targets in designing therapies, given their significant involvement in the pathophysiology of several diseases, including cancers. In the microenvironment of solid tumors, tumor associated macrophages (TAMs), either promote or suppress tumor growth depending on activating cues from the tumor milieu. Both *in vitro* and *in vivo* studies have recently identified fungal polysaccharides as potent macrophage activators capable of stimulating TAMs into tumoricidal phenotypes.

In this study, an optimized protocol for generating human macrophages from peripheral blood monocytes *in vitro* using Granulocyte macrophage colony stimulating factor (G-MCSF) or macrophage colony stimulating factor (M-CSF) was established.

Fungal polysaccharides isolated from the medicinal fungus, *Inonotus obliquus,* stimulated human macrophages *in vitro* to secrete the pro-inflammatory cytokines, tumor necrosis factor (TNF)-α, interleukin (IL)-6 and IL-12p70, essential for a complete anti-tumor immune response. Next, we showed that murine bone marrow-derived macrophages activated with the fungal polysaccharides induced an anti-tumor response against cancer in mouse models. This study shows that the novel fungal polysaccharides from *I. obliquus* play a significant role in activating an anti-tumor phenotype in macrophages and could be exploited as a potentially effective candidate for cancer immunotherapy.

ABBREVIATIONS

AcF1	Acidic fraction 1
APC	Antigen presenting cell
BMDM	Bone marrow derived macrophage
CD	Cluster of differentiation
CTL	Cytotoxic T lymphocyte
DAMP	Danger associated molecular pattern
GM-CSF	Granulocyte macrophage colony-stimulating factor
HLA	Human leukocyte antigen
IFN-γ	Interferon gamma
IL	Interleukin
MHC II	Major histocompatibility complex II
MoDM	Monocyte-derived macrophage
M-CSF	Macrophage colony stimulating factor
MDSC	Myeloid-derived suppressor cell
NF-κB	Nuclear factor κ light chain enhancer of activated B cells
NK cell	Natural killer cell
PAMP	Pathogen associated molecular pattern
PRR	Pattern recognition receptor
TAM	Tumor associated macrophage
TGF-β	Transforming growth factor β
TIL	Tumor-infiltrating lymphocyte
TLR	Toll-like receptor
TME	Tumor microenvironment
TNF-α	Tumor necrosis factor- alpha

1 INTRODUCTION

1.1 THE IMMUNE SYSYTEM

The immune system of mammals consists of a delicately complex and pervasive network of cells, tissues and organs that function generally to prevent or limit infection. Its role is underscored in immuno-compromised individuals with congenital immune disorders, HIV & AIDS, and even pregnant women, as they are extremely vulnerable to host of infections that typically healthy individuals are protected from (1–3). The immune system is highly organized to effectively detect and eliminate foreign invaders such as viruses, fungi, bacteria and even host cells that have become infected or cancerous. There are various immune cell types that play unique roles and are found either circulating throughout the body or resident in specific tissues (1).

The body mounts two distinct immune defenses upon invasion by an infectious or threatening agent, as will be discussed in the next section. The first and immediate response is known as innate immunity and the latter, more specific and delayed reaction, called adaptive immunity. It is extremely important to study and understand the physiological mechanisms behind this labyrinth network of cells as this enables scientists to optimize immune responses to deal with abnormalities ranging from minor infections to complex diseases such as cancer (3).

1.1.1 The Innate Immune System

The innate immune system is the immediate, antigen-nonspecific, and pre-existing first line of defense elicited against all sorts of foreign invasions and internal ‘danger’ signals. It encompasses a set of genetically organized and diverse components such as the physical and anatomic barriers of the skin and mucosa and various effector cells including natural killer (NK) cells, macrophages, dendritic cells (DCs), monocytes, granulocytes and the recently discovered innate lymphoid cells (ILCs). Innate immune cells recognize and eliminate a pathogen either by direct phagocytosis or other humoral mechanisms like secretion of cytokines or complement proteins (1,2,4).

Several families of pattern recognition receptors (PRRs) including toll-like receptors (TLRs), expressed by innate immune cells, facilitate the recognition and direct engagement of pathogen associated molecular patterns (PAMPs) (5). PAMPs are conserved features found in almost all

pathogens but missing in host cells; allowing immune cells to distinguish 'self' from 'non-self'(6). These receptors (PRRs) bind a host of microbial ligands: polysaccharides, proteins, glycolipids, peptidoglycans and nucleic acids from viruses, bacteria, and fungi (6,7). Neutrophils are short-lived phagocytes of the innate immunity, and normally the first to arrive at the site of a bacterial infection. They engulf and degrade pathogens by releasing microbicidal molecules and proteases (8). ILCs are a growing family of recently discovered immune cells that straddle both innate and adaptive immune systems. Like innate immune cells, they respond promptly to infections and tissue damage and lack antigen-specific receptors; however, they exhibit striking phenotypic and effector functions likened to polarized CD4+ T cell subsets (4),(9). Mast cells are essential in defending the host during parasitic worm infestations and allergic reactions (6,10) while professional antigen presenting cells like DCs reside in and patrol the skin and mucosal surfaces for invading microbes with subsequent activation of T lymphocytes (11). Details on some specific roles of innate immune cells like macrophages, in host defense against infections and cancers are later discussed in this thesis.

The general function however of the innate immunity is to prevent or suppress infections and diseases at an early stage. Consequently, a dysfunctional innate immune system, although rare, always has lethal consequences (1,12). Despite the prompt and effective mechanisms to defend its host, the innate immunity may sometimes be overwhelmed, leading to the launch of a stronger and more specific type of response, the adaptive immune response (2).

1.1.2 The Adaptive Immune System

It is referred to as the adaptive or 'acquired' immune response mainly because it is formed during an ongoing infection and adapts to the distinctive features of the infectious agent (2,10,13). Thus, the response is delayed, highly specific, and improves as the infection gets underway. B and T lymphocytes make up cells of adaptive immunity with incredibly unique receptors that bind to specific antigens. The B cell receptors (BCRs) and T cell receptors (TCRs) are extremely diverse and recognize highly specific antigens of an exact molecular type. Diversity is achieved through random somatic recombination of the various gene segments leading to the generation of billions of genetically distinct and highly specific receptor variants (13–15).

An activated B or T cell undergoes selective clonal expansion and fosters an effectively targeted immune response against a unique pathogen alongside the development of long-lived memory cells. The immunological memory provided by adaptive immunity promotes a more rapid and robust

response during future encounters with the same antigen (2,13). Effector mechanisms in both immune systems, leading to acute and chronic tissue inflammation, have been implicated in diseases like cancer (16,17). The B cell receptor exists as a membrane-bound or secreted immunoglobulin (Ig) that mediate a humoral immune response. Activated B cells undergo proliferation and differentiation into antibody-producing effector cells called – plasma cells. Effector functions of antibodies include opsonization, antigen neutralization, complement activation, and antibody-dependent cellular cytotoxicity (16).

T cells originate from bone marrow progenitors and undergo development in the thymus. They express highly variable membrane-bound receptors which recognize specific antigens. CD4+ (T helper cells) and CD8+ (cytotoxic T cells) are the major types of T cells. They efficiently coordinate various facets of adaptive immunity involving responses to microbes, allergens, and cancers (14). TCRs recognize and bind to antigens presented as peptides by antigen presenting cells (APCs). The molecules on which peptides are presented are a group of protein complexes called major histocompatibility complex (MHC), which are encoded for by genes in the MHC locus in all jawed vertebrates.(18) In humans, the MHC genes are located on chromosome 6 and encode the molecules referred to as human leucocyte antigen (HLA) complexes (19). There are two types of MHC molecules – MHC I and MHC II, on which antigens presented are recognized by CD8+ and CD4+ subsets, respectively. As indicated by the name, T helper cells 'help' B cells to produce antibodies, and also help activate NK cells, macrophages and DCs by secreting cytokines, whereas cytotoxic T cells directly 'kill' target cells that are infected or cancerous (15,16). An immune response is initiated when a naïve T cell first engages its cognate peptide-MHC complex followed by secondary signal generated by the binding of co-stimulatory ligands – CD80/ CD86 on APCs to CD28 on T cells, a third signal in the form of cytokines from APCs determine which subset of effector T cells are produced. For example, CD4+ T cells exposed to IL-12p70 differentiate into Th1 cells while IL-4 and TGF-β/IL-6 induces Th2 and Th17 cells, respectively (14,20). Effector T cells following activation and differentiation migrate to the site of infection or inflammation where they amplify the immune response to eliminate the infectious agent.

Only some effector cells (10-15%) persist after the immune response wanes and become long-lived memory T cells which enhance an immediate and efficient response upon subsequent re-exposure to the same pathogen. Current advances in cancer immunotherapy seek to generate a memory response, as this will potentially inhibit tumor recurrence or limit metastasis after removal of the primary tumor (16).

1.2 TUMOR IMMUNOLOGY

Cells within the human body are subject to a constant cycle of proliferation, destruction, and repair. New cells are continuously produced to replace the many dead and destroyed ones through a complex and tightly regulated mechanism. However, an enormous number of errors (mutations) could arise, either randomly or through exogenous factors, during normal processes such as cell proliferation. Over time, these neoplastic cells acquire several traits such as resisting programmed cell death, avoiding immune destruction, sustaining proliferative signaling independent of other cells, inducing angiogenesis among others; proposed as the hallmarks of cancer by Hanahan & Weinberg (2000), shown in **Figure 1** (21,22)**.** The body relies on sophisticated mechanisms including the immune system, as part of its normal functions, to detect and eliminate these abnormal cells. However, some of them escape destruction and become cancerous after selective mutations accumulate. There is accruing evidence that the immune system certainly provides defenses against tumors(23,24). The relationship between the immune system and cancer, and by extension, the field of tumor immunology is intricate – this has over the past decades, remained a subject of great flux with fundamental concepts highly debated. Nonetheless, it is imperative to understand the complex relationship that exists between tumor cells and the immune system since it holds a potential promise for new insights into tumorigenesis and novel ways of treating human cancers (25).

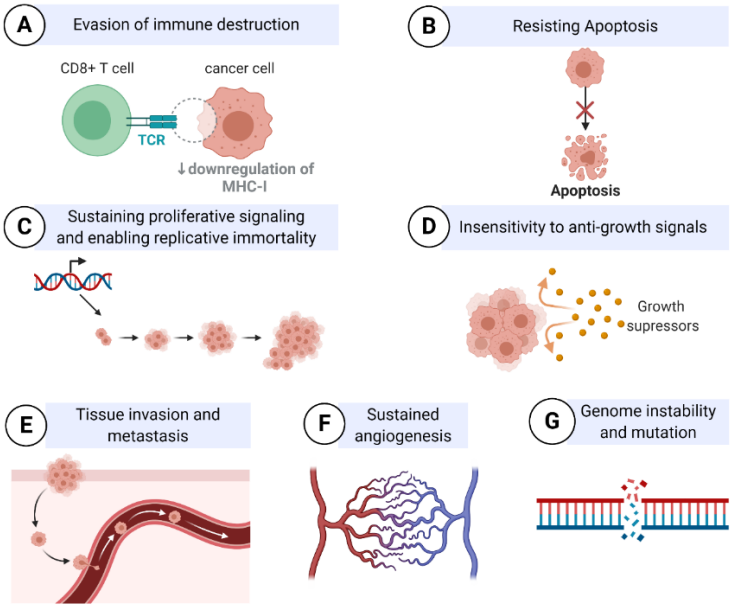

Figure 1. Hallmarks and acquired characteristics of cancer.

Hallmarks of cancer can be defined as functional capabilities that cancer cells acquire to be able to survive, proliferate, and disseminate. These functions are developed in different tumor types through unique mechanisms and at various times during multistep tumorigenesis. Recent significant breakthroughs in cancer therapy are designed to target one or more of these enabling characteristics and hallmarks. Modified from (21)

1.2.1 Cancer Immunosurveillance and Immunoediting

The subject of tumor immunology was predicted centuries ago by William Coley in 1893, when he used live bacteria to stimulate immune cells to treat cancer (26); he then suggested the concept of the immune system capable of recognizing and controlling tumor growth (27). Few years later, in 1909, Paul Ehrlich, hypothesized that the immune system suppressed neoplastic cells from growing into carcinomas that would have potentially occurred at a much higher rate (28–30). Although his hypothesis spurred the field of cancer immunotherapy, better understanding of the relationship between immune cells and cancer was necessary. Several decades following Ehrlich's unproven hypothesis, Sir Frank Mac Farlane Burnet and Lewis Thomas suggested that the immune system recognized neo-antigens from transformed (cancer) cells and induced an immunological reaction to destroy them (24,31). This was demonstrated in immunodeficient mice as they were highly susceptible to both induced and spontaneous tumors, in contrast to their immunocompetent counterparts (29,32). They concluded that the immune system certainly protects its host from cancers, and subsequently established the "**Immune Surveillance Theory**". This theory many years on, was proven by some and challenged by others (29,33).

Janeway further expounded the concept of tumor immunology when he developed the theory of "extended self vs. nonself", which postulated that the immune system is able to discriminate infectious nonself from non-infectious self, using a variety of germ-line encoded receptors that recognize molecular patterns present in microbes but missing in the host (5,34). Despite originating from normal cells, cancer cells undergo cellular transformations such as lack of self MHC I molecules, however, this allows recognition and killing by NK cells (missing self hypothesis) (28,35). Some innate immune cells – specifically macrophages and NK cells, have an intrinsic ability to quickly identify foreign invaders, 'stressed' or infected cells and mark them for destruction. Also, cytotoxic CD8+ T cells of the adaptive immune system have been extensively studied and shown to be directly involved in the killing of neoplastic cells (1,28,36).

Schreiber *et al.* (2002) developed a novel approach to describe the dual role of the immune system in not only protecting against but also shaping the formation of neoplastic disease (33). Unlike the immune surveillance theory, which proposed only one function of the immune system in protecting the host and acting only at the initial stages of cellular transformation, (29) the model by Schreiber et. al accurately described the broader roles and involvement of both innate and adaptive immunity in cancers (33). They proposed the theory of **"Cancer Immunoediting"** which elucidated an overly broad function of the immune system in 3 phases, also known as the **three Es of cancer**

immunoediting. The first phase is total **Elimination** of some tumors, by NK cells, CD4+ and CD8+T cells, which is akin to immunosurveillance (24,33). Phase two is the **Equilibrium** state where the immune system is non-protective, modifies environmental conditions that favor the growth of some resistant tumor variants. In the third phase, **Escape**, the immune system becomes tolerant or indifferent and fails to destroy the selected variants, tumor cells then grow uncontrollably in an immunocompetent host (33,37). The theories of immune surveillance and cancer immunoediting proposed decades ago remains relevant today since it has enhanced efforts to fully understand the extremely complicated mechanisms by which the immune system suppresses and/or promotes tumor growth. This insight will ultimately advance the approach and search for cancer therapies through immunological processes.

1.2.2 Tumor Microenvironment and Tumor-infiltrating Immune Cells

The tumor microenvironment (TME) is a site of complex interaction within and around the tumor mass where various cell populations and cellular products from the host; both healthy and cancerous are found (38). Among these cell types are fibroblasts, endothelial cells, cancer stem cells, immune cells – both resident and infiltrating, as well as secreted growth factors, extracellular matrix proteins, cytokines, and chemokines. Important immune cells associated with the TME secreting various forms of cytokines and chemokines include tumor associated macrophages (TAMs), myeloid derived suppressor cells (MDSCs), DCs, NK cells, granulocytes (basophils, eosinophils, neutrophils), B and T lymphocytes (39). Collectively, this complex milieu of cells and cellular products formed and influenced mainly by the cancer cells, determine the fate of the primary tumor from invasion to metastasis (37,40,41). The TME was recently identified to be the resultant effect of crosstalk between various cell types, exemplified in the interaction between cancer cells and stromal cells, where the latter support tumor progression by secreting growth factors and essential chemokines needed for survival and proliferation of tumor cells (38,40–42).

Notably, neoplastic cells can modify the immune system to enhance their establishment and, in some instances, chronic inflammation caused by cells of the immune system, could precede certain cancers. For example, inflammatory bowel diseases and chronic hepatitis, are inflammatory conditions that predisposes its hosts to colorectal cancers and hepatocellular carcinomas respectively (42,43). Due to its importance in shaping the overall outcome of tumor progression or suppression, tumor-infiltrating lymphocytes have become the target in recent cancer therapies, such as immune checkpoint inhibitors (ICI) – which has so far been hailed as the gold standard treatment for many cancers (44,45). Nevertheless, treatment with ICIs have been faced with major setbacks such as poor tumor

immunogenicity, infiltration of TME by immunosuppressive cells such as MDSCs, regulatory T cells (Tregs), along with inhibitory cytokines (46).

1.2.3 Role of Tumor-infiltrating Immune Cells

Generally, solid tumors are infiltrated by several immune and inflammatory cells via cytokines and chemokines secreted by tumor cells and by TAMs, however, their exact roles remain a subject of great debate (37,38). Earliest theories presumed that these immune cells were part of the body's response to reject newly transformed cells. Undeniably, this argument still holds that at the initial stages of tumor inception, the immune system responds to the presence of cancer by activating macrophages and T cells, which clear the tumor and prevents the occurrence of cancer (33). However, once tumors progress past this elimination stage, immune cells in the TME undergo modification to support and promote tumor progression while suppressing any immune cell-mediated cytotoxicity (47). Moreover, the type, location, and density of these infiltrating immune cells have been established as a valuable prognostic tool in cancer therapy, and numerous studies have supported claims that the presence of pro-inflammatory immune cells in the TME are linked with better prognosis (42,48). Tumor-infiltrating immune cells that derive from lymphoid precursors constitute B cells, plasmacytoid dendritic cells (pDCs) and the two main T cell lineages: CD4+ and CD8+ T cells. Whereas tumor associated macrophages (TAMs), conventional dendritic cells (cDCs), neutrophils, platelets and mast cells are among immune cells from myeloid precursors(38,43).

T cells are among tumor-infiltrating lymphocytes (TILs), and accumulation of T cell infiltrates such as Th1, Th17, cytotoxic CD8+ T cells along with pro-inflammatory cytokines within a tumor characterizes the tumor as 'hot'(49–51). '**Hot tumors'** usually undergo mutations and may present neoantigens which are easily recognized by T cells, leading to a subsequent attack on the cancer cells. As a result, hot tumors are believed to better respond to treatments with immune checkpoint blockades than non-immunogenic tumors (50). In sharp contrast, '**cold tumors**' refer to tumors lacking T cells infiltrates, also known as 'non-inflamed' tumors. They largely indicate non-responsive adaptive immunity and are usually resistant to immunotherapy drugs(49). T cells thus play essential roles in fighting cancers, either through direct killing by cytotoxic activities or indirectly orchestrating and organizing other immune cells to fight the cancer (51,52). This was illustrated in studies with mouse model for myeloma by Corthay et al, proposing that tumor-specific $CD4^+$ T cells played a fundamental role in inhibiting early tumorigenesis by secreting IFN-γ, which subsequently activated TAMs into a tumoricidal phenotype to prevent tumor development (53).

Natural killer (NK) cells of the innate immunity share some similar characteristics with cytotoxic T lymphocytes and are also involved in protecting host from viral infections, alongside playing pivotal roles in host defense against cancers (37). NK cells as well as CD8+ T cells express a repertoire of activating receptors such as NKG2D, which recognize NKG2D ligands/receptors (stress signal) on the cell surface of transformed and infected cells. Binding to this ligand activates the NKG2D pathway, which serves as a mechanism for the immune system to detect and directly kill cancer cells through cell-mediated cytotoxicity (54).

1.2.4 Cancer Immunotherapy

Cancer immunotherapy involves unique strategies to manipulate components of the immune system to combat tumors (55). The well-established conventional treatments for cancer: chemotherapy and radiation therapies and are associated with numerous detrimental effects, while surgeries are usually not applicable in metastatic cancers. This has pushed forward the need for relatively safer biological therapies (56,57). However, treatments combining conventional and immune therapies have by far, proven to be the most efficacious for several malignancies (58). Current treatment modalities harnessing the anti-tumor effects of the immune system include: cytokines, adoptive cellular therapy, therapeutic vaccines and the recently developed gold standard immune checkpoint blockade, which is based on monoclonal antibodies (mAbs) (59). Immunotherapies have increasingly become integrated in the standard of treatment for solid and hematological malignancies in preclinical models, clinical trials, and practice (55).

Monoclonal antibodies may work by blocking inhibiting receptors on immune cells or opsonizing cancer cells to enhance cellular mediated or antibody dependent cellular cytotoxicity (ADCC) (60). Example is Herceptin (trastuzumab), a recombinant humanized mAb, targeted at the extracellular domain of the Her-2 protein – which is expressed in nearly a quarter of metastatic breast cancers and associated with poor prognosis (55,61). Herceptin is shown to inhibit cellular signaling pathways, arrest cell proliferation and induce ADCC (61). Cytokine therapy on the other hand work to advance or attenuate immune responses. Recombinant IFN-α and IL-2 (Proleukin) are examples of cytokines that have received FDA approvals for use as adjuvants in the treatment of metastatic melanoma and renal carcinomas – although associated with high-dose toxicities (62,63). Evaluation in a phase II clinical trial revealed that metastatic melanoma patients treated with high-dose ipilimumab, combined with sargramostim (GM-CSF), had lower toxicities and improved survival compared to those treated

with high-dose ipilimumab alone (45,62). A number of other cytokines including IFN-γ, IL-7, IL-12p70, and IL-21 have shown efficacies in several murine carcinomas and are currently being investigated in clinical trials for human use (59,62).

T cells have been used in cancer therapies through direct cytotoxic activities (CD8+ T cells) or indirectly by activating helper CD4+ T cells, which orchestrate the recruitment of other immune cells. Adoptive cellular therapy against cancer is an approach that utilizes tumor-infiltrating lymphocytes from surgically resected tumors of patients. Specifically, tumor specific T cells are grown *ex vivo* then transferred adoptively together with high dose IL-2 into the patient (60). Chimeric antigen receptor (CAR) T cell therapy is another breakthrough in cancer immunotherapy in which T cells are genetically engineered with synthetic receptors to improve their specificity and avidity for cancer cells in a non-MHC restricted fashion (62,64).

Cytotoxic T lymphocyte antigen-4 (CTLA-4), a costimulatory molecule expressed on T cells acts as an immune checkpoint under normal physiologic conditions, by regulating inflammatory responses subsequent to T cell activation (46). It outcompetes CD28 for binding to B7 on APCs, thus preventing the costimulatory (second) signal required for the priming and activation of T cells (55) . Allison et al., developed CTLA-4–blocking antibodies which inhibit the regulatory signal produced from B7-CTLA-4 interactions, consequently increasing the activation threshold of T cells. In their study, they revealed that treatment with anti CTLA-4 antibody alone was effective against only immunogenic mouse tumors but combining them with tumor lysate-loaded dendritic cells and Treg-depleting antibodies, induced a significant anti-tumor response in highly metastatic and non-immunogenic tumors (65–68). Ipilimumab, an anti-CTLA-4 antibody (mAb) and immune checkpoint inhibitor, was FDA-approved in 2010 for the treatment of advanced melanoma, and has been reported to remarkably improve survival rates in patients for which conventional treatments had failed. (58,69,70).

Programmed death-ligand 1(PD-L1) expressed on cancer cells binds to its immunoinhibitory receptor, programmed cell-death protein 1 (PD-1), on T cells. The PD-1/PD-L1 is another immune checkpoint interaction that suppresses the effector phase of T cell activation during infections, mainly by dampening immune responses that could otherwise lead to autoimmune diseases (60,71). Many cancer cells however engage these inhibitory receptors as a mechanism of immune evasion and avoiding T cell killing – antibodies blocking these interactions, unleash the T cells for destruction of malignant cells (71). Pembrolizumab, an immune checkpoint inhibitor based on mAbs, which target programmed cell death-1 (anti–PD-1) has been reported to be relatively efficacious in several cancers including

advanced non–small cell lung cancer (NSCLC), with up to 21% response rates (72) and significantly lower toxicities compared to other immunotherapies(71,72).

Indeed, immunotherapy is a scientific breakthrough that has revolutionized cancer treatment and expanded our understanding of how the immune system responds to many malignant cells. Overall, the clinical goal of this rapidly evolving, front-line treatment is to harness the immune system to induce an active or passive immunity against malignancies (60). However, some shortfalls have been identified; while some therapies are precisely targeted at tumor antigens, others are broadly activating, causing side effects ranging from mild and localized to serious systemic, and often lethal consequences (59). Also, mitigating factors such as high-dose toxicities, poor immunogenicity of tumors, complexity of the immune system, coupled with the heterogeneity of individual cancers leaves a broad swathe of patients disadvantaged, hence the call for improved strategies (44,45,59,73).

1.3 MACROPHAGES

1.3.1 History, Ontogeny and Function

Macrophages, a cornerstone of the innate immunity, are phagocytic white blood cells, resident in many tissues and organs and represent a significant population of innate immune cells. Initially identified over a century ago by Ilya Metchnikoff, macrophages are believed to be important phagocytic cells in ancient Metazoan phylogeny which cleared fungal infections from crustacea and bacterial infections from rabbits (74,75). Metchnikoff cut the larvae of starfish and observed a population of cells that quickly migrated to the injury site and observed these cells also rapidly ingesting substances foreign to the digestive tract of the starfish. He called them phagocytes- ‘eating cells’ and later white blood cells- for their primary defensive role in its host. This astounding discovery on immunity won him the Nobel prize in physiology or medicine in 1908 (76–78). In 1924, Aschoff introduced the concept of reticulo-endothelial system (RES) to denote all specialized cells, which actively cleared vital stains from circulation (79). While RES has been exclusively linked with macrophages, recent findings have shown that scavenger endothelial cells efficiently functioned like macrophages by also clearing vital stains but were immunologically distinct cells. Many years later, his model was replaced with mononuclear phagocytic system (MPS), to precisely distinguish macrophages, monocytes, and their precursor cells from other cells of the RES (78,80,81). In adult mammals, macrophages are considered the most ubiquitous cells which display great anatomical and functional diversity (77,82,83). They are

retained throughout life by local proliferation and steady-state recruitment from the bone marrow, and generally function in host defense against infection by coordinating an immediate immune response through phagocytosis, antigen presentation and cytokine production. However, their role is not limited to the immune system; as they are also pivotal in other aspects of embryonic development, homeostasis, and wound repair (76,82).

1.3.1.1 *In vivo* vs. *in vitro* maturation of macrophages

Recent studies and techniques in cellular ontogenesis have invalidated the long-held belief that monocytes from the bone marrow were the exclusive source of tissue macrophages in adults (84). Macrophages have been established to have come from two sources – embryo derived macrophage precursors and the other group that originated from hematopoietic stem cells in the bone marrow (85). It has also been proven that many tissue-resident macrophage populations are derived during the embryonic stage of fetal development and self-maintain independently of bone marrow contribution during adulthood (84). Examples are the microglia of the brain and Kupffer cells which derive from the yolk sac and fetal liver, respectively. On the other hand, macrophages in organs like the heart, skin and gastrointestinal tract are known to be constantly replenished by bone marrow derived monocytes (86).

Several *in vivo studies* in mouse models have also established the standard paradigm that monocytes in circulation, extravasate into mucosal or inflamed tissues where they differentiate into either macrophages or DCs depending on signals from the microenvironment (87). However, observations in mouse models do not always translate to humans due to some genetic and physiological disparities (87). To fully understand the role of monocytic-derived cells in human diseases and steady-state conditions, human studies are therefore necessary to complement such findings. Human macrophages for example, express typical blood monocyte markers, such as CD14, CD11b, CD16 and HLA-DR; a clear indication reminiscent of its monocytic precursors (88). In humans, circulating monocytes are classified into three main populations based on the expression of the surface markers CD14 and CD16; identified as LY6C and CD43 respectively in mice (88). These monocyte populations are: **classical** ($CD14^{++}CD16^{-}$), which represent about 85% of monocytes, with **non-classical** ($CD14^{+}CD16^{++}$) and **intermediate** ($CD14^{++}CD16^{+}$), each constituting 5-10% of the total monocytic population (87). Besides the differential expression of surface markers, each of these subsets are further distinguished by their distinct gene expression profiles and unique functions in homeostasis and disease, some of which persist after maturation into DCs and macrophages (89). The concept that human bone marrow-derived monocytes later mature into macrophages has been reinforced by *in vitro* experiments; given

that monocytes derived from either blood or bone marrow, can be readily differentiated into macrophages when cultured in serum and/or with defined growth factors (85). Many recent *in vivo* studies have shown that migrating monocytes can develop in many ways: (a) they may remain in the tissues as monocytes and subsequently undergo local apoptosis, or (b) upregulate antigen presenting ability and chemokine receptor, CCR7 then move into draining lymph nodes or also (c) differentiate into macrophages in the presence of cytokines such as interleukin-3 (IL-3) and granulocyte macrophage colony stimulating factor (GM-CSF) (77,85,90). Additionally, there have been findings that mature differentiated macrophages resident in affected tissues can themselves proliferate to boost cell numbers (91). *In vivo* maturation of blood monocytes into macrophages reportedly occurs in a non-coordinated manner compared to *in vitro* settings, given the effects of differences in growth factors, metabolic requirements, oxygen concentrations and tissue matrix as well as influences from other immune cells (85). Evidently, during inflammation (*in vivo*), newly emigrating monocytes are exposed to pro-inflammatory, anti-inflammatory stimuli and other localized factors, which will subsequently shape the outcome of differentiated cells, a condition which may be tightly regulated *in vitro*. Furthermore, monocyte-to-macrophage transition takes a number of days *in vitro*, it is speculated to occur at faster rate *in vivo* even though the precise period is still unknown (85). However, conventional *in vivo* monocytic/macrophage phenotypes and functions have been reported in *in vitro* differentiated macrophages as well (87,88,92).

1.3.2 Role of Macrophages in Immunity

Macrophages are found in strategic positions throughout tissues of the body and their main function is to constantly survey the body and engulf foreign invaders. Their expansive role goes beyond the widely acknowledged function in innate immunity. They provide protective and pathogenic functions which include, ingestion and processing of foreign substances, apoptotic cells, cellular debris, cancer cells and any particle lacking the specific proteins found on healthy cells. In addition, they recognize danger signals via their broad range of pattern recognition receptors (PRR's), such as scavenger and toll-like receptors, which easily binds to polysaccharides, lipoproteins, lectins, oligonucleotides, and other microbial molecules. They also initiate immune responses by recruiting other immune cells through cytokine and chemokine secretion. Macrophages are key players in angiogenesis, wound repair, tissue development and maintenance of homeostasis as shown graphically in **Figure 2** (75,78,93).

Following decades of research, it has become increasingly evident that macrophages do greater than merely defending the host from pathogens. For the objective of this master thesis, three major roles of macrophages will be discussed in this section. That is, the role in phagocytosis, antigen presentation and perhaps most significantly, production of cytokines – that are essential for host immune responses against infections and cancer, along with repair of local tissue damage (77,82,83).

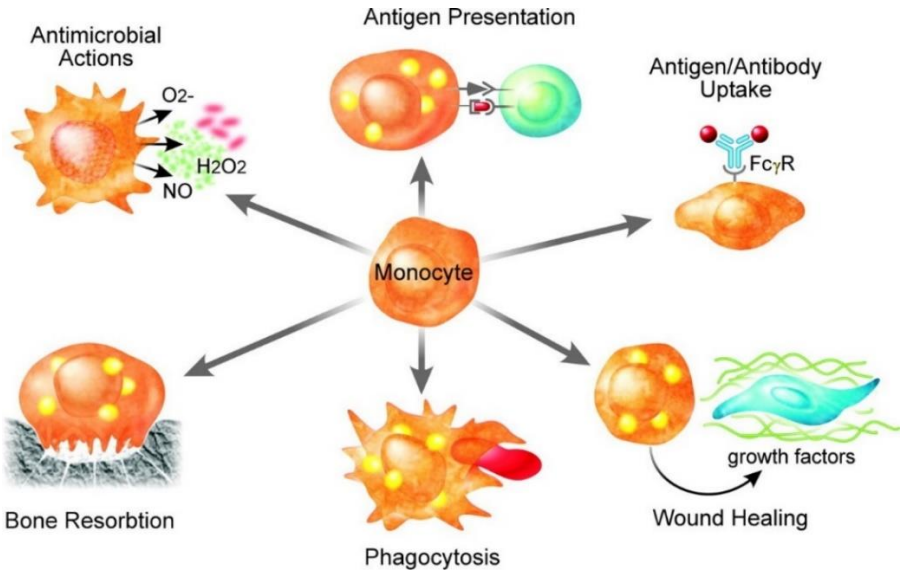

Figure 2. Heterogenous functions of macrophages in immunity and homeostasis

Resident and recruited macrophages in tissues derive from monocytic lineages and display remarkable functional diversity. Various roles depicted here involve host defense against intracellular microbes by producing inflammatory mediators such cytokines and reactive oxygen species, initiating an adaptive immune response through antigen presentation, phagocytosis and clearance of immune complexes to regulate inflammation, secretion of growth factors to mediate wound healing and repair of damaged tissues, specialized macrophages such as osteoclasts are crucial for bone remodeling all through adult life. Adapted from (93)

1.3.2.1 Macrophages in Phagocytosis

Phagocytosis is a process by which a cell detects, engulfs, and degrades a pathogen or cellular debris; in simple terms, it is a receptor-mediated uptake of particles larger than 0.5 µm (94). Macrophages are professional phagocytic white blood cells purported to have evolutionary cousins in all species; from single-celled amoeba to complex multicellular mammals. Ilya Metchnikoff, proposed that macrophages first evolved to regulate development by phagocytosing unwanted cells and maintaining order (74,77). Phagocytosis became an important property retained during evolution and remains one

of the most essential roles of tissue macrophages as it initiates the innate immune response, which then orchestrates an adaptive response (94).

Programmed cell death, also known as apoptosis, is an important part of normal development in almost all living organisms. Although an enormous number of cells die during embryonic development, they are quickly phagocytosed and that way, a massive number of senescent cells are removed. Studies conducted in mammalian development underscored the importance of macrophages in developmental phagocytosis. It was reported that mice lacking functional macrophages (by deletion of the crucial macrophage transcription factor PU.1), were inefficient in clearing dead cells and tissue remodeling was greatly hampered (95,96).

In addition to ingesting and clearing apoptotic cells, macrophages possess a plethora of restricted phagocytic receptors with which they discriminate potential pathogens from self, as earlier described. The term "Pattern-Recognition Receptors" (PRRs), which recognize conserved motifs called pathogen associated molecular patterns (PAMPs) on microbes and danger associated molecular patterns (DAMPs) on host cells was initially proposed by Janeway and is now widely acknowledged in immunology (5,34). There are four main families of the PRR's classified according to their location on either the plasma and endolysosomal membranes or within the cytosolic compartment (83,97). Toll-like receptors (TLRs) and C-type lectin receptors (CLRs) are among the specialized membrane-bound receptors whereas nucleotide-binding oligomerization domain (NOD)-like receptors (NLRs), retinoic-acid-inducible gene I (RIG-I)-like receptors (RLRs) and absent in melanoma 2 (AIM2)-like receptors, are examples of several other cytosolic receptors (83,98,99).

Lipopolysaccharide (LPS), a unique component of the gram-negative bacteria, is one of the most exemplified PAMPs recognized by TLR4 (100). Detection and binding of the receptor to the PAMP, spurs a series of downstream signaling events resulting in actin polymerization and rearrangement of the cytoskeleton. The cellular membrane protrudes around the particle, fuses behind it, and finally ingests into a membrane bound vesicle known as a phagosome. Maturation of the phagosome into a phagolysosome occurs through series of membrane fusion and fission events in the endocytic pathway. Once in the phagolysosome, the pathogen is digested by a wide range of hydrolytic and microbicidal mechanisms including toxic reactive oxygen and nitrogen species. This generates microbial peptides which are loaded onto specialized molecules – MHC, through a complex route of membrane trafficking. The MHC-peptide complex is subsequently transported to the surface membrane where it engages its cognate T- cell receptor in a process known as antigen presentation (94,99,101).

1.3.2.2 Macrophages in Antigen Presentation

Macrophages, DCs, and B cells have been classified as the three professional antigen presenting cells (APCs) (102). For a cell to function optimally in antigen presentation, it must meet three requirements. These are: ***(i)*** surface expression of both MHC I and II molecules alongside co-stimulatory molecules and PRR's; ***(ii)*** ability to phagocytose and process antigen; and ***(iii)*** synthesize and secrete cytokines-interleukin 1 (lL-1) (102–104). While DCs are key in antigen presentation to initiate primary immune responses, macrophages are considered the professional APC type most important in inflammatory sites and dedicated for clearing dead cells (105).

Digested microbial peptides (antigens) generated from phagocytosis, are loaded onto the MHC molecule to form a peptide-MHC II complex. The complex is then transported to the cell surface, where it binds to a corresponding helper T cell, programmed to recognize antigens, through complex physical and chemical interactions. (It is important that the peptide binds strongly to the MHC molecule during membrane transport, as weakly- bounded peptides may fail to engage its cognate T – cell receptor, which may prevent an immune response). Following this interaction, T cells secrete cytokines that activate various immune cells, for example B cells. Activated B cells in turn produce antibodies which coat the pathogen or target cell by binding to the antigens on their surfaces- a process known as opsonization. The opsonized particle is then readily phagocytosed by macrophages (75).

Antigen presentation by macrophages to T cells is a mutually beneficial interaction since the later secrete cytokines (IFN-γ), which activates macrophages to in turn produce IL-12p70, needed for the proliferation and differentiation of naïve CD4 T cells toward type 1 helper (Th1) T cells. (101,103,106). The process of phagocytosis and antigen presentation by macrophages is vital, given its significance in bridging the innate and adaptive immune systems. It is to this effect that pathogens target and impair antigen presentation pathways to evade destruction by the immune system. Several studies have also revealed that tumor cells have likewise evolved numerous means of manipulating antigen presentation pathways to escape detection and elimination by the immune system (75,107).

1.3.2.3 Macrophages in Cytokine Production

Cytokines are small cell-signaling molecules secreted by many cell types which play prominent roles in regulating many biological functions in both the innate and adaptive immune systems (108). Among leucocytes, macrophages are one of the major producers of cytokines even though they can also be

produced by non-immune cells such as epithelial cells and connective tissues. Depending on the activating stimuli, macrophages produce both pro and anti-inflammatory cytokines which regulate immune responses in health and diseases (75,109). Many signals trigger the production of cytokines in macrophages. For example, stimulation of most TLRs activate transcription factors needed for cytokine production. Notably, recent studies have identified that both interferon types, I and II, in combination with TLR stimulation can activate antitumor macrophage phenotypes (110). In addition, they identified that two signals; involving synergy between IFN-γ and TLR ligands was required to efficiently trigger macrophage tumoricidal activities through the production of nitric oxide (NO) and pro-inflammatory cytokines such as TNF-α and IL-12p70 (111).

Furthermore, immunological stimuli which occur during antigen presentation to T cells lead to secretion of inflammatory mediators (cytokines), which initiate an adaptive immune response. Corthay et. al, demonstrated the collaboration between macrophages and Th1 T cells in providing primary immunity against cancer (112). In their study based on a murine model for myeloma, it was discovered that IFN-γ, secreted by tumor specific Th1 T cells, triggered anti-tumor functions in macrophages within the tumor microenvironment. They hypothesized that the activated macrophages could inhibit proliferation of tumor cells through secretion of tumoricidal compounds like nitric oxide (NO) and reactive oxygen intermediates (ROI), which are established killing mechanisms previously reported by Mantovani et al. (53,113).

I. Pro-inflammatory Cytokines

Tumor necrosis factor α (TNF-α), IL-1, **IL-6**, and **IL-12p70** are examples of pro-inflammatory cytokines produced to initiate an inflammatory response when macrophages encounter pathogens. TNF is one of the rapid response cytokines released by activated macrophages upon pathogen invasion. It is an effective pyrogenic cytokine which produces fever and acute phase proteins by acting on the hypothalamus. Excessive production of this acute inflammatory cytokine however, has been implicated in diseases such as inflammatory bowel disease, cancer, rheumatoid arthritis, and other auto-immune pathologies (75).

IL-1 is mainly produced by monocytes and macrophages, even though they can sometimes be secreted by NK cells, B cells and DCs. IL-1 is also an inflammatory cytokine secreted in the preliminary stages of an immune response to infection. It exists in different forms- IL-1α and IL-1β, acting as a potent

mediator of fever and pain. Among other functions, it induces the expression of adhesion molecules on endothelial cells, which is required for transmigration (diapedesis) of immune cells to infection sites. IL-1β, besides functioning as a chemoattractant for granulocytes, also helps in the activation and differentiation of CD4+ T cells (75,114).

IL-6 is one of the cytokines with a pleiotropic effect- both pro-inflammatory and anti-inflammatory functions. It is produced by macrophages in response to infections and local tissue damage. IL-6 is essential in the activation of CD8+ T cells, and regulates important biological processes related to immunity, tissue repair and metabolism. Akin to other pro-inflammatory cytokines, IL-6 induces the production of acute phase proteins, by hepatic cells, which are vital in host defense against pathogens (75,109).

Interleukin 12p70 (IL-12) is largely produced by activated macrophages and other professional antigen-presenting cells. It is a heterodimer encoded for by two distinct genes, IL-12A (p35) and IL-12B (p40). The 70kDa protein binds IL-12 receptor (IL-12R) on macrophages, DCs, T and NK cells (60). Macrophage-derived IL-12p70 plays an essential role in cell-mediated immunity by stimulating the differentiation of naïve T cells into Th1 subsets and also induces the production of IFN-γ as well as TNF-α by T cells and NK cells (75). While IL-12p70 is vital in the immune response to infections, many studies have reported its potency in fighting cancers through its antiangiogenic activities (115), as well as enhancing the cytotoxic functions of CD8+ T cells and NK cells (116).

II. Anti-inflammatory Cytokines

While macrophages are key in provoking inflammatory responses, they are also an important source of anti-inflammatory cytokines, which have inhibitory or regulatory effects. Examples are transforming growth factor beta (TGF-β) and IL-10, which function to inhibit the synthesis of pro-inflammatory cytokines. In addition, regulatory cytokines such as IL-4 produced by activated T cells can suppress the inflammatory functions of macrophages (75).

IL-10, also known as human cytokine synthesis inhibitory factor (CSIF), is primarily a suppressive cytokine produced by monocytes and macrophages. It inhibits the pro-inflammatory and microbicidal activities of macrophages including restricting the synthesis and secretion of IL-1, TNF, IFN-γ and IL-12p70 (117). Apart from diminishing cytokine production, IL-10 impedes the process of antigen presentation in activated macrophages by down-regulating the expression of MHC II molecules. *In vivo* studies in mouse models revealed that elevated levels of IL-10 significantly reduced inflammation

secondary to cytokine production. In contrast, neutralization or complete blockade of IL-10 synthesis led to an increased production of pro-inflammatory cytokines such as TNF and IL-6. Recombinant IL-10 and blockade of TNF-α has thus proven to be a potentially effective treatment for some chronic gastrointestinal inflammatory diseases like Ulcerative colitis and Crohn's disease (75,116,118).

Transforming growth factor beta (TGF-β) is mainly an inhibitory cytokine produced by many cell types, including macrophages. It is a key cytokine involved in the embryogenesis, cell proliferation and regeneration, as well as homeostasis of tissues. Myeloid cells such as macrophages, produce TGF-β to suppress the effects of pro-inflammatory cytokines, as well as regulate macrophage activation. TGF-β is also known to inhibit the synthesis of cytokines needed for T cell proliferation (119). It promotes the maintenance and functions of Tregs while effectively suppressing the functions of Th1and Th2 cells (120).

III. Other Cytokines

Macrophages produce some specialized cytokines which stimulate the differentiation of hematopoietic cells. The **Granulocyte macrophage colony-stimulating factor (GM-CSF)** is an example of such cytokines that promote the differentiation of both granulocytes and macrophages from bone marrow precursor cells. GM-CSF is reportedly induced under inflammatory and pathologic conditions, but its expression markedly reduced in circulation under homeostatic conditions (121). Besides its role as growth factors, GM-CSF has been shown to play various inflammatory roles in host's defense to some pulmonary infections and other autoimmune reactions (122). GM-CSF is commonly considered to be a pro-inflammatory cytokine, since it stimulates monocytes and macrophages to increase the production of pro-inflammatory cytokines like TNF and IL-6 (123).

Macrophage-colony stimulating factor (M-CSF), also termed colony stimulating factor-1 (CSF-1); is a cytokine produced ubiquitously by many cells and tissues of the body, including bone macrophages termed osteoclasts (121). In contrast to GM-CSF, it is constitutively expressed under homeostatic conditions and is essential in stimulating growth, differentiation, and survival of monocytes into mature macrophages in various tissue (124). Studies have reported that while GM-CSF induces the expression of MHC class II molecules in murine bone marrow derived macrophages, M-CSF on the other hand, suppresses it (125). Further *in vivo* findings also revealed that the receptor for M-CSF is one of the markers initially expressed by developing macrophages and that mice lacking these cytokine receptors had deficiencies in several macrophage populations (123,126,127). M-CSF is also widely

used in generating 'alternatively activated' macrophages *in vitro*, which will be discussed later in this thesis (128).

IV. Chemokines

Chemokines are a large family of cytokines that control movement of cells in a process known as chemotaxis. Chemokines are produced by many cell types including macrophages, and function to recruit immune cells to sites of infection. Some chemokines are also key in the formation of new blood vessels during development as well as trafficking of cells to the tissues providing signals for cellular differentiation of cells (75). Chemokines secreted by macrophages are essentially classified as either inflammatory or homeostatic when they are induced by inflammation or involved in tissue homeostasis, respectively (129). Within inflamed tissues, both resident and infiltrating macrophages secrete inflammatory chemokines upon activation of their PRR's by the pathogen, this helps in trafficking the initial wave of innate immune effector cells. In general, chemokines shape immune responses to infections and tissue damage (130). Homeostatic chemokines on the other hand, are essentially produced in both lymphoid and non-lymphoid tissues and are responsible for physiological trafficking of cells needed for development and immune surveillance. However, some homeostatic chemokines like CCL19 and CCL21 are also induced at inflammatory sites (129).

CXCL1 and **CXCL2,** also referred to in mice as keratinocytes-derived chemokine (KC) and macrophage inflammatory protein 2-α (MIP-2α) respectively, are angiogenic chemokines induced by IFN-γ and secreted by monocytes and macrophages. They function as chemoattractant for neutrophils and hematopoietic stem cells and are also known to play a role in the development of tumors like melanoma (131,132).

Another important chemokine secreted by macrophages is **CXCL8** or IL-8, which is primarily responsible for trafficking of neutrophils and other granulocytes to the site of injury or infection during an innate immune response (133). Because macrophages are usually one of the first immune cells to encounter antigens, they are believed to be first in releasing IL-8. Apart from attracting other leucocytes, CXCL8 also functions to induce several physiological responses in target cells to increase their phagocytic ability on arrival at the infection site. As an important neutrophil chemotactic factor, CXCL8 additionally stimulates degranulation of neutrophils, which acts a vital intermediary in inflammatory diseases such as psoriasis, gingivitis and cancer. (134–136).

CXCL9 and **CXCL10,** also known as monokine induced by gamma interferon (MIG) and interferon gamma-induced protein 10 (IP-10) respectively, are both chemokines secreted by many cells,

including macrophages. Their secretion is induced by IFN-γ and they function to attract T cells to inflammation sites. While CXCL9 helps recruit immune cells necessary for inflammation and repair of damaged tissues, CXCL10 is plays a critical role in inducing apoptosis, inhibiting angiogenesis, and regulating cell proliferation in inflammatory diseases and cancer. Both chemokines are known to have potent anti-tumor effects and have been therapeutic targets for various infectious diseases and cancers (129,137,138).

1.4 MACROPHAGE ACTIVATION AND POLARIZATION

1.4.1 History and definition of macrophage polarization

In contrast to lymphocytes where phenotypic changes are "permanent" after exposure to polarizing cytokines, macrophages exhibit a plastic gene expression profile primarily influenced by the type and concentration of stimuli, as well as the duration of exposure to the stimulating agents (139,140). Immunologists have been divided over the definition and use of the terminologies macrophage 'polarization' and 'activation'. The lack of consensus is largely due to a myriad of interpretations encompassing macrophage activation studies. Nonetheless, Adams et al., defined macrophage activation as 'acquisition of competence to complete complex functions' such as phagocytosis, antigen processing and presentation, as well as cytokine secretion (141). Briefly, acquired properties such as the expression of surface receptors, production of cytokines, chemokines, and reactive oxygen species are either upregulated or repressed following macrophage polarization (140,142,143). In this research, the terms 'activation' and 'polarization' are used interchangeably to mean the stimulation of macrophages with external factors.

The term 'classically activated' originated in the 1960's by Mackaness in an infection context, when he first described an enhanced microbicidal activity of murine macrophages toward BCG (bacillus Calmette-Guerin) and Listeria upon re-exposure to the pathogens (144). Soon after that, the enhancement was linked with Th1-type cytokine, IFN-γ produced by antigen-activated immune cells. This was identified as the first macrophage activating factor, capable of transforming resting macrophages into active ones (145). Activated macrophages showed enhanced antigen presentation functions as well as complement mediated phagocytosis, they also secreted more pro-inflammatory cytokines and toxic mediators (146). Since the phenotypic and functional effects induced by IFN-γ was the first type observed in macrophages, it became known as the 'classical activation' of macrophages (146). It is worth noting that the term 'classical activation', which exclusively referred

to macrophages activated with IFN-γ, is now interchangeably used with IFN-γ and/or TLR stimulation (by LPS). (128)

Stein et. al (1992), later devised the name 'alternative activation' to describe the difference in activation and gene expression observed when macrophages were stimulated with IL-4 and IL-13 (147). Alternative activation was hence used to distinguish the effects of IL-4 stimulated macrophages from the earlier-discovered classically activation. IL-4-induced macrophages adopted an alternative macrophage phenotype, a state entirely different from IFN-γ activation but also far from deactivation, as will be later described (140,141,148).

1.4.2 M1 and M2 Macrophages

Many years after the 'classically' and 'alternatively' activated terminologies were introduced, Mills et.al (2000) proposed the M1 and M2 nomenclature to denote the classically and alternatively activated macrophages, respectively (149). This concept was borne out of observations that the metabolism of arginine was completely at variance in macrophages from the prototypical Th1 mice strain, (C57BL/6) and Th2 strain (BALB/c). Macrophages from the Th1 strain made the toxic nitric oxide (NO), while the Th2 strain macrophages made the trophic polyamines. He associated these metabolic differences with Th1 and Th2 responses in the respective strains and proposed that macrophages could make 'M1' or 'M2' responses analogous to T helper cells. (128,140,149).

Macrophages were therefore believed to be polarized into two main categories; first are the classically activated (also called 'M1' macrophages), with pro-inflammatory properties arising from immune responses generated by activating TLRs and interferon signaling (142).Additionally, classically activated macrophages were established to upregulate expression of MHC class II molecules, secrete pro-inflammatory cytokines and high production of reactive nitrogen and oxygen intermediates with tumoricidal functions (150). The second category referred to as the alternatively activated (or 'M2' macrophages) are characterized by anti-inflammatory properties induced by Th2 cytokines such as IL-4, and IL-13, and are important in wound healing and maintenance of tissue homeostasis. In contrast to M1 macrophages, M2 dampens inflammatory responses, secrete endothelial growth factors, and can promote tumor growth (140,147,151).

Several years down the line, when macrophage plasticity in response to different environment was gradually studied, this nomenclature has been considered as oversimplified and highly debated, with robust evidence suggesting that the diversity and overlap of cues from the microenvironment can generate a spectrum of macrophage phenotypes and functions *in vivo* (152). It now appreciated that

macrophages exist as a continuum of two the extremes with a dynamic polarization process; this include TAMs, which falls under neither M1/M2 categories (153,154). Also, other cytokines and factors, such as IL-10 and TGF-β, later identified as regulatory factors, did not fit in the Th1-Th2 context, even though they elicited responses similar to Th2 phenotypes (128). Another complication in clearly defining M1 and M2 macrophage phenotypes *in vitro* is the lack of constitutively expressed markers. An illustration is Arginase-1, which is a considered a classic M2 marker, is equally up-regulated in M1 macrophages (140,142,155). Moreover, the expression of Arginase-1 or CD206 is generally below detectable levels for realistic immunophenotyping (152,156). These factors coupled with the heterogeneity and many intermediary stages during polarization could not be satisfactorily described with the 'black' or 'white' model. This led Mantovani and colleagues, to classify macrophages as a continuum between two extreme polarized states, based on effects of the activating stimuli. They proposed M1 macrophages as (IFN-γ plus LPS or TNF-α) and 'M2-like' subdivided into groups namely: M2a (IL-4), M2b (immune complexes plus TLR ligands), and M2c (IL-10, and glucocorticoids); with their respective activating stimuli in parenthesis. (113,153,154).

Toll-like receptors play a significant role in recognizing pathogens and initiating inflammatory immune responses. Stimulation of TLRs by microbial products initiate signaling pathways that result in the activation of antimicrobial genes and inflammatory cytokines (101). As stated, M1 activated macrophages are typically induced upon stimulation with LPS and IFN-γ, and are characterized by upregulation of HLA-DR, co-stimulatory molecules: CD80 and CD86, and chemokines such as CXCL9 and CXCL10 which recruit Th1 T cells to inflammatory sites. M1 also secrete a myriad of cytokines, as mentioned in the previous section, these cytokines and surface receptors enhance the interaction of macrophages with other immune cells (146). For example macrophage-induced IL-12p70 drives the proliferation and differentiation of naïve T cells into helper T cell subtypes (154). Additionally, M1 activation triggers the inducible Nitric oxide synthase (iNOS) gene, which is essential for generating reactive oxygen species such as NO, needed for local tissue destruction. Due to the harsh inflammatory and cytotoxic effects, M1 macrophages are crucial in the elimination of pathogens, cancer cells and initiation of inflammation, however, chronic and unresolved inflammation under certain conditions can be detrimental to the host (16,157,158).

Alternatively activated (M2-like) macrophages on the other hand, are induced upon exposure to IL-4, IL-13, immune complexes, parasitic infections, and fungal cells to produce anti-inflammatory cytokines and chemokines including CCL17, CCL22 and CCL24 (159) Furthermore, M2 macrophages produce TGF-β, IL-10, and high expression of Arginase, which competes with NOS for their common

limiting substrate, L-arginine, thereby inhibiting NO production (159,160). M2 macrophages are mainly involved in clearing apoptotic cells and debris, resolving inflammation, secretion of growth factors needed for tissue healing and repair, and have also been reported to play significant roles in tumor progression (**Figure 2**) (154,160,161).

Another postulate for M1 and M2 characterization, reported in several studies and worth mentioning, is based on the cytokines used for generating the macrophages in *vitro,* which have substantial polarizing effects (140,162). GM-CSF and M-CSF growth factors, apart from inducing macrophage differentiation, are known to "prime" or "activate" them towards M1 and M2 phenotypes respectively (163). Studies comparing both colony stimulating factors in mice bone marrow derived macrophages (BMDMs) showed they displayed significant differences in transcription factors and cytokine production, as well as opposing roles in inflammation (164). It was established that GM-CSF macrophages exhibited pro-inflammatory properties (TNF expression), whereas M-CSF anti-inflammatory and tissue healing state (IL-10 expression), after LPS stimulation; hence were assigned the names M1 and M2, respectively, shown in **Figure 2**. (121,163–165).

Having acknowledged these, it is important to note that the activation status and ultimate function of macrophages as either promoting or antagonizing inflammation, is highly dependent on environmental cues. Additionally, the nomenclature proposed by Murray et al. (140), defining polarization states by the activating stimuli [e.g., M (IFN-γ)], seem to resolve some of the M1-M2 controversies; however this may not be applicable *in vivo* where the activating stimuli are very complex, not restrictive and especially usually unknown (152). Moreover, an imbalance in the steady-state of M1 and M2 may result in pathological events: while overproduction of M1 may well induce chronic inflammatory diseases, an excess number of M2 could also promote severe immune suppression (166). Additionally, the M1 and M2 nomenclature, even though widely used, remains controversial and efforts are continuously advancing to unambiguously define polarization. Notwithstanding, the terms 'M1' and 'M2' macrophages used herein refers to the pro-inflammatory and anti-inflammatory macrophages, respectively.

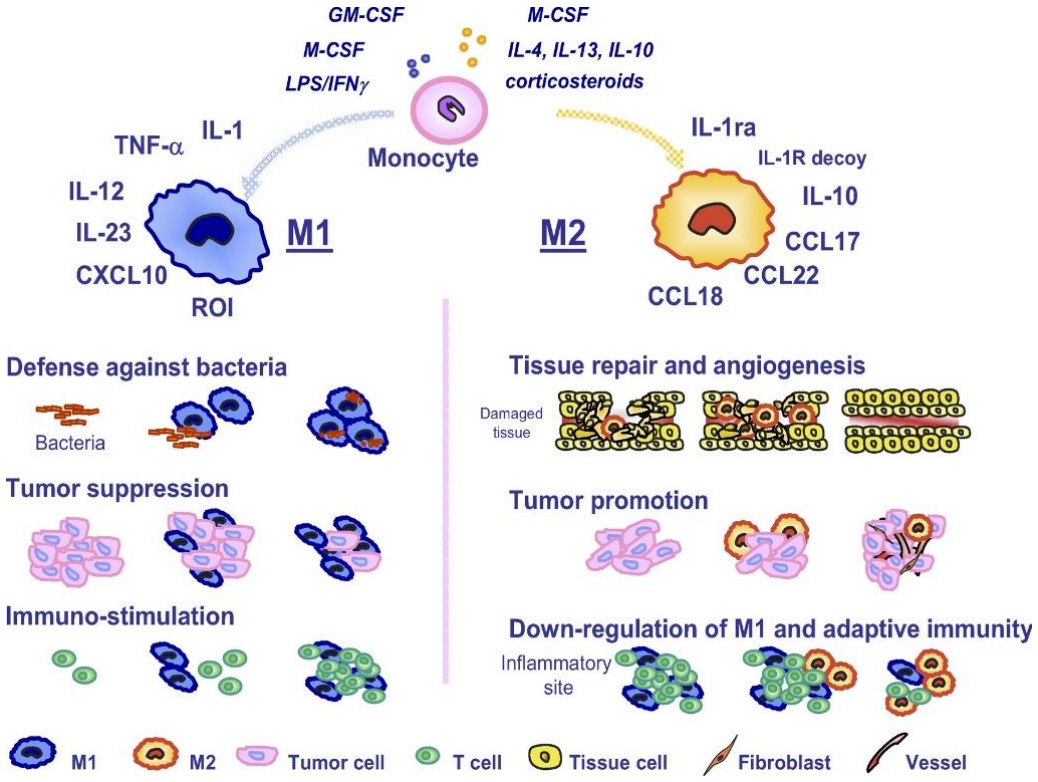

Figure 3. Macrophage polarization and function.

The two polarized states of macrophages: M1(classically activated) and M2 (alternatively activated). Shown above are activating stimuli LPS/IFN-γ and IL-4, IL-13, or IL-10 for M1 and M2 phenotypes respectively and their corresponding roles in host defense and diseases. Adapted from (167).

1.4.3 Tumor Associated Macrophages (TAMs)

In the strictest sense, tumor associated macrophages (TAMs) are almost not regarded as a distinctly separate subset of macrophages because they are only studied in tumors and not present at normal physiological conditions (158). It is widely acknowledged that solid tumors are infiltrated by immune cells, of which macrophages form a significant percentage. TAMs can originate from both tissue-resident macrophages and circulating monocytes recruited into the tumor microenvironment via chemokines and factors secreted by tumor cells and stromal cells (168). TAMs, like conventional macrophages, are heterogenous, multifunctional and highly plastic cells, which have been established to play dual roles in either promoting or suppressing tumor growth, and have also been characterized into 'M1' and 'M2' phenotypes (169). The role of TAMs remains enigmatic among immunologist, with many aspects still unclear, however the general opinion is that since TAMs share both M1 and

M2-like signatures, their roles within and around the TME are key in the establishment or elimination of tumors (53,168).

Many studies have highlighted the correlation of TAM phenotype, density, and microlocalization with overall prognosis. Particularly, high densities of M1 ($CD68^+$) TAM in the tumor islets of human NSCLC is associated with longer survival, while high $CD68^+$ TAM density in tumor stroma correlated with poor survival (170–172). Other reports supporting the concept of pro-tumorigenic activities of M2 TAMs, provide evidence that macrophage depletion in breast cancer models, for instance, have almost no effect in preventing neoplasm, and in some cases were even beneficial to the host (173). Inferences from these studies suggest that high M2 TAM densities in the TME are associated with poor prognosis (174–178). Consequently, recent therapies targeted at TAMs are largely aimed at inhibiting macrophage recruitment to the TME, depleting TAMs and reprogramming their initial tumorigenic properties (176,179). Nonetheless, other compelling studies also favor the theory that some TAM subsets have tumoricidal activities (158,168). Anti-tumor activities are reportedly induced by the classically activated 'M1' macrophages which secrete reactive oxygen and nitrogen species for local tissue destruction, as well as a wide range of inflammatory cytokines like IL-12p70, which function mainly to activate Th1 response to execute an anti-tumor response (158,168,169). One of the invaluable techniques providing evidence to support this claim was developed to enhance macrophage cytotoxicity within the TME of early-stage bladder cancer (180). This was achieved by stimulating TAMs with microbial particles from the bacteria bacilli calmette-guerin (BCG); activated macrophages produced enormous amounts of pro-inflammatory cytokines like IL-6, IL-1 and TNF-α, furthermore, they recruited other immunocytes like NK cells, CD4+ T helper and cytotoxic CD8+ cells to the bladder. Collectively, these cells create an inflammatory response, cytotoxic to bladder cancer cells (181,182).

Notably, TAMs exhibit remarkable degrees of functional and phenotypic plasticity in that, they can easily switch phenotypes depending on the location in the TME they occupy (169). For example, M2-like macrophages have been identified to inhabit necrotic and hypoxic environments within the tumor, with decreased antigen presentation and phagocytic activities (183,184). Also, immunophenotyping studies have established that TAMs can co-express markers established for M1 and M2 phenotypes, therefore providing a clear distinction between both phenotypes is almost impracticable (171,185). In light of their crucial roles in shaping the outcome of therapies, TAMs have increasingly become promising targets in designing and developing new strategies in cancer immunotherapy (186). More significantly, identifying key pathways in the recruitment, polarization, and synergistic effects between

TAMs and other TILs. This has paved the way for novel treatment approaches that target indirect pathways to stimulate cytotoxic T cell recruitment and activation (186). In some reported pre-clinical studies, synergizing this approach with checkpoint inhibitors and/or radiation and chemotherapies have proven remarkably successful (166,186).

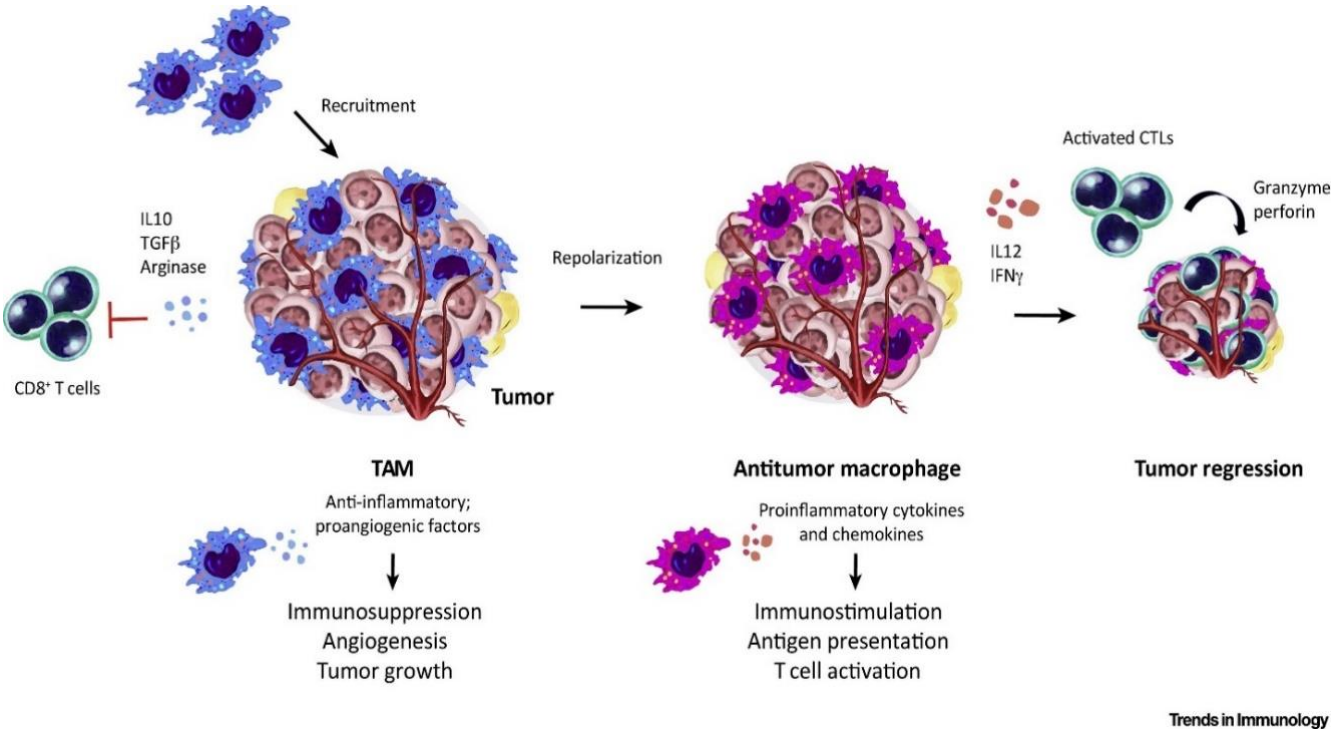

Figure 4. Reprogramming TAMs for cancer therapy

TAMs originate from tissue resident precursors or via recruitment from bone-marrow progenitors. Within the TME, they either promote or retard tumor progression. Tumorigenic TAMs (with 'M2-like' phenotypes) favor tumor progression and dampen inflammatory responses by down-regulating M1-mediated functions. Emerging strategies targeted at TAMs include inhibiting their recruitment to the TME, repolarization towards 'M1' phenotypes to produce pro-inflammatory cytokines, and upregulating antigen presentation mechanisms to stimulate adaptive immunity through activation of helper T cells and cytotoxic T lymphocytes (CTLs). Activated CTLs directly kill tumor cells through release of cytotoxic granzymes and perforin. Adapted from (186).

1.4.4 Surface Marker Expression

As stated previously, macrophages are resident in various tissues performing distinct roles and responding to niche-specific stimuli. Owing to the diversity, plasticity and overlapping functions of M1 and M2 polarized macrophages, identification of distinctive and unique markers to clearly differentiate them remains one of the most controversial subjects in macrophage biology (187). Moreover, various tissue macrophages and DCs derive from a common monocytic precursor and

express similar phenotypic as well as functional phenotypes, thus using surface markers as only means to distinguish both cells may not be entirely accurate (188). For instance, CD68 and MHC II are nonspecific surface markers equally expressed by both macrophages and DCs of the monocytic lineage. This is also consistent with the marker F4/80, which is shown to detect both macrophages and DCs infiltrating or being resident in murine kidneys (188).

Evidently, M1 and M2 activated macrophages may display differential gene expression profiles largely determined by the type of stimuli, concentration, and period of exposure, however some markers are conserved, such as some chemokines and their cognate receptors (154,187). An example is CXCL10, a chemoattractant secreted by M1 macrophages which recruit Th1 T cells while CCL17 and CCL22 secreted by M2 activated macrophages are involved in trafficking of T regulatory cells (Tregs) to the TME (189). Some commonly used macrophage markers such as CD14, CD16, CD68, CD163, CD206, among others, may be useful in studying both immunologic and metabolic functions of the various macrophage populations. The table below summarizes some key markers frequently used in identifying both human and murine macrophage subtypes.

Table 1. General phenotypic and functional markers used in characterizing macrophage polarization subsets. *Table provides an overview of macrophage subsets described in vitro. M1 macrophages predominantly drive inflammatory responses whereas M2 exhibit mostly homeostatic expression patterns. M2 macrophages encompass a functionally diverse group subdivided into M2a, M2b, M2c, and M2d, with each subclass activated by unique stimuli. Table shows an overview of different macrophage subtypes and subsets with their designated expression markers and characteristics. Adapted from (154)*

Macrophage phenotype	M1	M2a	M2b	M2c	M2d
Stimulation/ skewing condition	IFN-γ, LPS, GM-CSF	IL-4, IL-13, Helminth/Fungal infections	IL-1R, Immune Complexes	IL-10, TGF-β, Glucocor-ticoids	Adenosine, IL-6,
Cytokine profiles	TNF, IL-1b, IL-6, IL-12p70, IL-23	IL-10, TGF-β, IL-1ra	TNF-α, IL-1, IL-6, IL-10,	IL-10, TGF-β	TNF-α, IL-10, IL-12, TGF-β
Chemokines	CCL5, CCL2, CCL4, CCL8, CCL9, CCL10 CCL11, CCL3,	CCL22, CCL17, CCL24	CCL1	CCR2	CCL5, CXCL10, CXCL16
Molecular activation markers	CD68, CD80, IL-1R, MCH- II, TLR2, TLR4, iNOS, SOCS3	CD163, MHC II, CD200R, MMR / CD206, TGM2, IL-1R II	CD86, MHC-II	CD163, TLR1, TLR8	VEGF
References	(142,147,148,167, 190–194)	(96),(128),(134), (140),(143),(181)	(133),(134), (140),(145),(176),(178),(179)	(134),(140), (145),(182)–(184)	(64),(124), (140),(185)–(189)

1.5 IMMUNOMODULATORY POLYSSACCHARIDES

Alternative medicine using plant extracts in cancer treatment has become widespread the world over. The purported anti-cancer potential of these extracts is to a significant extent based on several experiments conducted in animal models, with many credible studies proving that the immunogenic effects stem from certain active biological compounds. One of the active compounds relevant for this thesis, and reported in numerous studies to induce cytotoxic and immunomodulatory effects on both human and mouse immune cells, is a complex carbohydrate molecule (polysaccharide) called beta-glucan (β-glucan) (204,205). β-glucans are major components of bacterial and fungal cell walls known to bind several PRRs including C-type lectin and TLRs found on macrophages, DCs, neutrophils, and NK cells, to initiate an anti-microbial immune response (204). Fungal polysaccharides (carbohydrates), like other microbial particles are recognized by immune cells as PAMPs which specifically bind Dectin-1 and complement receptor (CR3). This consequently prime leucocytes (macrophages) to phagocytose tumor cells opsonized with complement fragments (iC3b) (206). Also, activation of these innate immune receptors mediated by fungal polysaccharides have been demonstrated to efficiently enhance antigen presentation and even significantly, the production of pro-inflammatory mediators, which can further trigger the initiation of an adaptive immune response against tumor targets (205–207).

1.5.1 Chaga (*Inonotus obliquus*)

Previous studies carried out by Wold et. al, identified and purified six novel immunomodulatory polysaccharides isolated from the medicinal fungus, *Inonotus obliquus,* popularly known as Chaga (208); this forms the premise for much of the investigations conducted in this master thesis. One Slovakian botanist, Pilàt in 1936, who is believed to have extensively studied chaga and proposed its scientific name, observed that it has oblique pores, hence the source of its species name *obliquus* (209). Chaga mushroom is a white rot 'medicinal fungus' mainly found growing on the bark of birch trees in cold climates; and is commonly used in folk medicine in Russia, Asia, and Northern European countries to treat several ailments. In northwestern Russia, Finland and Siberia, the fruiting body of chaga mushroom is decocted to treat cancer patients (210). Many *in vitro* studies examining the clinical significance of chaga have discovered anti-tumor, anti-mutagenic, anti-viral, antioxidant, immunomodulatory and anti-inflammatory activities in chaga (210–213). An *in vitro* experiment demonstrated that water soluble compounds isolated from chaga, selectively arrested growth cycle in

human hepatoma cancer cells at the G0/G1 phase and thereafter induced cellular apoptosis while healthy cells remained unaffected (213).

Various *in vivo* studies have also confirmed immunostimulatory, cancer treatment and prevention properties in chaga. A study conducted in mouse models for metastatic Lewis Lung carcinoma revealed that extracts of *I. obliquus* caused significant reduction in tumor size, (approximately 60%), with a remarkable boost in energy metabolism observed following oral administration of chaga extracts (211). In a separate report, polysaccharides from *I. obliquus* were indirectly involved in inhibiting tumor growth by stimulating the immune system. In their study, purified endo-polysaccharides administered both orally and intraperitoneally were reported to significantly prolong the survival rate of mice implanted with highly metastatic-B16F10 murine melanoma cells. It was detailed that nearly 67% of the initial number of mice survived with no tumor incidence or cytotoxic effects observed 60 days post tumor-implantation (214). Interestingly, anti-inflammatory immune responses have also be reported in chaga polysaccharides, where activated mouse BMDMs significantly inhibited the production of NO and dampened pro-inflammatory responses induced by LPS activation (215).

In spite of the substantial amount of experimental evidences supporting the anti-tumor activity exhibited by chaga compounds and extracts, the underlying mechanisms and signaling pathways inducing the immunomodulatory and anticancer effects are still not clearly elucidated (211). However, some reports have revealed that biological compounds from *I. obliquus* extracts harbor high antioxidative properties, which can prevent the growth of tumors, reduce oxidative stress in immune cells, especially among patients with ulcerative colitis and healthy individuals alike (210,216). Furthermore, endo-polysaccharides purified from chaga extracts is believed to specifically activate macrophages and induce humoral immunity through B cell activation (214). Additionally, another study highlighted that polysaccharides isolated from the fruiting body of chaga effectively promotes macrophage activation by initiating the phosphorylation of classical MAP kinases (MAPKs), particularly, ERK1/2, JNK and p38; which subsequently activated the transcription of NF-κB. The activated macrophages upregulated phagocytosis, production of ROS/ NO, and secretion of TNF-α. Moreover, TNF-α secretion was reportedly inhibited by anti-TLR2 monoclonal antibodies, suggesting that production of TNF-α was possibly induced via the TLR2 receptor signaling pathway (217).

1.5.2 Investigating the tumoricidal potential of chaga polysaccharides.

Expounding on the existing experimental proofs and to further investigate the receptor signaling involved in the anti-tumor activities exerted by chaga polysaccharides, Wold *et al*. (2018) demonstrated that polysaccharides isolated from *I. obliquus* exhibited some immunomodulatory effects by increasing NO production in murine macrophage and DCs *in vitro* (208).In this study, the six isolated polysaccharides were characterized into 3 main groups based on their structural and chemical properties as follows: ***i*)** water-soluble and neutral compounds ***ii*)** water-soluble and acidic compounds, and ***iii*)** neutral, particulate compound. The structure-function relationship and signaling receptors possibly involved in the immunomodulatory function have been further investigated and this laid the groundwork for this thesis.

2 AIMS AND OBJECTIVES OF THE STUDY

2.1 Principal Aims

Many macrophage studies reported in the literature are often conducted in mouse models or immortalized cell lines, largely due to practical limitations in accessing human tissues and the inability of human cells to survive *in vitro* following isolation. However, the culture of primary human monocyte-derived macrophages provides an excellent option, as it relatively mimics *in vivo* conditions compared to cell lines; even more, blood monocytes can also be readily obtained in large numbers. Consequently, one major goal of this study is to provide an optimized, multistep method for generating and polarizing human monocyte-derived macrophages *in vitro.*

Additionally, few studies, if any, have focused on understanding how the active soluble molecular compounds found in the medicinal fungus, Chaga, can induce an antitumor response in macrophages. The second aim of this research is to provide insight into the immunostimulatory properties responsible for the tumoricidal activity observed in macrophages activated by fungal polysaccharides.

2.2 Research Objectives:

The following research objectives were laid out to facilitate the achievement of these aims:

1. Establish an optimized protocol for *in vitro* differentiation of human monocyte-derived macrophages from CD14+ monocytes using GM-CSF or M-CSF.
2. Examine surface marker expression and cytokine secretion profiles of *in vitro* polarized human macrophages using flow cytometry and Luminex technology, respectively.
3. Investigate the tumoricidal potential of novel fungal polysaccharides in mouse models for Lewis lung carcinoma.

3 MATERIALS AND METHODS

3.1 Materials

Table 2. Common materials, reagents, and manufacturer's information.

Name	Company	Cat. Number	Storage
Cell scraper	TPP©	99002	Dry storage
CD14 MicroBeads	Miltenyi	130-050-201	2-8ºC
Dimethyl sulfoxide (DMSO)	VWR®	0231	Room temperature
Falcon tube (50 mL)	SARSTEDT AG & Co. KG	62.547.254	Dry storage
Falcon tube (15 mL)	SARSTEDT AG & Co. KG	62.554.502	Dry storage
Fetal Bovine Serum (FBS)	BioWest	S181BH-500	Frozen
Flat bottom 48-well plate	Costar®	CLS3548	Dry storage
Glasstic® slides	Kova	87144E	Room temperature
LS columns	Miltenyi	130-042-401	Dry storage
Lymphoprep™	Progen	1114545	Room temperature, in the dark
MS columns	Miltenyi	130-042-201	Dry storage
Non-treated tissue culture dish	SARSTEDT AG & Co. KG	734-2796	Dry storage

Nunc™ CryoTube	Thermo Fisher	363401	Dry storage
Pre-separation Filters (30 µm)	Miltenyi	130-041-407	Dry storage
Penicillin-Streptomycin (P/S) 100 X Solution	Biowest	L0022-100	Frozen
Polypropylene centrifuge tubes (50 mL)	Corning®	CLS430290	Dry storage
Polypropylene centrifuge tubes (1.5 mL)	Corning®	CLS3620	Dry storage
Polypropylene centrifuge tubes (15 mL)	Corning®	CLS430791	Dry storage
RPMI 1640 with L- Glutamine	Biowest	L0500-500	4ºC
Sterile DPBS no calcium no magnesium ($DPBS^{-/-}$)	Gibco	14190-144	4ºC
Sterile PBS no calcium no magnesium ($PBS^{-/-}$)	Made in-house		4ºC
Sterile DPBS plus calcium plus magnesium ($DPBS^{+/+}$)	Sigma-Aldrich	D8662	4ºC
Trypan blue	Invitrogen	T10282	Room temperature
96 V-bottom well plate	VWR®	732-2470	Dry storage
0.5 M EDTA	ThermoFisher	AM9260G	4ºC

Table 3. Cytokines and ligands used in the differentiation and polarization of human monocyte-derived macrophages.

Name	Abbreviation	Manufacturer	Cat. Number	Storage
Recombinant Human GM-CSF	rhGM-CSF	Peprotech	300-03	- 80ºC
Recombinant Human M-CSF	rhMC-SF	Peprotech	300-25	- 80ºC
Recombinant Human IFN-γ	rhIFN-γ	Peprotech	300-02	- 80ºC
Recombinant Human IL-4	rhIL-4	Peprotech	200-04	- 80ºC
Recombinant Human IL-10	rhIL-10	Peprotech	200-10	- 80ºC
Lipopolysaccharide *E. coli* K12 (Ultrapure)	LPS	InvivoGen	Tlrl-peklps	- 80ºC

3.2 METHODS

3.2.1 Isolation of peripheral blood mononuclear cells (PBMC) from buffy coat

Reagents and solutions

- Lymphoprep™ (Progen, Cat. # 1114545; Heidelberg, DE)
- DPBS $^{-/-}$ (Gibco, Cat. # 14190-144)
- Fetal bovine serum (FBS), (BioWest, Cat. # S181BH-500)
- Trypan Blue Stain (0.4%) (Invitrogen, Cat. # T10282)

Buffy coats were obtained from the Blood bank at Oslo University Hospital, Ullevål, and approved for use by the Norwegian Regional Committee for Medical and Health Research Ethics, REK no. 2019/113.

Procedure:

1. Blood from buffy coats were diluted in an equal volume of PBS containing 2% FBS and mixed by inversion before gently layered on to recommended volumes of Lymphoprep™ in 50 mL falcon tubes. One buffy coat (approximately 55 mL) was typically divided into 4x 50 mL tubes; each tube containing 15 mL PBS with 2% FBS before the mixture was layered on 15 mL Lymphoprep™.
2. The tubes were then centrifuged at 800 g for 20 min at room temperature (RT), in a fixed-angle Beckman Model TJ-6 centrifuge, with brakes off, to achieve density gradation. The upper layer containing plasma and platelets was carefully drawn off leaving the mononuclear cell layer at the interface of plasma and Lymphoprep™ undisturbed.
3. Next, the layer of mononuclear cells was transferred into a sterile 50 mL centrifuge tube and washed twice with 20-30 mL $DPBS^{-/-}$ by centrifugation at 400 g for 7 min at RT to remove any contaminating platelets, plasma and Lymphoprep™.
4. Supernatant was removed with a 25 mL pipette to avoid disturbing the loose pellet.
5. The isolated mononuclear cells were then resuspended in approximately 10 mL $DPBS^{-/-}$ containing 2% FBS before being sifted through a 30 µm pre-separation filter to remove cell clumps and debris. Filter was pre-wet with 1 mL $DPBS^{-/-}$ before use.
6. Cell count and viability analysis were done manually using Trypan blue exclusion method on Glasstic® microscopic slides.

3.2.2 Cell counting

Reagent

- Trypan Blue Stain (0.4%), (Invitrogen, Cat. #: T10282)

Procedure:

To determine the number of viable cells, a portion of the cells in suspension was stained with Trypan Blue and counted manually under a light microscope. This method is based on the theory that live (viable) cells with intact cell membranes do not take in certain dyes, whereas cells which have lost membrane integrity, dead (non-viable) cells, do.

1) A 1:1 mixture of the cell suspension and trypan blue was prepared by adding 10 µL of cell sample to 10 µL of 0.4% trypan blue and thoroughly mixed by gently pipetting.

2) Cells were counted within 5 min of mixing by loading 10 µL of the mix into each chamber of the Glasstic® microscopic slide (KOVA, Cat. #: 87144), using a micropipette. Loading was done through the cutout notch.
3) Counts were performed in duplicate for each sample, starting with chamber 1 of the slide under a 40× objective according to the manufacturer's standard methodology (218,219)
4) Specifically, the number of cells in each of the four corner small grids/quadrants (denoted A, B, C, D) were counted – separate counts were kept for viable (unstained) and non-viable (stained) cells.
5) Next, the average of these four readings was multiplied by $9x10^4$ (multiplication factor); to obtain the number of cells per mL in the sample applied. The result was then multiplied by two, to take into account the 1:1 dilution of the sample in the trypan blue. This was finally multiplied by any dilutions in the original sample preparation of the cell suspension.
6) Number of cells (Viable or non-viable) in the sample:

$$= \frac{(A + B + C + D)}{4} x\ 9(10^4)\ x\ 2\ x\ sample\ dilution$$

7) The percentage of viable was calculated as:

$$\%\ Viable\ cells = \frac{Number\ of\ viable\ cells}{Total\ number\ of\ cells}\ x\ 100$$

3.2.3 Monocyte isolation by magnetic beads conjugated with anti-CD14 antibody

Reagents and solutions

- 0.5 M EDTA (Thermo Fisher, Cat. # AM9260G)
- FBS (BioWest, Cat # S181BH-500)
- $PBS^{-/-}$ (made in-house)
- MACS buffer: $PBS^{-/-}$ +10% FBS +1% EDTA
- CD14 MicroBeads (Miltenyi, Cat. # 1300-502-01)

Monocyte isolation was done by positive selection using magnetic-activated cell sorting (MACS) technology. An isolation (MACS) buffer was prepared with PBS containing 10% FBS and 1% EDTA, then later degassed under vacuum to remove air bubbles that could block the magnetic columns. MS

columns were used if the number of mononuclear cells was below 1x 10^8, if not LS columns were used to sort out monocytes labelled with anti-human CD14 antibodies (CD14 MicroBeads).

Procedure:

1. The PBMCs (isolated as described in 3.2.1) to be separated was resuspended in cold MACS buffer before CD14 MicroBeads was added as follows: 80 µL MACS buffer plus 20 µL CD14 MicroBeads per 1x 10^7 PBMCs. (The volumes of MACS buffer and MicroBeads were adjusted appropriately with cell number according to the protocol from the manufacturer).
2. The cell suspension with beads was uniformly mixed by vigorously vortexing for 20 secs, then incubated for 15 min in the fridge (2-8 °C).
3. Next, the cell mixture was washed by adding 1-2 mL of cold MACS buffer per 1x10^7 cells and centrifuged at 400 g for 7 min at 4°C to remove any excess of unbound beads.
4. The pellet was then resuspended in 500 µL of MACS buffer per 1x 10^8 cells for use in MS columns or 3 mL MACS buffer per 1x 10^9 cells in LS columns: scaling up the buffer volume accordingly with increased numbers of cells.
5. A column was placed on a magnetic separator (MS columns: OctoMACS, Miltenyi #130-042-109; LS columns: QuadroMACS, Miltenyi #130-090-976) and rinsed with 500 µL or 3 mL of MACS buffer for either MS or LS column, respectively.
6. The cell suspension was applied to the column and non-adherent cells washed away thrice with 500 µL (MS) or 3 mL (LS) MACS buffer, adding new buffer to the column only when previous one had been eluted.
7. The column was removed from the magnetic separator after final washing step and magnetically labelled cells were immediately flushed out with 1 mL (MS) or 5 mL (LS) MACS buffer, using a plunger provided in the kit.
8. The purified monocytes were counted using trypan blue exclusion method on Glasstic® microscopic slides.
9. An aliquot of cells was then prepared to check for cell purity by staining with anti-human CD14 antibody, followed by flow cytometry, as described in the immunostaining protocol in section **3.2.5**
10. Remaining cells were differentiated in the presence of either GM-CSF or M-CSF cytokine, detailed in the next section, or pelleted by centrifugation at 400 g for 7 min, 4° C before cryopreservation.

3.2.4 In vitro differentiation of human monocyte-derived macrophages

Reagents and solutions

- Recombinant human GM-CSF (r*h*GM-CSF): used at 50 ng/mL (Peprotech, Cat. # 300-03)
- Recombinant human M-CSF (r*h*M-CSF): used at 50 ng/mL (Peprotech, Cat. # 300-25)
- RPMI: RPMI 1640 w/ L- Glutamine: (Biowest, Cat. # L0500-500)
- Growth medium for moDMs: RPMI + 10% FBS + 1% Pen/Strep
- Detachment buffer (50 mL): 45ml $PBS^{-/-}$ + 5 mL FBS + 250 µL of 0.5M EDTA.
- Flow buffer (FB): $PBS^{-/-}$ + 10 % FBS

Procedure:

Day 0: Culture of monocytes

1. Purified monocytes freshly isolated or thawed were resuspended in growth medium consisting of RPMI 1640 w/ L-Glutamine, 10% FBS, and 1% Pen/Strep.
2. Cells were seeded at a density of 3.0 x 10^6 into a 10 cm non-treated tissue culture dish containing 10 mL growth medium.
3. Either cytokine was added to the growth medium to attain a final concentration of 50 ng/mL of fresh GM-CSF or M-CSF, which will ultimately generate GM-CSF or M-CSF moDMs, respectively.
4. Culture dishes were then incubated at 37 °C and 5% CO_2.

Day 3: Replenishing culture media and cytokines

5. Half (5 mL) of the medium per culture dish was removed into a clean 15 mL Falcon tube and centrifuged at 400 g for 7 min at RT.
6. The supernatant was discarded, and the cell pellet resuspended in 5 mL of fresh growth medium, then combined with the remaining cells in the culture dish.
7. Fresh r*h*GM-CSF or r*h*M-CSF was added to the culture medium to a final concentration of 50 ng/mL of newly added cytokines (as on day 0), for GM-CSF and M-CSF cultures, respectively.
8. Culture plates were incubated at 37°C and 5% CO_2 for 3 days.

Day 6: Macrophage polarization

9. All culture media was removed from each culture dish and replaced with 10 mL fresh growth medium, brought to room temperature.

10. Polarizing cytokines were added to the cultures (experimental conditions) and the cells incubated at 37 °C and 5% CO_2 for 24 hours at the following conditions:
    - IFN-γ: 40 ng/mL
    - LPS: 100 ng/mL
    - IFN-γ + LPS: 40 ng/mL + 100 ng/mL, respectively
    - Untreated: Control

Day 7: Cell harvesting

11. Polypropylene centrifuge tubes (Corning® 50 mL) were pre-coated with FBS by adding 1 mL serum to the wall of the tube and tube swirled to enable serum to coat the inner surface uniformly.
12. The serum-coated tubes were then placed on ice.
13. Culture medium from the dish was removed into the pre-coated centrifuge tubes (each condition in a new tube).
14. Next, 5 mL detachment buffer (detailed above) – used at RT was added to the culture plates and incubated at 37 °C for 30 min.
15. After incubation, the plates were observed under the microscope to check for rounded up cells.
16. Detached cells were harvested by pipetting up and down (about 5 times) and were combined with the cells in centrifuge tubes then place back on ice.
17. Following this, 5 mL detachment buffer was added to each culture plate and the few adherent cells remaining (approximately 10% of the cultured cells) were gently scraped using a cell scraper (TPP©, Cat. # 99002).
18. Scraped cells were collected, and the plates were finally rinsed with 2 mL detachment buffer and later combined with the harvested cells in the serum-coated centrifuge tubes.
19. Cell count was determined by trypan blue exclusion method.
20. Next, tubes containing harvested cells were centrifuged at 400 x g, 4 °C for 7 min.
21. All supernatant was removed, and the cell pellet was resuspended in 1 mL flow buffer
22. Cells were counted after resuspension in the flow buffer.

3.2.5 Immunophenotyping by flow cytometry

A. Immunostaining for cell-surface markers

Reagents and solutions

- Flow buffer: containing $PBS^{-/-}$ + 10% FBS (BioWest)
- Specific mAb see Table 4.
- Isotype-matched control mAb, see Table 4.
- Blocking agent: Human TruStain™ FcX; BioLegend, # 422301; San Diego (CA), USA or mIgG; Sigma-Aldrich, # I8765, Darmstadt, Germany).
- Propidium iodide (PI; BioLegend, # 421301; San Diego (CA), USA)

Procedure:

Harvested cells were prepared into single cell suspension in the flow buffer and incubated on ice for at least 15 min. The antibody mixes were made immediately prior to use and were kept in light protective (amber) microcentrifuge tubes on ice. Cell surface immunostaining was done in 96 well cell culture plates with V bottom, in a total volume of 50 µL per well. Concentration- and isotype-matched control antibodies were used to determine the level of background caused by non-targeted binding of antibodies and to help set the threshold for positive staining. All steps of the immunostaining procedure were performed on ice and with ice-cold buffers, unless otherwise stated.

1. Cell suspension was divided into 96 V-bottom well plate, with approximately 2.0 x 10^5 cells per well and pelleted by centrifugation at 400 g, 4 °C for 7 min.
2. Cells in each well were then resuspended in a blocking solution before incubation on ice for 30 min; Fc receptor blocking solution contained 50 µL flow buffer with 25 µg/mL FcX or mIgG.
3. After blocking, cells were centrifuged at 400 g, 4°C for 7 min and the pellet was resuspended in 50 µL flow buffer containing the required volume of staining antibody or isotype-matched control in each well. (**Tables 4** and **5**).
4. An additional cell sample, which was resuspended in only 50 µL flow buffer was also prepared as an unstained sample and negative control.
5. Cells were incubated in the dark, at 4 °C for 20 min.
6. Next, cells were washed twice in flow buffer by centrifuging for 7 min, at 400 g, 4 °C, and supernatant tossed off.

7. Cell pellet was resuspended in 200 µL flow buffer, transferred into flow cytometry tubes and kept on ice in the dark.
8. Cells were later stained with 6.25 µg/mL Propidium iodide right before acquisition on BD LSRFortessa™ flow cytometer.
9. Data obtained on BD LSRFortessa was further analyzed using FlowJo v10 10.7.1 (FlowJo, LLC, Ashland, OR).

B. Preparation of beads for fluorophore compensation

eBioscience™ UltraComp eBeads (Invitrogen, Cat. # 01-2222-42; Carlsbad (CA), USA) were used to adjust for spectral overlap in cases where several fluorophores were mixed in samples. Prior to data acquisition, 1 drop of eBeads was used per 500 µL flow buffer consisting of $PBS^{-/-}$ with 10% FBS, divided to match the number of fluorophores used, then incubated with 2.5 µL of antibodies per 100 µL of flow buffer for 5 min on ice and in the dark.

Table 4. List of primary detection antibodies and isotype-matched control antibodies.

Specificity	Fluorochrome	Clone	Cat. No.	Company	Isotype	Clone	Cat. No.
CD14	APC/Cy7	HCD14	325620	BioLegend	Mouse IgG1, k	MOPC-21	400128
HLA-DR	BV605	L243	307640	BioLegend	Mouse IgG2a, k	MOPC-173	400269
CD11c	Pacific Blue™	3.9	301626	BioLegend	Mouse IgG1, k	MOPC-21	400151
CD86	APC	IT2.2	305412	BioLegend	Mouse IgG2b, k	MG2b-57	401210

Table 5. Antibody volumes and concentrations

Antibody/matched- Isotype control		Stock concentration of mAb (µg/mL)	Volume of Antibody in 200 µL FB	Final Ab. Conc. in 50 µL FB (each well)
Antibody	HLA-DR	100	5µL	2.5µg/ mL
Isotype	mIgG2a, k	100	5µL	2.5 µg/ mL
Antibody	CD14	400	5µL	10 µg/ mL
Isotype	mIgG1, k	200	10µL	10 µg/ mL
Antibody	CD11c	400	5µL	10 µg/ mL
Isotype	mIgG1, k	200	10µL	10 µg/ mL
Antibody	CD86	200	5µL	5 µg/ mL
Isotype	mIgG2b, k	100	10µL	5 µg/ mL

Table 6. Antibody volumes and concentrations used for experiment described in Figure 8

Antibody/matched- Isotype control		Stock concentration of mAb (µg/mL)	Volume of Antibody in 200 µL FB	Final Ab. Conc. in 50 µL FB (each well)
Antibody	HLA-DR	100	10 µL	5 µg/ mL
Isotype	mIgG2a, k	100	10 µL	5 µg/ mL
Antibody	CD14	400	10µL	20 µg/ mL
Isotype	mIgG1, k	200	20µL	20 µg/ mL
Antibody	CD11c	400	10µL	20 µg/ mL
Isotype	mIgG1, k	200	20µL	20 µg/ mL
Antibody	CD86	200	10µL	10 µg/ mL
Isotype	mIgG2b, k	100	20µL	10 µg/ mL

3.2.6 Cryopreservation of cells

Reagents:

- Dimethyl sulfoxide (DMSO; VWR, Cat. # 0231)
- Freezing medium: FBS + 10% DMSO

Procedure:

1. For long term preservation, cells were pelleted by centrifugation at 400 g, 4 °C for 7 min, and live cell count determined by trypan blue exclusion method.
2. Next, cells were resuspended in a small volume of FBS and cooled on ice for approximately 15 min and were later resuspended to 1-2 x 10^7 cells/mL in freezing medium and aliquoted into Nunc™ CryoTube vials.
3. Cryo vials were labelled appropriately and pre-cooled at -80 °C for 24 hours in a Nalgene™ Mr. Frosty Cryo 1°C freezing container (ThermoFisher, # 5100-001; Rochester (NY), USA)
4. Vials containing cells were then relocated into a -150 °C freezer or liquid nitrogen tank for indefinite preservation.

3.2.7 Thawing of preserved cells

Reagents and solutions:

- Complete RPMI medium: RPMI 1640 w/ L- Glutamine + 10% FBS + 1% Pen/Strep

Procedure:

1. Complete RPMI medium was pre-warmed and cryovial containing cells rapidly thawed in a 37 °C water bath (until about 20% ice remained).
2. Cells were quickly transferred into a 15 mL falcon tube containing 10 mL pre-warmed complete RPMI medium (10 times volume of thawed sample) and washed twice, each in 10 mL medium by centrifuging at 400 g for 7 min, RT.
3. Supernatant was completely aspirated, and cells resuspended in fresh RPMI medium.
4. An aliquot was taken to determine live cell count by trypan blue exclusion method. Remaining cells were allocated for cell culture, immunostaining, or further analysis.

3.2.8 Stimulation of human monocyte-derived macrophages with fungal polysaccharides

Reagents:

- RPMI 1640 w/ L-Glutamine
- Activating fungal polysaccharides, see Table 6
- PRR ligands, see Table 7
- Recombinant human IFN-γ (Peprotech, Cat. # 300-02)

Procedure:

1. Cells were harvested on day 6 of *in vitro* differentiation of monocyte-derived macrophages as described in harvesting method (section **3.2.4**)
2. Cells were pelleted by centrifuging at 400 g for 7 min, RT then resuspend in 5 mL RPMI medium supplemented with 10% FBS, without antibiotics.
3. Live cell count was determined, and 1 x 10^5 cells were plated in 150 µl medium per well in a 48-well flat-bottom tissue-culture treated plate.
4. Cells were made to attach by incubating at 37°C for 2 hours, then stimulated for 24 hours by adding 150 µl fresh RPMI media with 10% FBS, supplemented with selected fungal polysaccharides; with or without IFN-γ at 37°C, 5% CO_2. See **Tables 7** and **8** for activating polysaccharides and PRR ligands used as controls, respectively.
5. After 24 hours, culture media were collected into a V-bottomed 96-well plate and spun down at 1000 g for 15 min at 4°C, to remove cellular debris.
6. Next, supernatant was transferred into a new V-bottomed 96-well plate and centrifuged again at 1000 g for 15 min at 4°C.
7. Supernatant was then collected and divided into 2 new V-bottomed/round-bottomed 96-well plates: with each well containing approximately 130 µl supernatant.
8. Samples were stored at -80 °C for a maximum of 8 days until cytokine analysis by magnetic Luminex® technology.

Table 7. Isolated polysaccharides from I. obliquus and their chemical properties.

Polysaccharide fraction	Abbreviation	Water solubility	Molecular Weight (kDa)	pH sensitivity	Concentration (µg/mL)
IOI-WN	IWN	High	60	Neutral	100
IOE-WN	EWN	High	73	Neutral	100
IOI-WAcF1	AcF1	High	28	Acidic	100
IOI-WAcF2	AcF2	High	14	Acidic	100
IOI-WAcF3	AcF3	High	10	Acidic	100
IOI-A1	A1	Non soluble	>450	Alkaline	100

Abbreviations/names: IOI = I. obliquus Interior part; IOE = I. obliquus Exterior part; WN = Water-extracted, Neutral; WAc = Water-extracted, Acidic; F1-F3 = Fraction 1-3; A1 = Alkaline-extracted polysaccharide 1. (Wold et. at, 2018).

Table 8. Pattern recognition receptor (PRR) ligands and cytokines used as controls in the stimulation of human monocyte-derived macrophages for cytokine quantification assay.

Ligand	Abbreviation	Target	Concentration	Cat. No.	Provider
Pam3CysSerLys4	Pam_3CSK_4	TLR1/2	100 ng/mL	tlrl-pms	InvivoGen
Lipopolysaccharide *E. coli* (Ultrapure)	LPS	TLR4	100 ng/mL	tlrl-peklps	InvivoGen
Lipoteichoic acid *(S. aureus)*	LTA	TLR2/6	100 µg/mL	tlrl-pslta	Sigma-Aldrich
Zymosan crude *(S. cerevisiae)*	ZymC	TLR2, Dectin-1	100 µg/mL	Z4250	Sigma-Aldrich
Zymosan purified *(S. cerevisiae)*	ZymP	Dectin-1	100 µg/mL	tlrl-zyd	InvivoGen
Laminarin *(L. digitata)*	Laminarin	Dectin-1	100 µg/mL	L9634	Sigma-Aldrich
Recombinant Human IFN-γ	r*h*IFN-γ	IFN-γR	40 ng/ mL	300-02	Peprotech

3.2.9 Cytokine quantification using Magnetic Luminex® technology

Reagents, solutions, and buffers

- Standard (Bio- Rad, # 12007919)
- Standard diluent (Bio- Rad, # 9703888)
- Bio-Plex Pro® Human magnetic beads 10x (Bio- Rad, # 10043482)
- Bio-Plex Detection Antibody Diluent HB (Bio-Rad, # 10032400)
- Assay buffer (Bio- Rad, # 9723892)
- Streptavidin-PE concentrate (Bio- Rad, # 171304501)
- Deionized/ distilled water (Made in-house)
- Human TNF- α detection antibody 10x (Bio- Rad, #171B5026M)
- Human IL-6 detection antibody 10x (Bio- Rad, # 171B5006M)
- Human 12p70 detection antibody 10x (Bio- Rad, # 171B5011M)

Procedure:

Flat-bottom, 96-well Bio-Plex Pro® plates (Bio-Rad, #171-025001) were used for Magnetic Luminex® assays. All reagents and buffers were brought to RT before use and the entire procedure was performed at RT unless otherwise mentioned. Plates were covered with aluminum plate sealers (Bio-Rad # 1814045) during every incubation, to protect the samples from light. Hand-held magnetic washer (Bio-Rad, #170-20100) was used to secure microparticles during washing, and the plates were left to stand for 1 min after each wash before the washing solution was tossed off, to prevent loss of beads. Polypropylene test tubes (Corning®) were used for dilution of standards and samples. Very importantly, half volumes of magnetic beads, detection antibodies and PE recommended by the manufacturer were used and dilutions were prepared just prior to the start of the assay.

1. Harvested supernatants, previously frozen, were thawed at RT and centrifuged at 16,000 x g for 4 min immediately prior to use, to further eliminate cell debris.
2. A single vial of standards provided by supplier was reconstituted by mixing the volume in vial in 500 µL of deionized water.
3. Next, a fourfold standard dilution series and blank was prepared to obtain a 9-point standard curve.

4. This was done by labelling nine 1.5 mL polypropylene tubes: S1 – S8 and the last tube labelled as blank, then 150 µL of deionized water was added to tubes S2 – S8 and blank, with 72 µL in S1.
5. Reconstituted standard was then vortexed for 5 secs then 128 µL was transferred to the S1 tube, containing 72 µL of the diluent, then mixed by vortexing.
6. With a new pipette tip, 50 µL was transferred from the S1 tube to S2 tube then vortexed for 5 secs. The 1:4 (fourfold) serial dilution was continued to S8.
7. Next, coupled beads dilution was prepared by first vortexing the 10x stock for 30 secs before pipetting 288 µL of beads into 2.8 mL assay buffer in a 15 mL polypropylene tube, then vortexed again for 30 secs.
8. After vortexing, 25 µL of the diluted coupled beads was added to each well of the assay plate.
9. Next, the plate was secured to a Bio-Plex® hand-held magnetic washer and washed by adding wash buffer (100 µL PBS + 1% Tween®) per well, then left to stand for 1 min before tossing off liquid. Washing was done twice.
10. Premixed standards, sample, and blank were vortexed for 30 secs and added to the assay plate by transferring 25 µL of each to the appropriate well, changing pipette tips between transfers.
11. The plate was then sealed and incubated for 1 hour at RT on a horizontal orbital microplate shaker at 800 ±50 rpm to mix.
12. Next, the plate was secured to a Bio-Plex® hand-held magnetic washer and left to stand for 1 min before tossing off liquid.
13. The plate was then removed from the magnetic washer and washed, as described in step **9**. repeated 3 times.
14. Detection antibody cocktail was prepared by diluting 150 µL of the 10x stock in 1.5 mL of antibody diluent.
15. Next, 12.5 µL of the diluted antibody cocktail was dispensed into each well of the assay plate using a multichannel pipette.
16. Plate was covered and incubated for 30 min at RT on the microplate shaker, as above.
17. Washing steps were repeated after incubation, as described in step **9**.
18. Streptavidin-PE, was diluted by mixing 30 µL, in 3 mL assay buffer, and 25 µL was added to each well before incubation on the microplate shaker for 10 min at RT.

19. The washing procedure described in step **9** was repeated three times before the beads were resuspended in 125 µL assay buffer per well, followed by incubation on the microplate shaker for 60 secs.
20. Following this, the cytokine concentrations were determined by Bio-Plex® MAGPIX™ Multiplex Reader; microparticles were resuspended again immediately prior to reading.
21. Samples were analyzed in duplicates.

3.2.10 Isolation and differentiation of bone marrow-derived macrophages

Reagents:

- $DPBS^{+/+}$ (Sigma-Aldrich, Cat. # D8662)
- FBS (Biochrom GmbH, Cat. # S0113)
- $PBS^{-/-}$ (Made in-house)

Procedure:

Bone marrow from mice was differentiated into macrophages by use conditioned medium containing macrophage colony-stimulating factor (M-CSF). The conditioned medium was generated by culturing L929 cells (Cell Lines Service, Cat. # 400260) in RPMI 1640 medium with L-Glutamine containing 10 % FBS (S0113, Biochrom GmbH, Berlin Germany). When the L929 cells had reached confluency, the cells were cultured for 10 more days, before the conditioned medium was collected from the L929 cells, centrifuged, filtered, and stored at -20 °C, and was used for the differentiation and maintenance of bone marrow-derived macrophages (BMDMs).

1. Femurs and tibiae of the hind legs from 8- to 12-week-old C57BL/6NRj mice were harvested and the marrows flushed with RPMI 1640 medium containing 10 % FBS. The procedure was performed under sterile conditions.
2. Bone marrow cells were then filtered through a cell strainer with 70 µm pores (Sigma-Aldrich, Cat. # CLS431751).
3. Cells were cultured in 10 cm non-tissue culture treated dishes in RPMI medium with L-Glutamine containing 10 % FBS, 1 % P/S and 30 % L929-derived conditioned medium.
4. After 5 days of culturing, non-adherent cells were washed off using $DPBS^{+/+}$
5. Adherent macrophages were further cultured for 2 days.

6. Macrophages were then harvested from the dishes after incubation with ice-cold $PBS^{-/-}$ for 20 min at 4°C.
7. Detached macrophages were then flushed off plates by pipetting up and down several times.
8. Cell count was determined, and 1 $x10^7$ cells aliquoted into each vial before cryo-preservation.
9. The purity of the cells as analyzed by flow cytometry, using the macrophage markers CD11b (M1/70, BioLegend) and F4/80 (BM8, BioLegend), was 99 % and the cells were then referred to as bone marrow derived macrophages (BMDMs).

3.2.11 Subculture of Lewis lung carcinoma (LLC) cells

Lewis lung carcinoma (LLC, also called LLC1) is a cell line originating from a spontaneous lung carcinoma in a C57BL/6 mouse and was obtained from CLS Cell Lines Service (Eppelheim, Germany).

Procedure:

1. One vial (approx. 5 x 10^6 cells; passage #34) was thawed and seeded into a T175 cell culture flask containing 35 mL fresh growth medium (RPMI 1640 with 10% FBS and 1% Pen/Strep).
2. The cell culture was split in a ratio 1:4 or 1:6 (depending on the growth rate) in a new flask every 1-2 days; to avoid cell clusters.
3. Cells were cultured for 10 days before harvesting.
4. On day 10, cells were collected by removing half of the medium and adherent cells scraped gently with a cell scraper before the flask was rinsed with 10 mL $DPBS^{-/-}$.
5. Next, cell washing was done twice by centrifugation at 400 g, 4 °C for 7 min and cell viability obtained by trypan blue exclusion method. The cell concentration was adjusted to $1x10^6$ cells/mL in $DPBS^{-/-}$ before being used in the experiment described below.

3.2.12 *In vivo* experiments using a Mouse model

Reagents and solutions:

- FBS (Biochrom GmbH, Cat. # S0113)
- $DPBS^{-/-}$ (Gibco, Cat. # 14190-144)
- Activating factors, see step 2

C57/BL-6 mice from Janvier Labs (Le Genest-Saint-Isle, France) were in house bred at the Department of Comparative Medicine, Oslo University Hospital, Rikshospitalet (Oslo, Norway). The research project was approved by the Norwegian National Committee for Animal Experiments (approval number 20/102031) and all the performed experiments conform with the national regulations and the EU directive 2010/63/EU. The Winn assay was used for the co-injection experiments.

Procedure:

1. One vial of BMDM (1 $x10^7$ cells) was thawed and plated in 5 non-tissue culture treated-petri dishes (10 cm) for 3 days in RPMI with 10% FBS and 10% L929 conditioned medium (=complete medium).
2. On day 3, the BMDMs were activated by carefully aspirating media and adding fresh complete medium (8-10 mL per dish) containing the activating factors in the concentrations indicated below. The BMDMs were cultivated with the factors for 24 h.
    a. 100 µg/mL AcF1 + 20 ng/mL IFN-γ
    b. 100 µg/mL AcF3 + 20 ng/mL IFN-γ
    c. 100 ng/ mL Pam_3CSK_4 +20 ng/mL IFN-γ
    d. 20 ng/mL IFN-γ
    e. No treatment (control)
3. BMDMs were harvested on day 4 by aspirating media and adding cold $PBS^{-/-}$, cell count was determined and adjusted to 15 $x10^6$ cells /mL in $DPBS^{-/-}$
4. Pre-cultured LLCs were harvested, and washed with $DPBS^{-/-}$, and the cell count adjusted to $1x10^6$ cells/mL in $DPBS^{-/-}$ as described in 3.2.11.
5. All harvested cells were stored in $PBS^{-/-}$ on ice for minimum 30 min.
6. Equal volumes of LLCs and BMDMs were mixed (1 mL from each), to obtain a 15:1 ratio of BMDMs: LLCs, and the tubes were stored on ice.
7. 100 µL of each condition mixture was injected subcutaneously on the left flank of the mice.

8. Tumor growth was monitored using a caliper every other day until humane end points were reached (15 mm in tumor diameter), and the animals euthanized by cervical dislocation.
9. Tumor growth was calculated using the formula: Tumor Volume (mm^3) = [$width^2$ x length] x 0.4 (220).
10. Mice in 'No treatment' and Pam_3CSK_4 groups served as negative and positive controls, respectively.

3.2.13 Statistical analysis

Statistical analysis was conducted using the GraphPad Prism 8.1.1 software (GraphPad). Values from control samples were used as a reference to each individual value, unless otherwise stated. The data were analyzed using one-way ANOVA test to generate P-values, or using two-way ANOVA followed by Sidak's test for comparison of multiple samples. Threshold of significance was set at $p<0.05$.

4 RESULTS

4.1 Monocyte isolation from Peripheral Blood Mononuclear Cells (PBMCs)

Monocytes were isolated from fresh buffy coats obtained from the Oslo University Hospital blood bank; this provided a valuable source of concentrated leukocytes as two buffy coats (2 x 55 mL) yielded up to 400 million PBMCs. Subsequent purification by positive selection using CD14 MicroBeads is one of the established quick and optimal purification methods (221). With this positive immunoselection strategy (MACS sorting with CD14 antibodies), we obtained over 100 million purified monocytes. Freshly isolated monocytes were used to generate monocyte-derived macrophages or cryopreserved for later use.

The gating strategy used to verify purity of isolated CD14+ monocytes from PBMCs of healthy donors is indicated as follows: mononucleated cell gate was first set using side scatter (SSC) vs forward scatter (FSC) parameters to remove debris from all recorded events. SSC provides information on the granularity or internal complexity of the events recorded, whereas FSC is used to assess the size of each event. In the FSC vs SSC plot, two distinct populations were observed: one cluster (smaller population) had events below 20K and 50K on the FSC and SSC scales, respectively. These events were excluded as debris since they were too small to be cells and the remaining (larger) population with FSC-A events above 50 K were gated as cells (**Figure 5A)**. Next, cells were gated in a single cell gate, using FSC-Height (FSC-H) and FSC-Area (FSC-A) as parameters to exclude doublets and cell clumps. Due to the linear correlation between these parameters on a density plot, single cells appear along the diagonal of the FSC-H/FSC-A plot, allowing single cells to be gated while doublets or clumps appearing outside the diagonal are discriminated (**Figure 5B**). From the single cell gate, dead cells which were filled up with the fluorescent dye, propidium iodide (PI), and appearing high on the PI (vertical) scale were excluded (**Figure 5C**). Single, live purified monocytes were defined as cells with CD14 expression, showing 96.1% purity (**Figure 5D**). Histograms obtained upon staining single live monocytes in (Figure 5C) with APC/Cy7-conjugated anti-human CD14 mAb (clone HCD14, BioLegend) **Figure 5E** (**blue)**. Background staining levels were detected with APC/Cy7-conjugated mouse IgG1, k mAb (clone MOPC-21, BioLegend) as an isotype-matched control **(Figure 5E, pink**). Data shown are representative of at least four successful independent experiments performed.

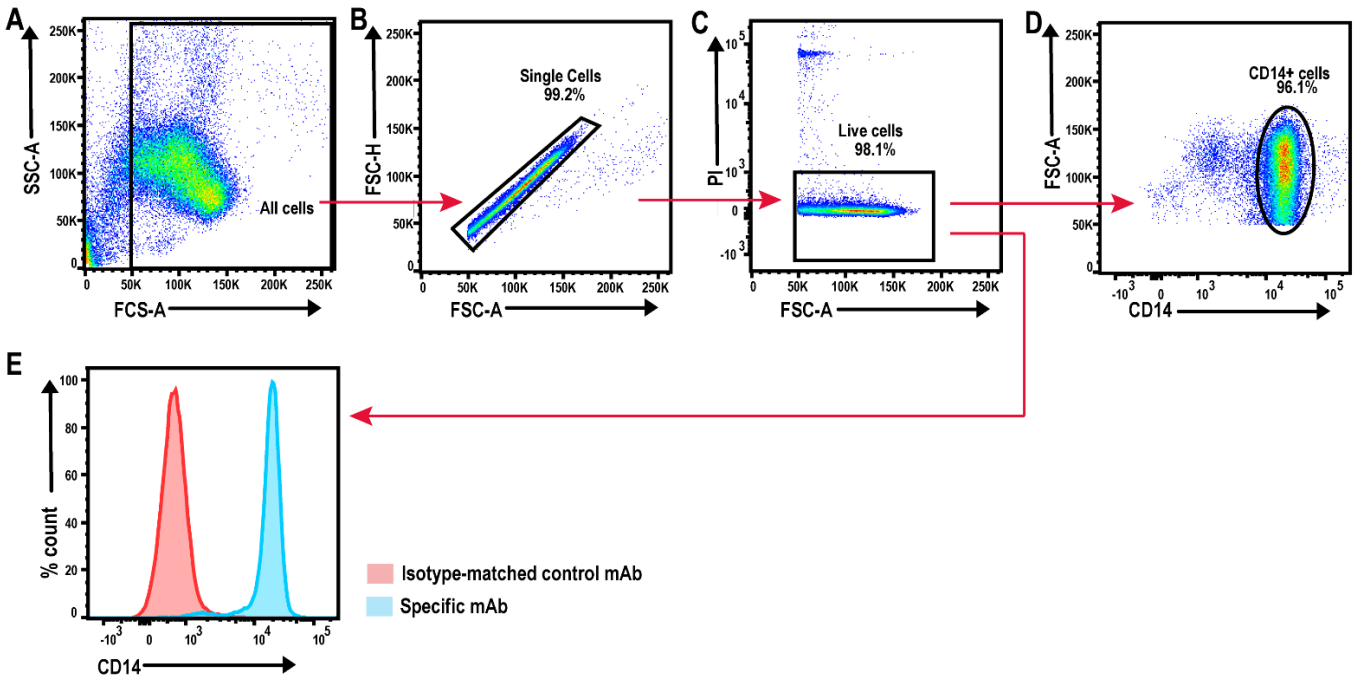

Figure 5. Verification of purified CD14+ monocytes.

*Monocytes were isolated from PBMCs by standard density gradient centrifugation with Lymphoprep™, followed by positive selection using magnetic beads conjugated to an anti-human CD14 antibody (CD14 MicroBeads®). CD14+ labelled cells were collected as monocytes and subsequently stained for flow cytometry. Percentage purity of positively selected monocytes was then verified by flow cytometry following these gating strategies: **(A)** Forward versus side scatter (FSC vs SSC) gating based on size and granularity (complexity) was used to exclude cellular debris from all events recorded; events below 50K (FSC-A) were discarded as debris. **(B)** Single cells were identified using FSC-A and FSC-H as parameters to gate out doublets. **(C)** Dead cells stained with the fluorescently active propidium iodide (PI) were excluded and **(D)** single, live cells expressing CD14 were defined as live monocytes (CD14+ 96.1%). **(E)** Histogram showing CD14 expression on single, live cell population in **C**. Data shown are representative of at least four independent experiments performed.*

4.2 In vitro differentiation of monocyte-derived macrophages (MoDMs)

Freshly isolated or thawed CD14+ cells were used in the differentiation of monocyte-derived macrophages *in vitro*. Monocytes were cultured by seeding 3 x10^6 cells into 10 cm non-tissue culture treated dishes containing growth medium (RPMI+ 10% FBS+ 1% Pen/Strep) enriched with either GM-CSF or M-CSF for six days. Many reports have indicated that monocytes can be differentiated into MoDMs without cytokines/growth factors, leading to the so-called uncommitted/M0 macrophage phenotype (195,222). A 'no cytokine' culture was differentiated simultaneously as control, per the differentiation protocol used. Cells were maintained at 37°C in a humidified 5% CO_2 atmosphere and culture medium replaced after 3 days. Monocytes (in all specific conditions) were monitored during

growth and differentiation into mature macrophages. Morphological changes observed were captured on days 3 and 6 using a phase contrast microscope (**Figure 6**), see also **Supplementary Figure 1** for morphological differences due to the choice of serum in differentiation cultures. Generally, cells remained unadhered to the culture plate following initial seeding and retained a monocytic appearance; small, amorphous for 3 days in all conditions (Figure 6, left column). At day 4-5 of culture, cells began to adhere to the plastic and morphological differences among cultures became apparent (not shown). *In vitro* differentiation of monocytes into macrophages was considered complete on day 6, where cells were observed to have tightly adhered to plastic with larger and more homogenous appearances across culture-specific conditions (Figure 6, right column). On culture day 6, cells differentiated without cytokines were noted to be well dispersed with a more rounded morphology. Additionally, they appeared homogenous with some few cells still in suspension (**Figure 6A, right column**). On the contrary, cells differentiated in the presence of GM-CSF had become larger, were more heterogenous regarding cell size and shape. Moreover, they were highly confluent and displayed an amoeboid morphology; seen as large and flattened with oval-shaped nuclei, a stark morphological difference compared to the control (**Figure 6B, right column**).

Similarly, M-CSF differentiated macrophages were uniformly adherent, appeared larger and more confluent than monocytes during initial seeding. Also, they portrayed as flat and slightly stretched-out cells similar to fibroblasts, with some spindle-like processes extending out from the ends of the cell body. Moreover, cell nuclei appeared well-defined with a flat oval shape (**Figure 6C**). The experiment was conducted 4 times and data shown are representative of three successful ones.

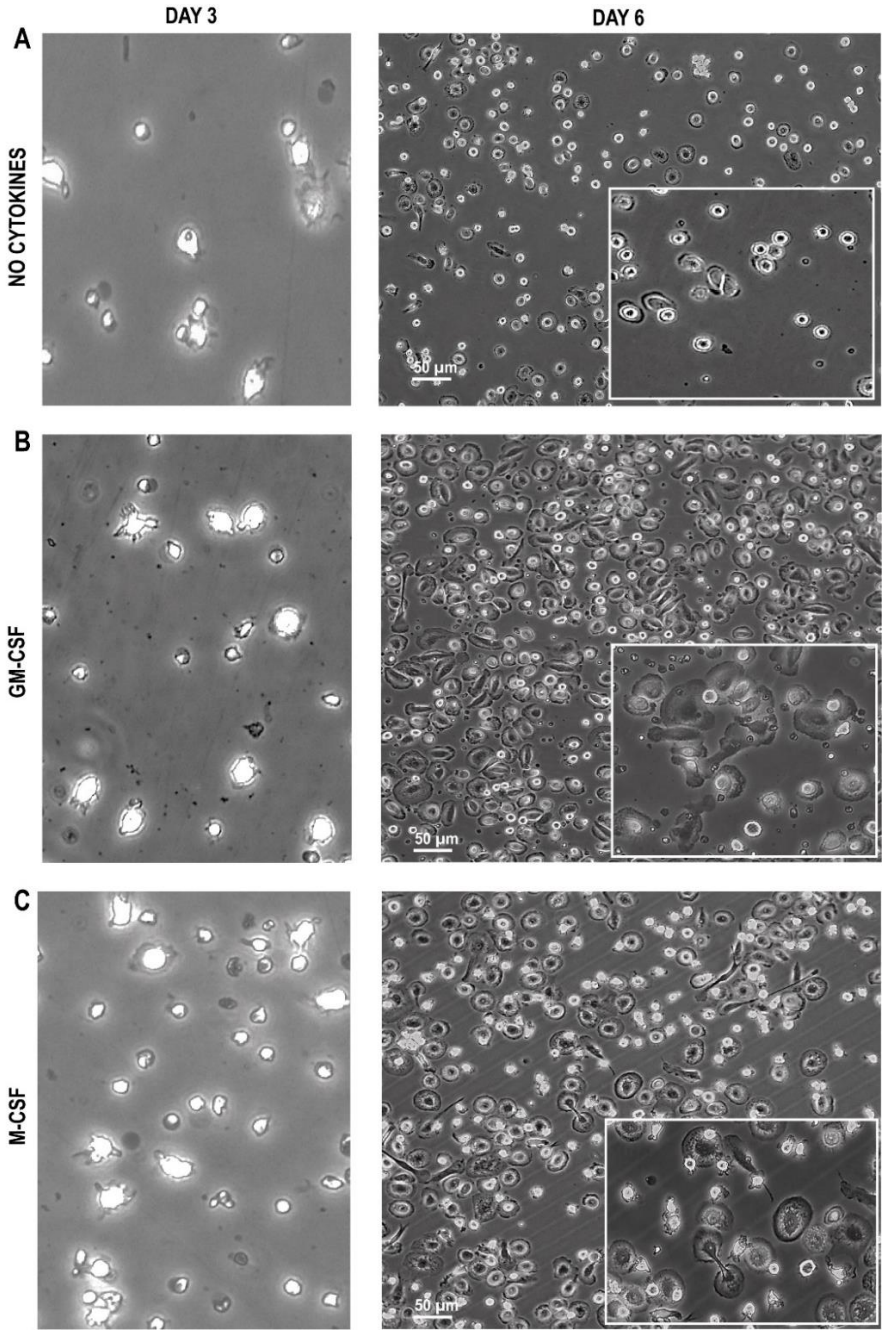

Figure 6. In vitro differentiation of monocyte-derived macrophages.

A schematic micrograph showing distinct sizes and morphologies on day 3 and 6 of thawed human monocytes differentiated into MoDMs under specific culture conditions. Cells appeared amorphous and remained largely in suspension on day 3 (left column) for all conditions. Fully differentiated macrophages appeared larger, mostly attached to the culture plate by day 6 with well-defined and generally homogenous morphology (right column). ***(A)*** *Cells differentiated without growth factors (no cytokines) were more rounded, equally sized, and less confluent compared with cytokine-differentiated cells.* ***(B)*** *Cells differentiated in the presence of GM-CSF were heterogeneous regarding cell size, but all cells appeared to have a flattened 'pancake-like' morphology, and relatively larger than the cells cultivated without cytokine.* ***(C)*** *M-CSF differentiated cells were uniformly adherent, showed a slightly stretched morphology with some spindle-like projections. The data are representative of three independent experiments. Images were captured with a phase contrast Zeiss AxioCam Mrc microscope, with original magnification at 60x. Scale bar, 50µm. Insert: enlarged image.*

4.3 Flow cytometric analysis of cell surface molecules on MoDMs.

On culture day 6, fully differentiated MoDMs were harvested by detaching tightly adherent cells from the culture dishes by 30 min incubation at 37°C in a nonenzymatic detachment buffer prepared in our lab, as described in section **3.2.4**. See **Supplementary Figure 2** for effects of different harvesting techniques on cell yield and viability. Mature MoDMs differentiated from the specific conditions: 'no cytokines', GM-CSF or M-CSF cultures were compared by analyzing the expression of typical pan-macrophage cell surface molecules using a flow cytometer. Thawed undifferentiated monocytes or freshly isolated monocytes from healthy donors were used as controls. All analyses were conducted on the day of staining and the following macrophage/monocytic lineage surface markers were examined on resting macrophages: CD14, HLA-DR and CD11c. CD14 is one of the widely used markers for the detection of myeloid lineage cells. It is a co-receptor for TLR4 and TLR2, and is constitutively expressed on the surface of monocytes, macrophages, and DCs at wide-ranging levels. HLA-DR, a human class II major histocompatibility complex (MHC) antigen is inherently expressed on monocytes and professional APCs which include macrophages, DCs, and B lymphocytes. CD11c, also known as integrin alpha X, even though a widely used defining DC marker, is also expressed on monocytes as well as macrophages. Refer to Tables 4 and 5 for lists of specific mAbs and the respective isotype-matched control mAbs used.

Cells were gated using FSC-SSC pattern by setting a size threshold at 50k on the FSC scale to exclude all events too small to be cells (**Figure 7A**). The threshold at 50k was determined by backgating the smallest events (below 50k), which were observed to be dead cells and cellular debris (not shown). From the cell gate, doublets and cell clumps were eliminated by setting a single cell gate, where FSC-H and FSC-A were used as parameters to remove all events appearing outside of the diagonal plot (**Figure 7B**). Dead cells were further excluded by staining each sample with the fluorescent dye propidium iodide (PI) right before data acquisition, and the uptake of photoactive PI by dead cells allowed gating of only live viable cells for the analysis (**Figure 7C**). The resulting population was then used for analysis (**Figure 7D**). Monocytes were used as control and identical gates were set for the 'no cytokines', GM-CSF and M-CSF differentiated macrophages. CD14, HLA-DR and CD11c expression levels were then analyzed on viable cells from resultant population in Fig. 7D.

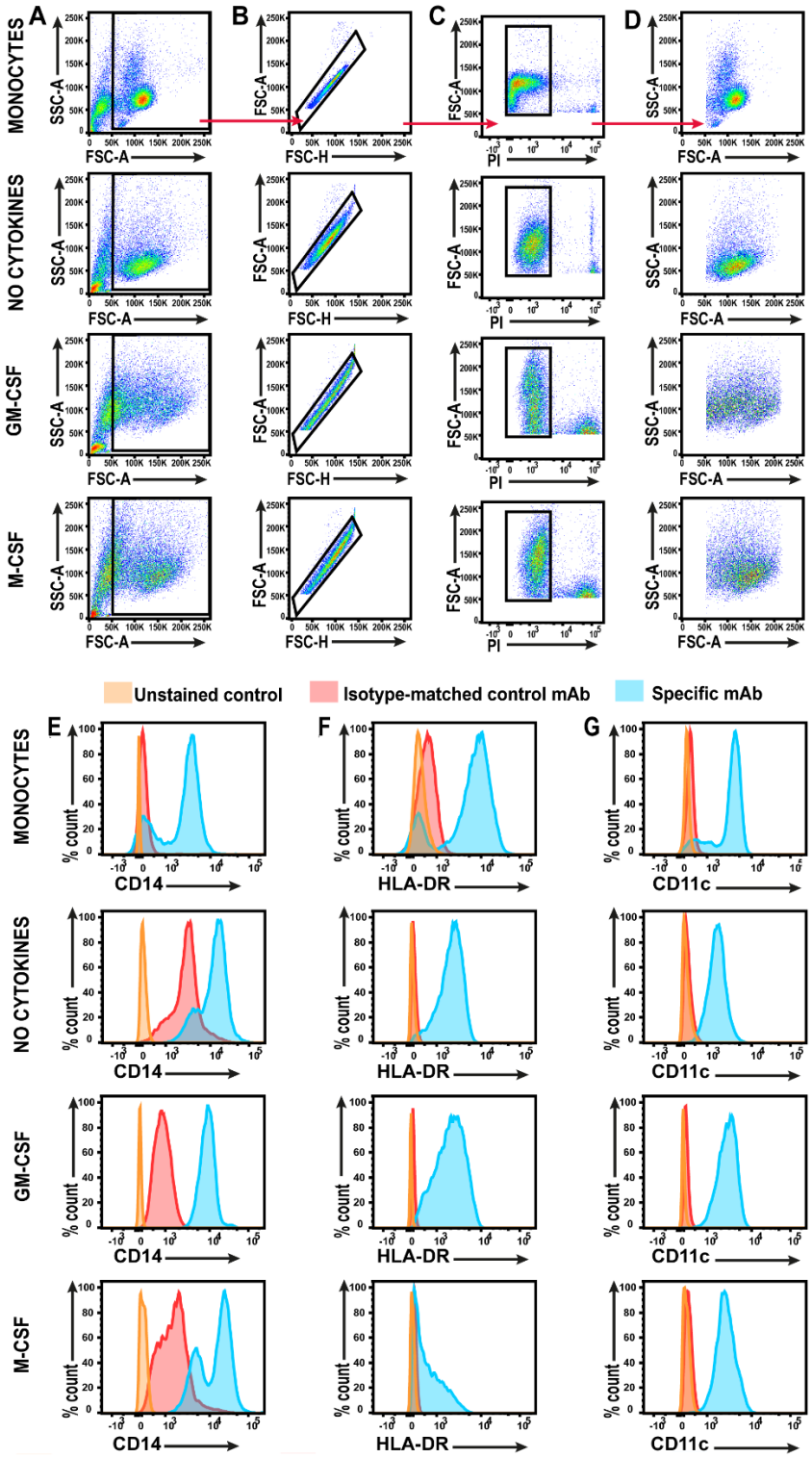

Figure 7. Surface marker expression of human monocyte-derived macrophages (MoDMs).
*MoDMs generated in the presence of hGM-CSF, hM-CSF, and culture medium (No cytokines) were analyzed by flow cytometry for typical macrophage and monocytic markers on culture day 6. (**A**) FSC vs SSC was used as a size exclusion parameter to gate out events below 50K (FSC-A). (**B**) Single cells were identified using FSC-A and FSC-H parameters, and (**C**) dead cells with high expression of propidium iodide (PI) were excluded. (**D**) Resulting population used for analysis. Monocytes were used as control and identical gates were set for the various conditions of fully differentiated macrophages. Histograms showing expression of established pan-macrophage lineage markers: (**E**) CD14, (**F**) HLA-DR and (**G**) CD11c on resting macrophages differentiated under specific culture conditions. Data are representative of 2 independent experiments.*

Overall, cell size was observed to have increased upon differentiation; a further validation of micrographs captured during culture and differentiation period (Fig. 6). Freshly isolated or thawed monocytes appeared to be the smallest, with FSC-A between 100-150K (**Figure 7A**). Macrophages differentiated without cytokines were slightly larger than undifferentiated monocytes with a wider size range around 80-170K on the FSC-A scale (Figure 7A, second row). However, both GM-CSF and M-CSF differentiated macrophages were evidently larger in size and complexity; with FSC-A between 100-200K and SSC-A around 150K (**Figure 7A**, third and fourth rows respectively). Further, CD14 expression level appeared to have increased, particularly in GM-CSF differentiated macrophages, compared to monocytes (**Figure 7E**). Meanwhile, HLA-DR expression slightly declined in GM-CSF and 'no cytokines but prominently in M-CSF differentiated macrophages (**Figure 7F**). CD11c showed a relatively similar expression level in all macrophages as well as monocytes (**Figure 7G**). The presence of a surface marker was only assumed if primary stains (blue) exceeded the levels of irrelevantly targeted isotype-matched stains (pink) and unstained (peach) controls. At least two independent monocyte/macrophage comparison experiments were performed, and similar expression patterns of all markers were observed in both.

4.4 Comparison of surface markers on Monocytes, MoDMs and MoDCs

Several *in vitro* and *in vivo* studies have reported that human monocytes can differentiate into MoDCs or MoDMs under the influence of cytokines such as GM-CSF, M-CSF and IL-4, with many overlapping phenotypic and functional characteristics among these cell types (4,5). To validate the successful *in vitro* differentiation of human CD14+ monocytes into MoDMs and MoDCs, we next compared the expression pattern of cell surface molecules on the three cell types. Again, CD14, HLA-DR and CD11c were the selected markers for analysis. MoDMs and MoDCs were harvested on culture day 6 and cell surface staining performed for flow cytometry, as previously described. See **Table 6** for list and concentration of antibodies used in this experiment. Peripheral blood monocytes previously isolated, was thawed 24 hours before staining and analysis.

Cells were gated using FSC-SSC pattern, and events below 50K on the FSC scale were discarded (**Figure 8A**). The events with a linear correlation between height and area, (FSC-A vs FSC-H) were selected as single cells (**Figure 8B**), then dead cells were removed from the analysis by excluding all cells stained with the fluorescent dye, PI (**Figure 8C)**, and the following population was used for analysis (**Figure 8D**).

Identical gates were set for both MoDMs and MoDCs. Monocytes produced two populations in the FSC-A vs SSC-A dimensional plot (**Fig. 8D**). A bigger population with lower granularity, between 50K-100K on the SSC-A scale, and a smaller cluster with higher complexity, around 150K-200K, appearing on top of the SSC-A scale. Analysis of CD14 expression on the two populations revealed that the less granular cells (bigger population) showed a high expression level (**Figure 8E**, higher blue peak), while the more granular population showed extremely low-to-almost absent CD14 expression (**Figure 8E**, smaller peak). The bigger population was therefore considered to be monocytes, with the smaller cluster believed to be early-stage apoptotic cells or granulocytes isolated along with the monocytes during the magnetic activated cell sorting (MACS) procedure. On a cursory observation, MoDCs appeared to be larger with more complexity than MoDMs and undifferentiated macrophages (**Figure 8A, MoDCs**). Analysis of MoDMs also produced two populations: one with a lower FSC-A, below 50K but wide range of granularity, up to 130K on the SSC-A scale. The second was relatively larger in size with high granularity; and was observed as the cluster of events with both FSC-A and SSC-A above 50K (**Figure 8A, MoDMs**). The threshold set to exclude the smaller but granular events was determined by backgating both populations (not shown). From this analysis, it was observed that events lower than 50K on the FSC scale were all filled up with the PI stain and were concluded to be both debris and early-stage apoptotic cells due to relatively harsh harvesting procedure of MoDMs; hence were excluded from the analysis.

The histograms (**Figure 8E**) depict cell surface markers analyzed by flow cytometry, with specific mAb staining in blue against the isotype-matched control mAb in pink. Monocytes expressed an increased level of CD14 with a prominent upregulation seen in MoDMs while MoDCs showed a sharp decline in CD14 expression upon differentiation (**Figure 8E**). In contrast, HLA-DR levels increased with cell differentiation, as observed in MoDCs and MoDMs, compared to undifferentiated monocytes (**Figure 8F**). Similarly, CD11c was heavily upregulated in MoDCs and MoDMs (**Figure 8G**). Results comparing geometric mean fluorescent intensities of the markers revealed a more graphic representation of the expression levels in all three cell types (**Figure 8H**). Macrophages showed the highest expression of CD14, followed by monocytes then DCs with the lowest. On the other hand, DCs appeared to express HLA-DR the most, while CD11c was upregulated almost equally in both DCs and macrophages. Altogether, macrophages differentiated from monocytes demonstrated an increased expression of all selected surface markers, while DCs upregulated only HLA-DR and CD11c.

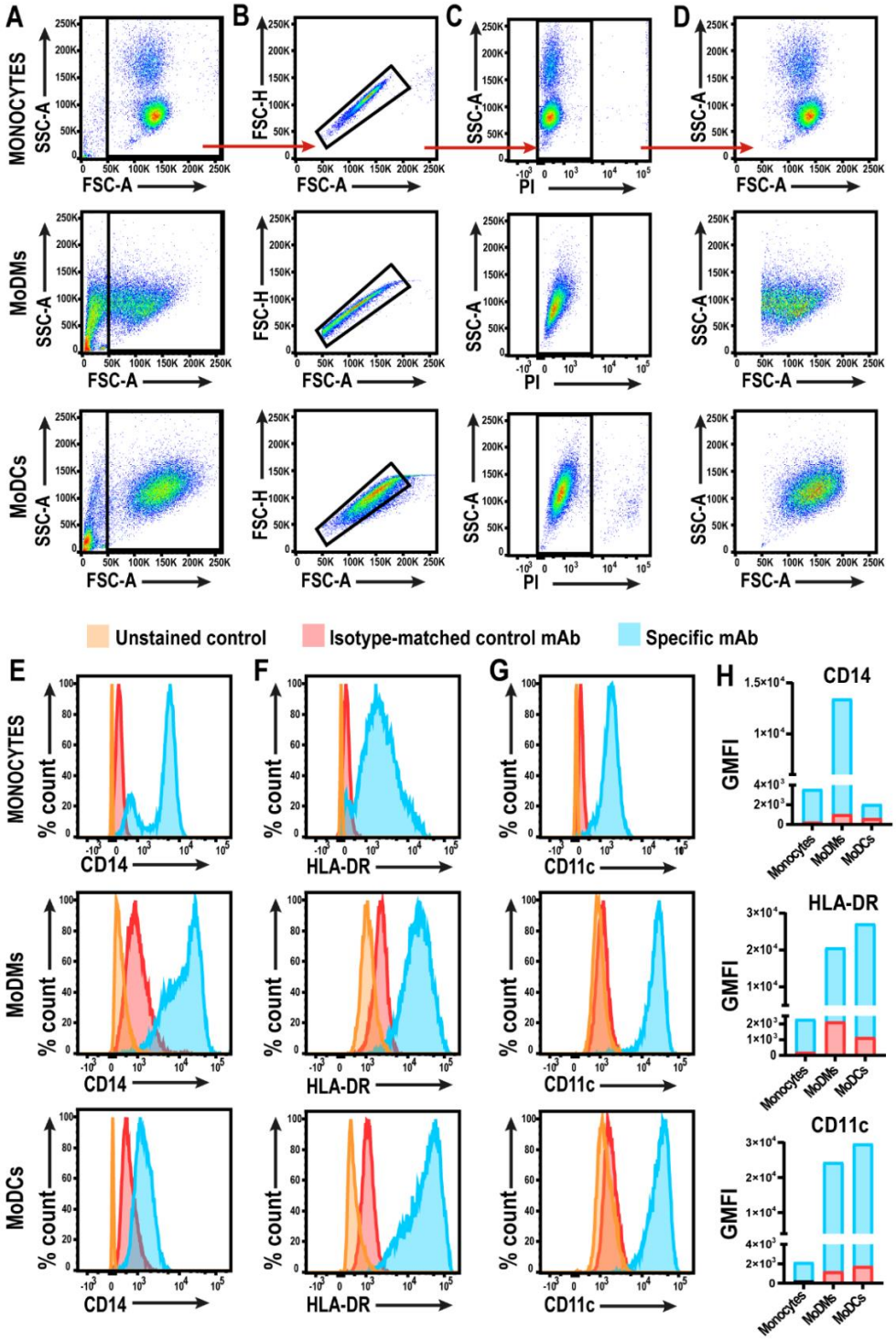

Figure 8. Flow cytometric analysis of surface markers on monocytes, MoDMs and MoDCs.
*MoDMs and MoDCs were differentiated in the presence of GM-CSF only or GM-CSF+IL-4, respectively. Cells were harvested on day 6 and surface markers on thawed monocytes, MoDMs and MoDCs were compared by flow cytometry. (**A**) FSC vs SSC was used as a size exclusion parameter to gate out events below 50K (FSC-A). (**B**) Single cells were identified using FSC-A and FSC-H parameters, and (**C**) dead cells with high expression of propidium iodide (PI) were excluded; (**D**) resulting population used for the analysis. Identical gates were set for MoDMs and MoDCs. Histograms showing expression of monocytic-lineage markers: (**E**) CD14, (**F**) HLA-DR and (**G**) CD11c on monocytes, macrophages and DCs. (**H**) GMFI values further confirmed expression patterns of selected markers. The experiment was performed four times, and results from a representative experiment are presented.*

4.5 In vitro polarized MoDMs undergo morphological changes upon activation.

In the literature, several terminologies and definitions have been used to describe *in vitro* macrophage activation and polarization following their exposure to an external stimulus (148,163,199). Cytokines are well-established extrinsic activating factors known to skew macrophages either towards a pro-inflammatory or anti-inflammatory phenotype *in vitro*. IFN-γ, is the main cytokine associated with M1 activation and the major product of Th1 T cells. An optimal antitumor response is induced when IFN-γ is combined with LPS or TNF, according to many reports (110,191,224). Bacterial LPS is the best-studied M1 macrophage signal, which is mainly recognized by TLR4 and eventually induces a prototypic inflammatory response (191). Here, MoDMs were treated with IFN-γ only, LPS (from *E. coli,* K12) only or LPS plus IFN-γ; referred to as classically activated (M1) macrophages, as described by Mantovani *et al.* (148). CD14+ monocytes were seeded at cell density 3.0 x 10^6 cells per 10 mL growth medium and were differentiated in the presence of 50 ng/ mL human GM-CSF. On culture day 6, differentiated macrophages were activated by replacing culture medium in each plate with either 100 ng/mL LPS, or 40 ng/mL IFN-γ. The other culture dishes were replaced with either medium containing LPS + IFN-γ (at concentrations indicated) or only culture medium (referred to as 'no treatment'). All cultures were incubated for at least 24 hours and then harvested for further analysis. Microscopic images were captured prior to cell harvesting and flow cytometric analysis on day 7.

The varied culturing conditions generated cells with distinct morphologies. Micrographs in **Figure 9** showed that pre-activated macrophages, otherwise termed 'resting macrophages', revealed the characteristic large, irregularly-shaped and flattened cells, consistent with the morphological features of GM-CSF differentiated MoDMs, described in section 4.2 (**Figure 6B, Figure 9A**). LPS-treated macrophages similarly maintained the flattened and amorphously shaped appearance of untreated macrophages, although some rounded cells were observed (**Figure 9B**). Macrophages treated with only IFN-γ exhibited the typically large, spread-out cells which appeared to be a quite homogenous population that is tightly adherent to the culture dishes and show prominent oval-shaped nuclei (**Figure 9C**). Macrophages treated with LPS in combination with IFN-γ displayed a somewhat unique morphological characteristic different from the remaining parallel cultures. Although some cells retained the round morphology in this culture condition, others revealed a striking contrast – mostly flat and elongated with spindle-like projections extending out of the cell body, a characteristic fibroblastic morphology. In addition, cell nuclei appeared stretched and larger, compared to the cytoplasm (**Figure 9D**).

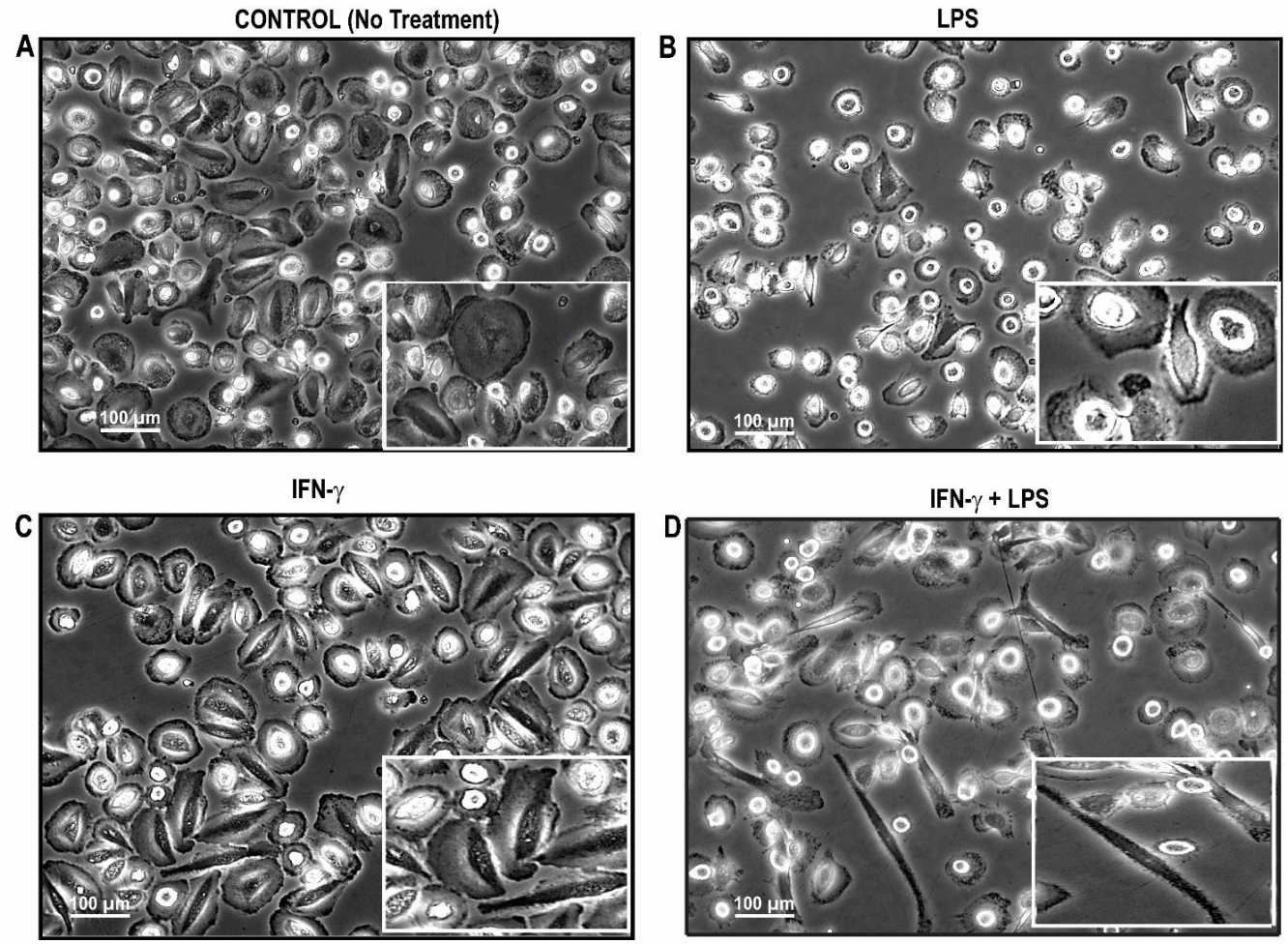

Figure 9. Micrograph of in vitro polarized (M1) human monocyte-derived macrophages.
Microscopic examination showing distinct morphologies of unstimulated macrophages and macrophages treated with either 40 ng/mL IFN-γ, 100 ng/mL LPS (from E. coli K12) or both (LPS+IFN-γ) for 24 h. ***(A)*** *Prior to activation, resting macrophages differentiated in the presence of GM-CSF exhibited the characteristic flattened-shape morphology for human MoDMs, shown as control.* ***(B)*** *Cells activated with LPS, or* ***(C)*** *IFN-γ only generally maintained the spread-out morphology of unactivated macrophages.* ***(D)*** *Cells treated with both LPS and IFN-γ were mostly elongated and spindle-like cells. Figure shown is representative of three individual experiments performed. Phase contrast images were taken on day 7 at 100 x magnifiction; scale bar 100 µm. Insert: enlarged image. Micrographs were taken on day 7 using a phase contrast Zeiss AxioCam MRc at 100x magnification; scale bar 100 µm. Enlarged image shown as insert.*

4.6 Different polarization conditions affect expression levels of activation markers.

In vitro polarized macrophages were harvested on day 7 and expression levels of selected activation markers compared by flow cytometry. We investigated how the various cytokines used in activating MoDMs affected the expression of HLA-DR and CD86. HLA-DR even though expressed on resting macrophages is known to be upregulated upon macrophage activation; a prerequisite in the process of antigen presentation to T lymphocytes, following activation by for example LPS or IFN-γ. CD86 is a membrane protein expressed on APCs including macrophages, and is known to provide the second/costimulatory signal essential for activating T cells, by binding to CD28 on the latter. Like HLA-DR, CD86 exhibits a broad constitutive expression pattern, being present at considerable levels on resting macrophages with significant upregulation upon stimulation (225).

Two separate cell populations were produced in the two-dimensional plot analyzed for non-treated macrophages, shown as 'unstimulated' (**Figure 10A**); similar populations were observed for LPS, IFN-γ, and LPS+ IFN-γ activated macrophages (data not shown). Cells were gated using FSC-A vs SSC-A to set a threshold around 70K on FSC scale to exclude debris, and cells believed to be undifferentiated monocytes (**Figure 10A**). Single and live cells were selected by gating with FSC-A vs FSC-H parameters and removing cells stained with PI, respectively (**Figure 10B** and **10C**). The final population of single, viable and fully differentiated activated macrophages were used in the further analysis (**Figure 10D**).

Unstimulated macrophages demonstrate a relatively lower expression of HLA-DR compared to LPS-treated macrophages (**Figure 10E and 10F**). However, macrophages polarized with only IFN-γ showed little to no difference in HLA-DR expression when compared with the unstimulated control (**Figure 10G**). More significantly, activation with combined stimuli (LPS+ IFN-γ), resulted in a quite substantial upregulation of HLA-DR (**Figure 10H**). An identical expression pattern was observed for the activation marker CD86; stimulation with LPS alone resulted in a noticeable increase in expression levels compared with the untreated control (**Figure 10I and 10J**). Alternatively, activation with IFN-γ alone, revealed no differences in CD86 expression with the control (**Figure 10K**). Again, the combination of LPS and IFN-γ exhibited a remarkable upregulation of the costimulatory molecule on macrophages (**Figure 10L**). The geometric mean fluorescence intensities (GMFI) were compared to further corroborate the obtained results.

The effects of LPS alone and LPS+ IFN-γ treatments were apparent for both HLA-DR and CD86 with the most striking representation for CD86 (**Figure 10M**). However, there seem to be no significant differences between the untreated and IFN-γ alone stimulated macrophages in both markers (**Figure 10M**). Surface marker expression was only assumed present if primary antibody exceeded the levels of irrelevantly targeted isotype-matched stains and unstained controls. Two successful experiments were conducted, see **Supplementary Figure 3** for data replicated in an independent experiment.

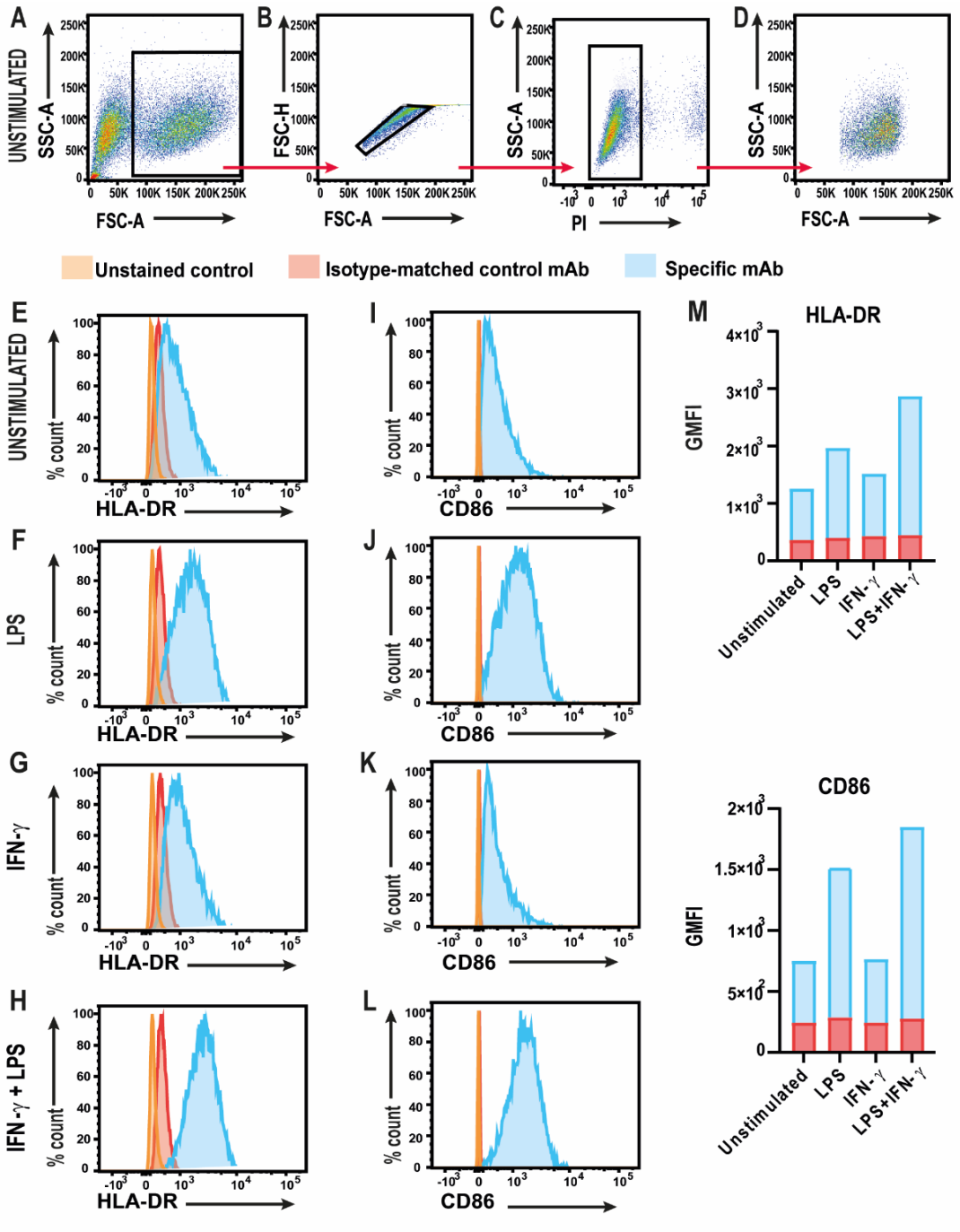

Figure 10. Flow cytometric analysis of M1 polarized macrophages.

*In vitro GM-CSF differentiated macrophages were analyzed for activation markers after overnight stimulation with 100 ng/mL LPS only (from E. coli K12), 40 ng/mL IFN-γ only or LPS+ IFN-γ at stated concentrations. (**A**) Size exclusion gate used to select cells above 50K on FSC scale. (**B**) Single cells were identified using FSC-A and FSC-H parameters and (**C**) dead cells stained with propidium iodide (PI) were excluded. (**D**) Resulting population was identified as live, fully differentiated MoDMs and used for the analysis. Unstimulated macrophages were used as control and identical gates were set for macrophages activated with either LPS or IFN-γ only, or LPS+IFN-γ (not shown). Histograms showing expression of established classically activated macrophage markers: HLA-DR **(E)**, **(F)**, **(G)**, **(H)** and CD86 **(I)**, **(J)**, **(K)**, **(L)** in unstimulated, LPS, IFN-γ and LPS+ IFN-γ, respectively. **(M)** The GMFI for all conditions were compared to further validate results obtained; blue bars show GMFI of the specific mAb while red bars show GMFI of the isotype-matched controls. Data have been replicated in an independent experiment.*

4.7 Quantification of pro-inflammatory cytokines released from Chaga-activated MoDMs

Our collaborator Christian Winther Wold isolated chaga polysaccharides and characterized them into 3 main groups based on their structural and chemical properties as follows: two water-soluble and neutral compounds (IWN and EWN), three water-soluble and acidic compounds (AcF1, AcF2, AcF3), and one alkaline, particulate compound (A1) (see manuscript in Annex). In subsequent experiments, it was demonstrated that the isolated polysaccharides could bind multiple PRRs to activate murine macrophages into a pro-inflammatory anti-tumor phenotype to secrete cytokines like IL-6 and TNF-α (manuscript in annex). TNF-α, previously known as TNF was originally discovered for its ability to induce necrosis in certain tumors, and is also reported to suppress the growth of transformed cells by activated macrophages (226,227). IL-6, a pleiotropic cytokine known for its dual role in inflammation, additionally activates cytotoxic T lymphocytes, which are essential immune cells in fighting cancers (75). IL-12p70 is primarily produced by APCs including macrophages and is actively involved in cell-mediated immunity via activation of Th1 T cells, NK cells as well as CD8 T cells. It also synergizes with other cytokines like TNF to stimulate the production of IFN-γ (228).

We investigated the potential of chaga polysaccharides namely: IWN, EWN, AcF1, AcF2, AcF3 and A1 to induce the production of pro-inflammatory cytokines in human MoDMs. MoDMs were generated in the presence of either GM-CSF or M-CSF and were seeded into 48-well plates; with 1x 10^5 cells in 150 µL growth medium per well. Cells were activated for 24 h with various polysaccharides (100 µg/mL), in the absence (black bars) or presence (red bars) of 20 ng/mL IFN-γ (**Figure 11**). LPS-EK, Pam_3CSK_4 (both 100 ng/mL), zymosan crude (ZymC), zymosan purified (ZymP) and laminarin (all 100 µg/mL) were positive controls. Untreated macrophages were used as negative control. Cell supernatant was collected after repeated cycles of centrifugation, and concentrations of human IL-6, TNF-α and/or IL-12p70 were measured. Samples in duplicates were analyzed using a MAGPIX Multiplex Reader and Bio-Plex Manager 6.1 software. Four independent experiments were conducted; two measured IL-6 and TNF-α production by GM-CSF MoDMs while IL-6, TNF-α and IL-12p70 production were quantified twice in M-CSF differentiated macrophages.

All six polysaccharides, except for A1, induced the production of IL-6 in GM-CSF differentiated macrophages. Similar pattern was observed with TNF-α production, notably AcF3 being the most active polysaccharide, with levels comparable to the positive controls – LPS, Pam_3CSK_4 and Zymosan. In general, the remaining polysaccharides, with the exception of A1, produced moderate amounts of IL-6, with a slight

increase noticed when combined with IFN-γ (**Figure 11**). A similar observation was made for TNF-α production, where co-incubation of IFN-γ together with the polysaccharides, moderately enhanced TNF-α secretion, apart from AcF3, which appeared to be less dependent on exogenous IFN-γ (**Figure 11B**). We compared the production of the same cytokines plus IL-12p70 in M-CSF activated macrophages. **Figures 12A and 12B** again show that AcF3, in the absence or presence of IFN-γ, stimulates the macrophages to secrete IL-6 and TNF-α. For IL-6, production, minor effects of co-stimulation with IFN-γ were observed in for example, IWN, EWN and AcF2. However, polysaccharide-mediated production of TNF-α was clearly enhanced by IFN-γ, except for AcF1 and AcF3. Additionally, A1 comparably secreted low levels of both cytokines. A more glaring contrast was observed in **Figure 12C**, where activated cells almost failed to produce IL-12p70 in the absence of IFN-γ. Among the polysaccharides, AcF1 and AcF3, through synergistic interactions with IFN-γ, appeared to secrete the highest levels of IL-12p70; equivalent to, or even higher than LPS and Pam_3CSK_4. In sum, chaga polysaccharides potentially activated MoDMs and induced the production of IL-6 and TNF-α at substantial levels, somewhat independent of IFN-γ, whereas IL-12p70 production required IFN-γ as an essential co-activation signal. Additionally, the polysaccharides AcF1 and AcF3 presented to be the most active in both GM-CSF and M-CSF MoDMs, while A1 showed as the least active, with little IL-6 and TNF-α production but none of IL-12p70.

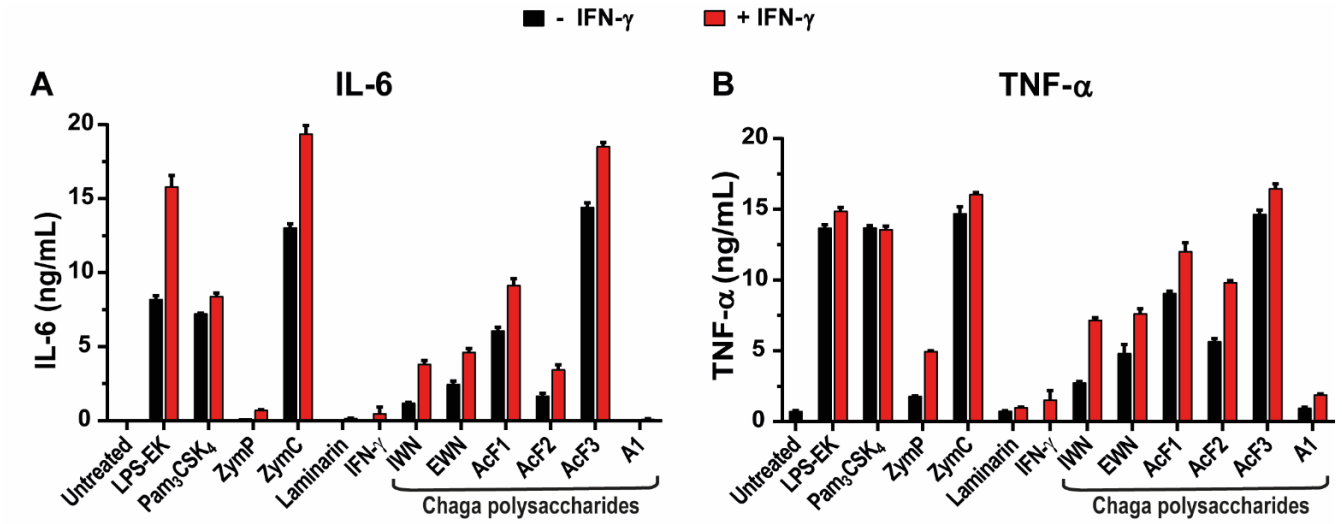

Figure 11. Cytokine quantification in media from GM-CSF MoDMs activated with Chaga polysaccharides.
GM-CSF differentiated moDMs (1 x10^5 cells in 150 µL per well) in 48-well plates were treated on culture day 6 with various polysaccharides: 100 µg/mL alone (black bars) or in combination with 20 ng/mL IFN-γ (red bars) for 24h. Cytokine concentration in cell media was then measured using a Bio-Plex MAGPIX Multiplex Reader; samples were analyzed in duplicates. LPS from E. coli K12, Pam_3CSK_4 (both 100 ng/mL), zymosan crude (ZymC), zymosan purified (ZymP) and laminarin (all 100 µg/mL) were positive controls. Untreated macrophages were used as negative control. Two independent experiments were performed; data shown represent mean and ± SD values from two experiments with cells obtained from the same donor. ***(A)*** *All six polysaccharides but A1 induced the production of IL-6.* ***(B)*** *TNF-α, production was induced by all polysaccharides with minor dependence on IFN-γ.*

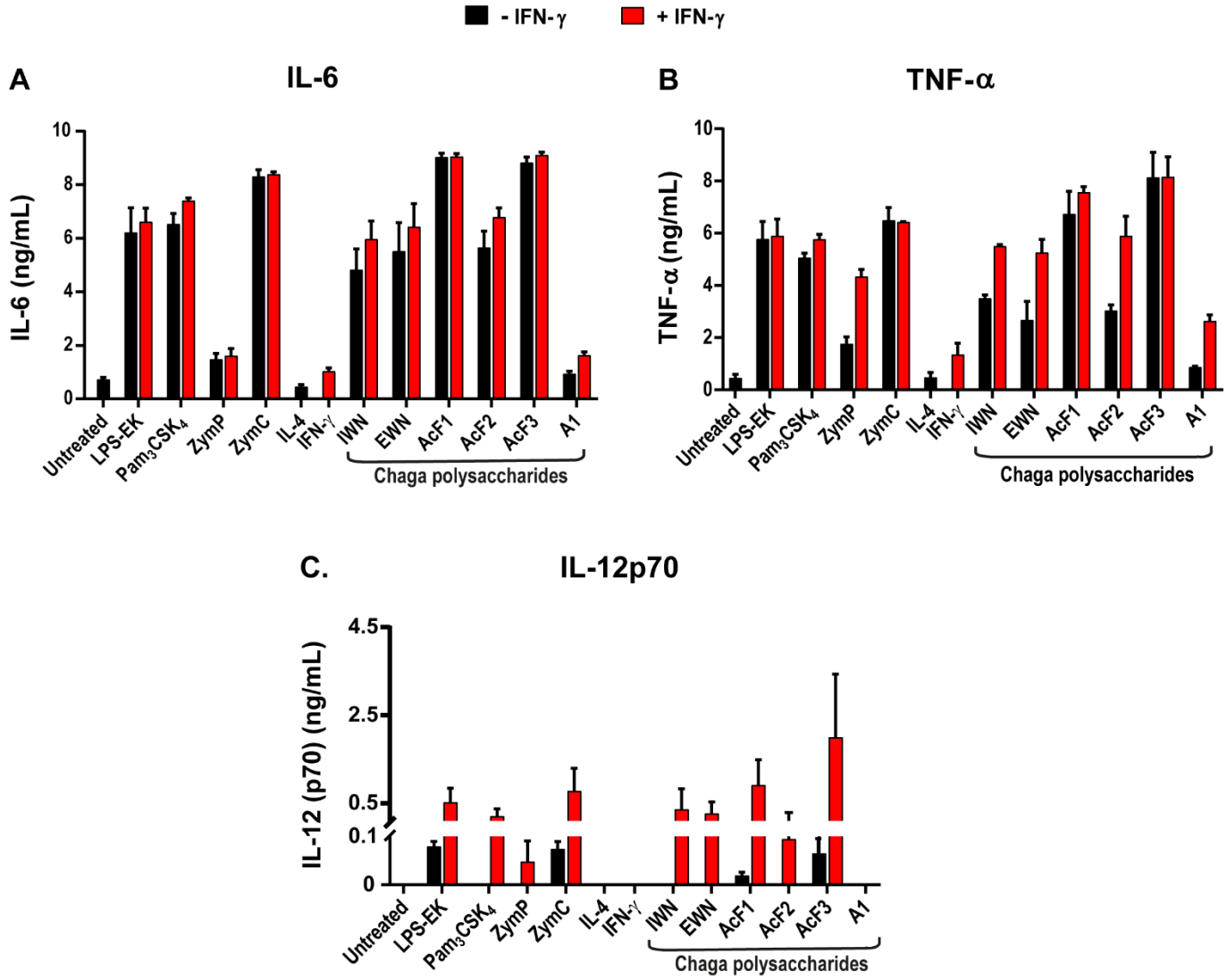

Figure 12. Effects of Chaga polysaccharides on IL-6, TNF-α and IL-12p70 production by M-CSF activated MoDMs. *M-CSF differentiated human macrophages: (1 x 10^5 cells) in 150 µL culture medium per well in 48-well plates were treated on culture day 6 with various polysaccharides at 100 µg/mL, alone (black bars) or in combination with 20 ng/mL IFN-γ (red bars) for 24h, before cytokine concentrations in cell media were measured using Luminex xMAP technology. LPS from E. coli K12 strain, Pam_3CSK_4 (both 100 ng/mL), zymosan crude (ZymC), and zymosan purified (ZymP), (both 100 µg/mL) were used as positive controls. IL-4 (20 ng/mL) and untreated macrophages were negative controls. All six polysaccharides induced the production of* ***(A)*** *IL-6 and* ***(B)*** *TNF-α, at varying levels with minor or no effect of co-stimulation with IFN-γ; conversely,* ***(C)*** *IL-12p70 production was mainly dependent on IFN-γ. Samples were analyzed in duplicates and graphs show mean values with ±SD pooled from two independent experiments obtained from the same donor.*

4.8 In vivo analysis of anti-tumor potential of Chaga polysaccharides

Promising results from the *in vitro* experiments revealed that chaga polysaccharides could activate both human and mouse macrophages into a pro-inflammatory, anti-tumor phenotype (see manuscript). However, we did not know whether this effect could be replicated *in vivo*. To test this hypothesis, we selected the two most active polysaccharides, AcF1 and AcF3, hereafter referred to as 'F1' and 'F3' respectively, for further *in vivo* analysis. Mouse models, C57B/L6, were randomly divided into five groups consisting of nine mice per group except for one group with eight mice. Each mouse was co-injected with LLCs and BMDMs pre-activated with F1, F3 or Pam_3CSK_4, together with IFN-γ. Nine mice each in F1+ IFN-γ and F3+ IFN-γ groups represented the treatment category, while nine mice in Pam_3 + IFN-γ formed the positive control group, and eight mice in IFN-γ only formed an additional control group. The negative control group, consisted of nine mice co-injected with LLCs plus non-treated BMDMs, and this was designated as 'Untreated' (**Figure 13**). The mice were subcutaneously inoculated with 0.1 mL of each condition mixture on day 0, and tumor growth was recorded every other day until humane endpoint was reached. The mice were sacrificed by cervical dislocation when the maximum tumor length measured 15 mm, and the entire experiment was terminated on day 48 post-inoculation, when the last tumor-bearing mouse was euthanized. Tumor volumes were recorded using the formula: Tumor Volume (mm^3) = [$width^2$ x length] x 0.4 (220).

Results obtained indicated that all nine mice in 'Untreated' group except for one, developed tumors; with tumors formed around twelve days after initial injection (**Figure 13A**). Quite interestingly, all eight mice that received LLCs plus macrophages treated with only IFN-γ developed tumors, with most mice showing visible tumors by day twelve – similar to the untreated group (**Figure 13B**). This was in sharp contrast to the Pam_3CSK_4 + IFN-γ treatment group, where all mice remained tumor free, except one in which tumor tissue was observed after 40 days of initial injection (**Figure 13C**). Also, the polysaccharides (AcF1 and AcF3) + IFN-γ treatment groups showed a remarkable absence of tumor development in most of the mice. Specifically, only two out of nine mice in both chaga-treatment groups developed tumors, with half of the tumors visible after 20 days post-inoculation (**Figure 13D and Figure 13E**). Data of all mice are presented in graph F, and all survivors were still tumor-free 48 days after initial inoculation (**Figure 13F**). Overall, 8/9 mice in the positive control group (Pam_3) and 7/9 in both chaga treatment groups remained tumor-free, most likely because all LLC cancer cells were killed *in vivo* by the activated macrophages. Meanwhile, mice in the 'Untreated' and IFN-γ only groups demonstrated the worst survival; with 1/9 and 0/8 survivors, respectively. Experiment was performed once, and statistical significance was calculated using Mantel-Cox test followed by Gehan-Breslow-Wilcoxon test to compare each treatment group with the untreated control.

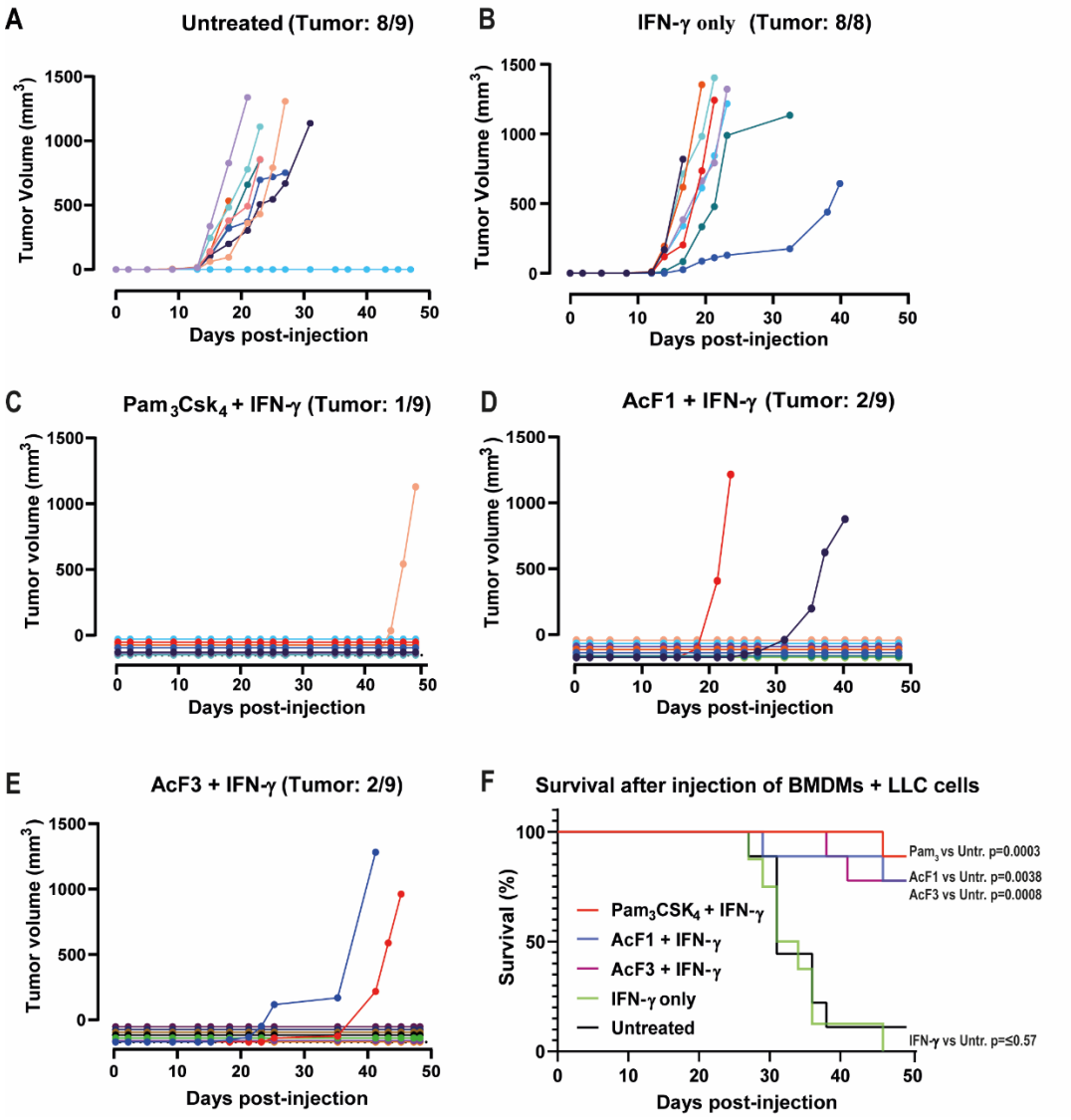

Figure 13. Anti-tumor response of macrophages activated by chaga polysaccharides.

Mouse BMDMs were left untreated or were pre-activated in vitro for 24 h with various activating factors: 20 ng/mL IFN-γ, 100 ng/mL Pam_3CSK_4 in combination with 20 ng/mL IFN-γ, or 100 µg/mL polysaccharides in combination with 20 ng/mL IFN-γ. Activated BMDMs were then mixed with LLCs in ice-cold PBS in a 15:1 ratio (BMDMs: LLCs) and co-injected subcutaneously on the left flank of each mouse. Tumor growth was measured every other day until humane endpoint was reached. Graphs show individual tumor volumes from C57BL/6 mice bearing subcutaneous Lewis lung carcinoma (LLC) tumors ***(A)*** *Untreated macrophages combined with LLCs served as a negative control.* ***(B)*** *Macrophages activated with IFN-γ only;* ***(C)*** *Pam_3CSK_4+IFN-γ as positive control.* ***(D)*** *Chaga polysaccharides: AcF1 + IFN-γ and* ***(E)*** *AcF3 + IFN-γ were treatment groups. (n=9 for each group, except IFN-γ only; n=8). All but one in the untreated group developed tumors whereas one and two out of nine mice established tumors in the Pam_3 and AcF1 groups, respectively. Two mice in the treatment group, AcF3 and all eight of the IFN-γ only group developed tumors.* ***(F)*** *Kaplan–Meier survival curves showing differences in survival between groups after inoculation with pre-activated BMDMs and LLCs. Overall, mice in the chaga and Pam_3CSK_4 treatment groups showed improved survival (red, blue, and purple curves); while those in the untreated and IFN-γ only groups demonstrate the worse survival rates. Statistical significance was calculated using Mantel-Cox test followed by Gehan-Breslow-Wilcoxon test to compare each treatment group with the untreated control; $p \leq 0.05$ were considered statistically significant.*

5 DISCUSSION

One of the major goals of this study was to establish a protocol for differentiating human monocytes into macrophages *in vitro*. Many studies have reported successful generation of human macrophages; nevertheless, with some variations. A common disparity and vital information very often missed or poorly described is the harvesting method utilized in these protocols (229–231). Therefore, we describe in this thesis, a practical model of generating human monocyte-derived macrophages *in vitro*, and successfully harvesting viable cells for further downstream applications. The second aim of this work was to examine the anti-tumor potential of macrophages stimulated with the novel chaga polysaccharides previously isolated by our collaborator Christian Winther Wold (208); which we investigated both *in vitro* and *in vivo*. We measured pro-inflammatory cytokines induced by chaga-activated MoDMs and examined the anti-tumor effect of murine BMDMs activated with these polysaccharides, using mouse models.

5.1 Monocyte purification

It is widely acknowledged that the monocyte isolation and purification method employed could subsequently affect the phenotypic and functional properties of MoDMs generated (232–234). Human primary macrophages are mostly obtained *in vitro* by purification of circulating blood monocytes through various techniques. The method used and described in this study is positive selection by magnetic beads through MACS technology, however other commonly used methods such as plastic adherence and negative selection by MACS, will be described. Magnetic activated cells sorting (MACS) is an extensively used and robust method which uses microbeads conjugated to antibodies against specific cell surface molecules to isolate subpopulations out of complex cell mixtures (235). Positive selection of monocytes involves labelling cells with magnetic beads conjugated to anti-human CD14 antibodies (CD14 MicroBeads). The cell suspension loaded onto a column is placed in a magnetic field, and the CD14+ magnetically labelled cells are retained within the column while unlabeled cells pass through and are collected as waste. The tagged (retained) cells are then eluted and collected as the positively selected cell fraction (221,236).

This method is based on the principle that CD14 molecule, an LPS sensing receptor, expressed on the surface of monocytic lineage cells including monocytes and macrophages, is a key marker for identifying monocytes (237). Positive immunoselection is reported to be the optimal procedure among the three, to

obtain a highly purified and viable monocyte population (221,232). With this technique we obtained an extremely pure monocyte population (96% purity), which were then differentiated towards macrophages, see **Figure 5D**. Another advantage suggested by some reports indicate that since CD14 lacks a cytoplasmic domain, the bound CD14 antibodies may be deficient in triggering a signal transduction pathway which would lead to activation of some sort. On the downside, the bound anti CD14 antibody has been reported to reduce responsiveness of isolated monocytes to LPS through internalization of TLR4 (238).

Unlike positive selection, negative sorting involves the use of monocyte enrichment cocktails, containing antibodies against all leucocytes other than monocytes. When placed in a magnetic field, the labelled (unwanted) cells, are retained and unbound cells that pass through are collected as the fraction of 'cells of interest'– negatively selected monocytes. This process, even though results in 'untouched' and non-activated cells, has however been described as costly, and produces a relatively lower yield and purity, since isolated monocytes are highly likely to be contaminated with platelets (232). The third commonly used method in monocyte purification, involves separation from lymphocytes by plastic adherence. PBMCs are plated on tissue culture treated dishes and allowed to adhere to the plastic by incubation for some period. Non-adherent cells are removed by several washing steps and adherent cells harvested as monocytes. While this technique is easy to perform and relatively cost effective, isolated monocytes are reportedly activated through binding and activation of some adhesion molecules like integrins. Also, due to repeated washing cycles and likelihood of some monocytes not adhering, overall yield and viability is proven as poor when compared with magnetic immunoselection (230–232).

Ideally, one must examine all three purification methods to exclude potential bias in drawing conclusions. Although we did not evaluate monocyte enrichment by negative immunoselection or plastic adherence, we generally considered positive selection by MicroBeads as an ideal method based on: ***i)*** previous reports comparing all methods (232), ***ii)*** the high percentage purity and viability of CD14+ monocytes we obtained, and ***iii)*** the ability of isolated monocytes to successfully differentiate into macrophages, given the optimal conditions.

5.2 In vitro differentiation of monocytes

Isolated CD14+ monocytes were cultured in growth medium, supplemented with 10% FBS and 1% Pen/Strep, with or without growth cytokines for 6 days. The specific culture conditions generated different populations of mature macrophages showing slightly different morphologies and surface marker expression patterns (**Figure 6**). Microscopic examinations revealed the characteristic large, flattened and

stretched out morphology of mature macrophages differentiated in the presence of cytokines. Comparable results were observed for both GM-CSF and M-CSF differentiated macrophages as reported in other studies (121,239–241), however one striking difference noted was that GM-CSF MoDMs were mostly round whereas M-CSF showed some spindle-like morphology. As seen in figures **6B** and **6C**, cells appeared larger, appeared densely populated, with nearly all tightly adhered to the plastic, compared to smaller and loosely attached cells in the cultures without growth factors (**Figure 6A**). This substantiates the established effects of these growth factors in not only influencing the growth of primary monocytes, but also foster their differentiating into macrophages (123,124,239,240). Other studies suggest that GM-CSF and M-CSF are mandatory for monocytes to survive and differentiate into macrophages *in vitro* (229), however, in our hands, differentiation without supplement of the growth factors GM-CSF or M-CSF was successful, albeit with some few observable differences.

The results obtained from the microscopic assessment of the various differentiation conditions for generating MoDMs was validated by flow cytometry analysis. Expectedly, cells differentiated in the presence of cytokines (GM-CSF or M-CSF) were found to be relatively larger and more granular, compared to 'no cytokine' macrophages (**Figure 7A**). Macrophages differentiated without cytokines showed size and complexity comparable to undifferentiated monocytes, used as control (**Figure 7A**, first and second rows). Many studies have supported claims that GM-CSF and M-CSF cytokines used in macrophage differentiation, tend to prime MoDMs towards pro-inflammatory and anti-inflammatory states respectively, without fully activating them (121,197,242). Additionally, it has been established that both cytokines independently induce different macrophage subsets with distinct morphologies and functions (243). This connotation must however be used cautiously as certain phenotypic markers, for example, CD200R, which is commonly accepted as an 'M2' marker is expressed at comparable levels in both M-CSF and GM-CSF differentiated macrophages (229). It must also be noted that most of these reports based their conclusions on combined differential expression patterns of genomic and phenotypic markers, as well as cytokine secretion profiles (121,197,242,243).

We however analyzed commonly used monocytic-lineage markers CD14, HLA-DR and CD11c among these cell types with undifferentiated monocytes as reference. As seen in **Figure 7E**, CD14, which is inherently expressed on monocytes and macrophages was higher in GM-CSF differentiated macrophages compared to monocytes. M-CSF and 'no cytokines' macrophages appeared to also have a higher CD14 expression, although with some high background signal from the isotype-matched control. Next, we noted that HLA-DR expression was identical in GM-CSF differentiated and 'no cytokines' macrophages,

but a sharp decline in M-CSF differentiated MoDMs. This pattern was observed in two independent experiments performed, a deviation from what is commonly reported in the literature; as HLA-DR is upregulated upon monocyte differentiation into macrophages (244). Even though this was unexpected, it would nonetheless be in agreement with the opinions of Ushach (2016) and Mia (2014) that both murine BMDMs and human MoDMs, differentiated with M-CSF and polarized into M2 macrophages demonstrated high phagocytic activities but low antigen presentation capacity due to their anti-inflammatory phenotypes (121,196).

Observations and findings during in vitro differentiation of monocytes

During the differentiation of monocytes into macrophages *in vitro,* we encountered a few challenges, which were often missing completely or poorly detailed in many established protocols. These observations enlightened us on how some minor factors, often overlooked, could have profound impact on the successful differentiation of human macrophages *in vitro*. One of such findings, even though common knowledge in cell biology, is the effect of sera used in the differentiation cultures. FBS, when supplemented with culture media is believed to provide essential components such as nutritional, hormonal, attachment and growth factors to cells (245,246). To address the cause of the poor survival and unusual morphologies observed in our MoDM cultures, we compared serum from two suppliers, Biochrom (Cat. # S0113) and BioWest (Cat. # S181BH-500). The aim was to determine if either of these could positively affect the growth and differentiation of primary human monocytes in culture. We monitored and captured images of simultaneous cultures set up with the differentiation conditions described in section **3.2.4**, but with separate sera. From our observations, media supplemented with serum from Biochrom was less efficient as most cells, about (50%) appeared dead, with many unadhered cells (possibly undifferentiated monocytes), by culture day 6 (**See supplementary figure 1**). In contrast cells in parallel culture, supplemented with serum from BioWest showed better survival, proliferation, and differentiation into typical macrophages on culture day 6. The serum-comparison experiments were conducted at least thrice, with cells obtained from the same donors in each comparison experiment. Similar reports have been documented in previous studies, asserting that differences in suppliers could have as much as double-fold discrepancies in growth and maintenance of certain cell types (247,248). Consequently, we concluded from our data, that serum from BioWest was a better option of the two, for growth and differentiation of primary human monocytes *in vitro,* although interestingly, results from our lab have suggested the opposite for growth and maintenance of murine BMDMs.

An additional challenge we faced was harvesting mature macrophages for further analysis. One characteristic of macrophages in culture is their strong adherence to any substrate, particularly with activated ones (249). As shown in **Figures 6** and **9**, macrophages adhere tightly to the plastic (non-treated) culture dishes by day 6 or 7 in culture, and are difficult to detach without enzymatic treatment or mechanical processes as many protocols suggest (229,230,232). While some recommend use of thermo-responsive substrates (250) which are costly, others use enzymes such as trypsin or accutase with or without scraping for dislodging cells; we observed poor cell viability and cell clumping with this method. Also, one commonly suggested technique is incubating cells in $PBS^{-/-}$ and on ice during harvesting, but in our experience, very few cells detached after an hour-long incubation. We however tried detachment with buffer prepared in our lab; $PBS^{-/-}$ + 2.5mM EDTA +1% FBS (BioWest), and incubation at 37°C, for 30 min. We compared this with incubation at 4°C and the results were remarkable. After 30 min incubation at 37°C, about 80% of cells were dislodged and the few adherent cells when observed under the microscope had rounded up, as opposed to cells kept on ice, where more than 70% remained firmly attached and needed to be incubated longer or scraped multiple times. Significant differences between these two methods became apparent during flow cytometry analysis of harvested cells. By incubation at 37°C, the percentage of dead cells post-harvesting was reduced by nearly 80%; as many cells were automatically dislodged, leaving fewer cells to be harvested mechanically (See **Supplementary Figure 2,** third and fourth rows**)**. In contrast, cells incubated at 4°C, were less viable, as almost 60% were filled with PI stain during flow cytometry analysis possibly due to mechanical stress evoked by scraping (**Supplementary Figure 2, first** and **second rows**).

As earlier mentioned, cultured macrophages strongly attach to any substratum and this presented an additional difficulty during centrifugation of harvested cells for other applications. We observed that harvested cells 'disappeared' after centrifugation at 400 g, 4°C and 7 min using falcon tubes. No visible pellets were seen, and there were no cells in the supernatant collected for cell counting, even though culture dishes observed under the microscope were empty. To solve this, we tried both glass and polypropylene centrifuge tubes and at different centrifugation speeds but without improvement. Next, we sought to provide 'lining' within the tubes by coating the inner surface of the centrifuge tube with serum to prevent cells from directly attaching to the tubes and again, our findings were astonishing. Recovery of cells harvested into serum-coated tubes were found to be 3-fold higher than cells in plain centrifuge tubes (See Supplementary Table 1). Taking everything into account, these observations,

seemingly trivial, posed major setbacks and finding solutions to them significantly improved the yield and viability of human monocyte-derived macrophages differentiated *in vitro*.

5.3 Comparison of MoDMs and MoDCs

Monocytes, macrophages, and DCs are commonly referred to as members of the mononuclear phagocytic system (MPS) with shared phenotypic markers and functions (223). *In vitro*, human monocytes can be differentiated into MoDMs or MoDCs, given specific culture conditions (221,230,251). We differentiated both MoDMs and MoDCs in the presence of GM-CSF, but with an additional cytokine, IL-4, and a higher concentration of GM-CSF (100 ng/mL) in the case of MoDCs. Next, we analyzed the different expression patterns of some markers commonly associated with cells of the mononuclear phagocytic system; CD14, HLA-DR and CD11c (87). CD14 is generally used as an identification marker for monocyte-derived cells, especially macrophages, and may be present on mature DCs, but at relatively lower levels (221). Similarly, CD11c, a classical DC identification marker is also expressed by monocytes and macrophages at distinct levels (252). HLA-DR, is a common surface molecule expressed by all professional antigen presenting cells, including MoDMs and MoDCs. As shown in **Figure 8E**, CD14 was highly upregulated in differentiated macrophages with a sudden decrease in DCs upon differentiation. It is believed that changes in protein expression levels are the result of a coordinated alteration in mRNA levels of the CD14 molecule. This occurs upon monocyte differentiation into DCs (221). Most evidently seen in the GMFI representation in **Figure 8H,** CD14 is clearly downregulated in DCs compared to their monocyte precursors, but not at all absent. As one would expect in professional APCs, HLA-DR showed upregulation upon differentiation into MoDMs and MoDCs. Unsurprisingly, CD11c seem to be expressed at almost similar levels in MoDMs and MoDCs, which is consistent with most reports that some macrophage subsets are positive for CD11c (253).

Although phenotyping is a fairly straightforward technique to characterize cellular subsets, it is a widely acknowledged fact that some markers are not unique to specific cells, hence analyzing a combination of morphological, phenotypic markers as well as transcriptomic analyses would be essential to accurately distinguish between cells of common precursors (87).

5.4 *In vitro* activated MoDMs undergo both morphological and phenotypic changes

Cytokines and microbial particles can activate macrophages *in vitro.* Bacterial LPS and the cytokine IFN-γ from Th1 T cells have been established as the classical macrophage stimulators, polarizing the macrophages into a pro-inflammatory (M1), tumoricidal phenotype (141,143,148). In theory, the activating stimuli applied is generally believed to result in substantial changes both morphologically and genetically (148). Here, MoDMs were polarized into M1 phenotype by treating cultures with either LPS, IFN-γ or both, then morphological and phenotypic changes that followed were examined. Photographs of the specific cultures showed that macrophages treated with either LPS or IFN-γ exhibit some slight morphological distinction, not so marked from non-activated ones. The more obvious difference was seen when both stimuli were combined, as microscopic examinations showed cells had undergone some noticeable structural changes; with elongated and spindle-like morphologies, as opposed to the classical 'fried egg' shape of non-activated macrophages (Figure 9). These findings clearly support the notion that gene expression profiles of macrophages activated with the combined stimuli are different from that displayed by LPS or IFN-γ profiles alone (128). Moreover, it is reported that following activation by an initial stimulus, macrophages could undergo multiple progressive functional phenotypes when additional cytokines are added in a sequential manner (199). In general, an indication from the microscopic results seem to provide proof of the concept that activated macrophages undergo additional modifications, both functional and biochemical, depending on whether the activating cytokine is used alone or synergized with other stimuli (163,199). This was validated by flow cytometry analysis of the activated MoDMs.

We compared the membrane expression of some M1 markers: CD86 and HLA-DR in the different polarization conditions. Activation with IFN-γ alone showed no difference in expression patterns when compared with the untreated control. This is in accordance with the concept that single ligands may not be sufficient for activation, as previously described (199,224). However, a remarkable observation was made with LPS alone, an apparent upregulation was noticed with single stimulation by LPS, to a level comparable to the co-stimulation, particularly in CD86 (Figure 10). This trend is however commonly reported, for example, LPS as a single exogenous stimulus is shown to sufficiently activate mouse macrophages to produce NO and pro-inflammatory cytokines, rendering them cytotoxic to tumor cells (110,111,254,255). Additionally, the literature contains numerous reports that single activation with LPS, is to some extent similar to two signals, as it triggers two signaling pathways mediating the production of both type 1 interferons and pro-inflammatory cytokines (111,256,257). Also, since CD14, the major receptor for LPS is expressed on macrophages, one possible explanation for the disparities could be that

the activated macrophages with an elevated CD14 expression are hypersensitive to LPS (255). However, IFN-γ, could possibly show similar activation pattern if used at a slightly higher concentration, but that we could not confirm.

Notwithstanding, the expression of HLA-DR and CD86 were appreciably upregulated when IFN-γ augmented the effect LPS (Figure 10M). Similar data have been replicated in a separate experiment, which corroborate our observations and several other reports that LPS alone seem to sufficiently activate MoDMs, and demonstrate enhanced activity when combined with other stimuli such as IFN-γ.

5.5 Quantification of pro-inflammatory cytokines in Chaga-activated MoDMs

Chaga polysaccharides have been fairly investigated and reported to stimulate macrophages into a pro-inflammatory phenotype (212,213). However, to our knowledge, much of the studies have been based on murine macrophages with limited data on human macrophages. We stimulated human MoDMs with the six chaga polysaccharides along with other commonly used PRR ligands, (see tables 7 and 8), and measured the concentrations of pro-inflammatory cytokines after 24 hours. All chaga polysaccharides, except for A1, induced GM-CSF MoDMs to secrete substantial amounts of the cytokines; IL-6, TNF-α and IL-12p70 in M-CSF MoDMs. Overall, TNF-α production mediated by AcF3, appeared to be less dependent on IFN-γ while IL-6 showed some slight dependency. In addition, all polysaccharides, synergized with IFN-γ to secrete IL-12p70, with notable effects observed in AcF1 and AcF3. Series of studies performed by Wold and colleagues, showed identical activation and secretion patterns in mice BMDMs (see manuscript). Chaga-activated mice BMDMs induced NO production, which ultimately inhibited the growth of cancer cells (LLCs) during co-culture. Evidence provided suggested that the immunological activity observed was devoid of LPS contamination, which could potentially produce false positive results. This was verified by activating mice BMDMs generated in TLR4 knock out mice (TLR4 KO), and comparing activation signals with the wild type. Results confirmed that NO production was retained in both wildtype and TLR4 KO BMDMs activated with chaga polysaccharides plus IFN-γ, while completely absent in TLR4 KO BMDMs activated with LPS (see manuscript).

One cytokine of particular importance in this study is IL-12p70, which has been shown to induce an anti-tumor response in animal models, by augmenting the cytotoxic activities of NK cells and CD8 T cells (228). MoDMs differentiated in the presence of M-CSF showed an impressive production of IL-12p70 upon activation with chaga polysaccharides. As shown in figure 12, an essential facilitator in the optimal

production of IL-12p70 is IFN-γ. IL-12p70 secreted by activated macrophages subsequently leads to the activation and differentiation of CD4 T cells with enhanced Th1-type effector functions, which in turn produce more IFN-γ to stimulate macrophages, in a positive feedback loop (259). In addition, cytolytic activities of NK cells, such as production of granzyme and perforin, believed to have direct anti-tumor effects are promoted by IL-12p70 (260). Due to its crucial role in bridging both innate and adaptive immune responses, harnessing various approaches to induce IL-12p70 production in macrophages is undoubtedly a beneficial tool in the treatment of many diseases, including cancers. Collectively, our findings in human MoDMs and results from Wold et al. on BMDMs, indicate that chaga polysaccharides can induce pro-inflammatory immune responses in both human and murine macrophages *in vitro.* Additionally, the acidic fractions, AcF1 and AcF3, were identified as the most promising candidates. We however interpret the data with caution since all polysaccharides were used at concentrations 1000x higher than the positive controls, LPS-EK and Pam_3CSK_4. Nonetheless, the immunostimulatory effect induced by chaga polysaccharides, provide hopeful prospects for cancer immunotherapy that needs to be further explored.

5.6 Chaga polysaccharides potentially induce tumoricidal macrophages in mouse models

The positive *in vitro* data on the chaga polysaccharides piqued our interest to further investigate their effect *in vivo*. From our findings, the polysaccharides AcF1 and AcF3, augmented by IFN-γ, demonstrated potent anti-tumor effects in mouse models. As shown in the survival graph, 78% of mice in both chaga-treatment groups remained tumor-free, as opposed to 10% survival rate in the untreated category. Again, our *in vivo* results demonstrate that even though IFN-γ is essential for inducing tumoricidal macrophage activities, it is insufficient when used alone, as there were no survivors in the group that received treatment with only IFN-γ. We show that chaga-activated BMDMs are polarized into anti-tumor M1 phenotypes, hence their anti-tumor effect. One mechanism of action could be direct elimination by phagocytosis of tumor cells by activated macrophages, with subsequent presentation of immunogenic peptides to B and T lymphocytes, as have been reported in M1 macrophages (259). Additionally, mice BMDMs activated with chaga polysaccharides have been shown to produce NO, which is not only cytotoxic, but reported to spawn various downstream toxic metabolites, that collectively constitute the anti-tumor capacity of M1 macrophages (261).

In principle, following acute inflammation due to the injection of activated macrophages and LLCs, circulating monocytes and granulocytes would be rapidly recruited into the tissues (262). Additional cytokines and chemokines released by infiltrating immune cells function as chemoattractant for further recruitment. For example, IL-1β secreted by monocytes during early stage inflammation, promotes the growth and differentiation of CD4 T cells (75,263). Moreover, pro-inflammatory cytokines secreted by macrophages, including IL-6, TNF-α, IL-23 and particularly IL-12p70, could dampen the action of regulatory cytokines like TGF-β, and inhibit the differentiation of regulatory T cells (259). Given the influence of other leucocytes *in vivo*, and the complex diversity of cells within the tumor microenvironment, one important question that arises is the evidence of direct killing effected by macrophages and the exact roles/ participation of other immune cells. As we cannot rule out the direct involvement and confounding effects of leukocytes such as DCs, NK cells, B and T lymphocytes, their activities in this context remains to be further explored.

It is worth mentioning that in a re-challenge experiment involving survivors of the initial experiment, tumor-free mice seemed to have acquired some long-term protection against the LLC cancer. However, this result could not be substantiated as only 3 out of 10 naive mice in the control group developed tumors, whereas all surviving mice in the F3 and Pam3 treatment groups remained tumor free (Results not shown). The low tumor take in the control group could likely be due to technical and human errors, albeit, since the experiment was conducted once, it would be plausible to replicate the data in order to provide strong evidence of a long lasting systemic immune response. With this in mind, an important concept that merits investigation is the concept of 'trained immunity'. This is defined as an improved innate immune response to different pathogens following an initial challenge; in the form of vaccination or infection (264). The long-held belief that innate immune cells lack memory has been disputed in recent years as several experimental reports have indicated that innate immune cells, including macrophages can acquire some form of primitive memory through epigenetic and metabolic mechanisms (264–266). Microbial ligands, including β glucans in the cell walls of bacteria and fungi, after binding specific PRRs, subsequently activate the transcription of pro-inflammatory genes. Normally, gene transcription is turned off or significantly downregulated when the initial stimulus is removed or diminishes, however there is evidence of a faster onset and an amplified pro-inflammatory response upon rechallenge with the same or different stimuli, which can protect against a secondary infection. This phenomenon has been linked to epigenetic imprinting in innate immune cells involving histone modifications at the promoter regions of pro-inflammatory genes (265,266).

5.7 Concluding remarks and future perspectives

In summary, this experimental study sought to describe a comprehensive protocol for differentiating human macrophages from monocytes *in vitro* and to investigate the tumoricidal potential of polysaccharides isolated from the medicinal fungus, *Inonotus obliquus*, both *in vitro* and in animal models.

Altogether, the protocol described in this thesis is straightforward, practical, and most importantly, reproducible. We highlighted pragmatic factors in the differentiation and harvesting processes which posed huge limitations initially but resolving them greatly improved on the overall yield and viability of macrophages generated. This optimized methodology will be extremely beneficial to researchers studying the important roles of human macrophages *in vitro.*

Investigating the immunomodulatory effects of chaga polysaccharides revealed two main findings: ***i)*** that chaga polysaccharides could stimulate human macrophages to produce the pro-inflammatory cytokines: IL-6, TNF-α and IL-12p70, with IL-12p70 production being heavily dependent on IFN-γ. ***ii)*** using mouse models, we established that activated BMDMs in the presence of IFN-γ induced a tumoricidal, M1 macrophage phenotype, which subsequently led to protection against LLC tumors inoculated subcutaneously. Coupled with previous findings on NO production and inhibition of growth of cancer cells in mice BMDMs, chaga-activated macrophages could potentially induce direct killing of tumor cells both *in vitro* and *in vivo.* However, since the *in vivo* study was performed once, the intriguing findings cannot lead to definitive conclusions and future efforts should aim at exploiting ways in which these compounds interact with the immune system to generate antitumor responses. In conclusion, there is ample evidence that chaga polysaccharides could generate a potentially powerful therapeutic effect against cancer and should be fully harnessed.

6 REFERENCES

1. Charles A Janeway J, Travers P, Walport M, Shlomchik MJ. The front line of host defense. In: *Immunobiology: The Immune System in Health and Disease*. New York: Garland Science 2001https://www.ncbi.nlm.nih.gov/books/NBK27105/ (accessed 1 Nov2020).

2. Pahram P. The immune system. In: *The immune system*. New York: Garland Science 2015: 24–31.

3. Overview of the Immune System | NIH: National Institute of Allergy and Infectious Diseases. https://www.niaid.nih.gov/research/immune-system-overview (accessed 1 Nov2020).

4. Eberl G, Colonna M, Di Santo JP, McKenzie ANJ. Innate lymphoid cells: A new paradigm in immunology. *Science (80-)* 2015;**348**:6566–6566.

5. Janeway CA. Approaching the asymptote? Evolution and revolution in immunology. *Cold Spring Harb Symp Quant Biol* 1989;**54 Pt 1**:1—13.

6. Alberts, B., Johnson, A., Lewis, J., Raff, M., Roberts, K., and Walter P. *Molecular Biology of the Cell (4th Ed)*. New York: Garland Science 2002https://www.ncbi.nlm.nih.gov/books/NBK26846/

7. Actor JK. *Elsevier's integrated review. Immunology and Microbiology*. Elsevier Saunders 2012

8. Wigley FM, Boin F. Clinical Features and Treatment of Scleroderma. In: Firestein GS, Budd RC, Gabriel SE, McInnes IB, O'Dell JRBT-K and FT of R (Tenth E, editors. *Kelley and Firestein's Textbook of Rheumatology*. Elsevier 2017: 1424-1460.e5.

9. Bando JK, Colonna M. Innate lymphoid cell function in the context of adaptive immunity. Nat. Immunol. 2016;**17**:783–789.

10. Turvey SE, Broide DH. Innate immunity. *J Allergy Clin Immunol* 2010;**125**:S24–S32.

11. Banchereau J, Steinman RM. Dendritic cells and the control of immunity. Nature. 1998;**392**:245–252.

12. Janeway CA, Medzhitov R. Innate Immune Recognition. *Annu Rev Immunol* 2002;**20**:197–216.

13. Atisha-Fregoso Y, Zou YR, Diamond B. B cells and generation of antibodies. In: *Dubois' Lupus Erythematosus and Related Syndromes*. 2018: 101–115.

14. Kumar B V., Connors TJ, Farber DL. Human T Cell Development, Localization, and Function throughout Life. *Immunity* 2018;**48**:202–213.

15. Goswami R, Awasthi A. Editorial: T Cell Differentiation and Function in Tissue Inflammation. *Front Immunol* 2020;**11**:289.

16. Raval RR, Sharabi AB, Walker AJ, Drake CG, Sharma P. Tumor immunology and cancer immunotherapy: Summary of the 2013 SITC primer. J. Immunother. Cancer. 2014;**2**:14.

17. Moriguchi Y, Kan N, Okino T, Harada T, Yamasaki S, Ichinose Y et al. A new model of active specific immunotherapy using interleukin-1 and sonicated tumor supernatant in murine tumor system. *J Surg Oncol* 1996;**62**:78–85.

18. Kulski JK, Shiina T, Anzai T, Kohara S, Inoko H. Comparative genomic analysis of the MHC: The evolution of class I duplication blocks, diversity and complexity from shark to man. Immunol. Rev.

2002;**190**:95–122.

19. Beck S, Geraghty D, Inoko H, Rowen L, Aguado B, Bahram S et al. Complete sequence and gene map of a human major histocompatibility complex. *Nature* 1999;**401**:921–923.

20. Smith-Garvin JE, Koretzky GA, Jordan MS. T cell activation. Annu. Rev. Immunol. 2009;**27**:591–619.

21. Hanahan D, Weinberg RA. Hallmarks of cancer: The next generation. Cell. 2011;**144**:646–674.

22. Hanahan D, Weinberg RA. The hallmarks of cancer. Cell. 2000;**100**:57–70.

23. Corthay A. Does the immune system naturally protect against cancer? Front. Immunol. 2014;**5**:197.

24. Burnet FM. The Concept of Immunological Surveillance. In: *Progress in experimental tumor research. Fortschritte der experimentellen Tumorforschung. Progres de la recherche experimentale des tumeurs*. Karger Publishers 1970: 1–27.

25. Weinberg R. *The Biology of Cancer*. 2nd editio. New York: Garland Science 2014

26. Coley WB. The treatment of malignant tumors by repeated inoculations of erysipelas: With a report of ten original cases. 1. *Am J Med Sci* 1893;**105**:487.

27. Yang Y. Cancer immunotherapy: Harnessing the immune system to battle cancer. J. Clin. Invest. 2015;**125**:3335–3337.

28. Gonzalez S, González-Rodríguez AP, González-Rodríguez AP, Suárez-Álvarez B, López-Soto A, Huergo-Zapico L et al. Conceptual aspects of self and nonself discrimination. *Self Nonself* 2011;**2**:19—25.

29. Ribatti D. The concept of immune surveillance against tumors. The first theories. Oncotarget. 2017;**8**:7175–7180.

30. Ehrlich P. Über den jetzigen Stand der Chemotherapie. *Berichte der Dtsch Chem Gesellschaft* 1909;**42**:17–47.

31. Thomas L. On immunosurveillance in human cancer. *Yale J Biol Med* 1982;**55**:329.

32. Shankaran V, Ikeda H, Bruce AT, White JM, Swanson PE, Old LJ et al. IFNγ, and lymphocytes prevent primary tumour development and shape tumour immunogenicity. *Nature* 2001;**410**:1107–1111.

33. Dunn GP, Bruce AT, Ikeda H, Old LJ, Schreiber RD. Cancer immunoediting: From immunosurveillance to tumor escape. Nat. Immunol. 2002;**3**:991–998.

34. Janeway CA. The immune system evolved to discriminate infectious nonself from noninfectious self. *Immunol Today* 1992;**13**:11–16.

35. Kärre K, Ljunggren HG, Piontek G, Kiessling R. Selective rejection of H-2-deficient lymphoma variants suggests alternative immune defence strategy. *Nature* 1986;**319**:675–678.

36. Dunn GP, Old LJ, Schreiber RD. The immunobiology of cancer immunosurveillance and immunoediting. Immunity. 2004;**21**:137–148.

37. Alsibai KD, Meseure D. Significance of Tumor Microenvironment Scoring and Immune Biomarkers in

Patient Stratification and Cancer Outcomes. In: *Histopathology - An Update*. InTech 2018 doi:10.5772/intechopen.72648

38. Galon J, Fridman WH, Pages F. The adaptive immunologic microenvironment in colorectal cancer: A novel perspective. Cancer Res. 2007;**67**:1883–1886.

39. Stankovic B, Bjørhovde HAK, Skarshaug R, Aamodt H, Frafjord A, Müller E et al. Immune Cell Composition in Human Non-small Cell Lung Cancer. *Front Immunol* 2018;**9**:3101.

40. Melero I, Rouzaut A, Motz GT, Coukos G. T-cell and NK-cell infiltration into solid tumors: A key limiting factor for efficacious cancer immunotherapy. *Cancer Discov* 2014;**4**:522–526.

41. Kornstein MJ, Brooks JSJ, Elder DE. Immunoperoxidase Localization of Lymphocyte Subsets in the Host Response to Melanoma and Nevi. *Cancer Res* 1983;**43**.

42. Whiteside TL. The tumor microenvironment and its role in promoting tumor growth. Oncogene. 2008;**27**:5904–5912.

43. Greten FR, Grivennikov SI. Inflammation and Cancer: Triggers, Mechanisms, and Consequences. *Immunity* 2019;**51**:27–41.

44. Longo V, Brunetti O, Azzariti A, Galetta D, Nardulli P, Leonetti F et al. Strategies to improve cancer immune checkpoint inhibitors efficacy, other than abscopal effect: A systematic review. *Cancers (Basel)* 2019;**11**. doi:10.3390/cancers11040539

45. Das S, Johnson DB. Immune-related adverse events and anti-tumor efficacy of immune checkpoint inhibitors. 2019;**7**. doi:10.1186/s40425-019-0805-8

46. Fares CM, Van Allen EM, Drake CG, Allison JP, Hu-Lieskovan S. Mechanisms of Resistance to Immune Checkpoint Blockade: Why Does Checkpoint Inhibitor Immunotherapy Not Work for All Patients? *Am Soc Clin Oncol Educ B* 2019;:147–164.

47. Gajewski TF, Schreiber H, Fu Y-X. Innate and adaptive immune cells in the tumor microenvironment. *Nat Immunol* 2013;**14**:1014–1022.

48. Galon J, Costes A, Sanchez-Cabo F, Kirilovsky A, Mlecnik B, Lagorce-Pagès C et al. Type, density, and location of immune cells within human colorectal tumors predict clinical outcome. *Science (80-)* 2006;**313**:1960–1964.

49. Bonaventura P, Shekarian T, Alcazer V, Valladeau-Guilemond J, Valsesia-Wittmann S, Amigorena S et al. Cold tumors: A therapeutic challenge for immunotherapy. Front. Immunol. 2019;**10**:168.

50. Duan Q, Zhang H, Zheng J, Zhang L. Turning Cold into Hot: Firing up the Tumor Microenvironment. Trends in Cancer. 2020;**6**:605–618.

51. Hadrup S, Donia M, Thor Straten P. Effector CD4 and CD8 T cells and their role in the tumor microenvironment. *Cancer Microenviron* 2013;**6**:123–133.

52. Martínez-Lostao L, Anel A, Pardo J. How Do Cytotoxic Lymphocytes Kill Cancer Cells? *Clin Cancer Res* 2015;**21**:5047–5056.

53. Corthay A, Skovseth DK, Lundin KU, Røsjø E, Omholt H, Hofgaard PO et al. Primary antitumor immune response mediated by CD4+ T cells. *Immunity* 2005;**22**:371–383.

54. Lanier LL. NKG2D receptor and its ligands in host defense. *Cancer Immunol Res* 2015;**3**:575–582.

55. Mellman I, Coukos G, Dranoff G. Cancer immunotherapy comes of age. *Nature* 2011;**480**:480–489.

56. Tannock IF. Conventional cancer therapy: Promise broken or promise delayed? *Lancet* 1998;**351**:SII9–SII16.

57. Couzin-Frankel J. Cancer Immunotherapy. *Science (80-)* 2013;**342**:1432 LP – 1433.

58. Buchbinder E, Stephen Hodi F. Cytotoxic T lymphocyte antigen-4 and immune checkpoint blockade. J. Clin. Invest. 2015;**125**:3377–3383.

59. Alatrash G, Jakher H, Stafford PD, Mittendorf EA. Cancer immunotherapies, their safety and toxicity. *Expert Opin Drug Saf* 2013;**12**:631–645.

60. Baxevanis CN, Perez SA, Papamichail M. Cancer immunotherapy. Crit. Rev. Clin. Lab. Sci. 2009;**46**:167–189.

61. Nahta R, Esteva FJ. Herceptin: Mechanisms of action and resistance. Cancer Lett. 2006;**232**:123–138.

62. Conlon KC, Miljkovic MD, Waldmann TA. Cytokines in the Treatment of Cancer. *J Interf Cytokine Res* 2019;**39**:6–21.

63. Proleukin® (IL-2) Immunotherapy for Metastatic Melanoma. https://proleukin.com/mm/how-proleukin-works/ (accessed 6 Nov2020).

64. Srivastava S, Riddell SR. Engineering CAR-T cells: Design concepts. Trends Immunol. 2015;**36**:494–502.

65. Leach DR, Krummel MF, Allison JP. Enhancement of antitumor immunity by CTLA-4 blockade. *Science (80-)* 1996;**271**:1734–1736.

66. Krummel MF, Allison JP. CD28 and CTLA-4 have opposing effects on the response of T cells to stimulation. *J Exp Med* 1995;**182**:459–465.

67. Sutmuller RPM, Van Duivenvoorde LM, Van Elsas A, Schumacher TNM, Wildenberg ME, Allison JP et al. Synergism of cytotoxic T lymphocyte-associated antigen 4 blockade and depletion of CD25+ regulatory T cells in antitumor therapy reveals alternative pathways for suppression of autoreactive cytotoxic T lymphocyte responses. *J Exp Med* 2001;**194**:823–832.

68. Liu Y, Zheng P. How Does an Anti-CTLA-4 Antibody Promote Cancer Immunity? Trends Immunol. 2018;**39**:953–956.

69. Pardoll DM. Immunology beats cancer: a blueprint for successful translation. *Nat Immunol* 2012;**13**:1129–1132.

70. Hodi FS, O'Day SJ, McDermott DF, Weber RW, Sosman JA, Haanen JB et al. Improved Survival with Ipilimumab in Patients with Metastatic Melanoma. *N Engl J Med* 2010;**363**:711–723.

71. Sunshine J, Taube JM. PD-1/PD-L1 inhibitors. Curr. Opin. Pharmacol. 2015;**23**:32–38.

72. Rizvi NA, Hellmann MD, Snyder A, Kvistborg P, Makarov V, Havel JJ et al. Mutational landscape determines sensitivity to PD-1 blockade in non-small cell lung cancer. *Science (80-)* 2015;**348**:124–128.

73. Gogas H, Ioannovich J, Dafni U, Stavropoulou-Giokas C, Frangia K, Tsoutsos D et al. Prognostic Significance of Autoimmunity during Treatment of Melanoma with Interferon. *N Engl J Med* 2006;**354**:709–718.

74. Metchnikoff E. *Lectures on the comparative pathology of inflammation delivered at the Pasteur Institute in 1891*. Рипол Классик 1893

75. Arango Duque G, Descoteaux A. Macrophage Cytokines: Involvement in Immunity and Infectious Diseases. *Front Immunol* 2014;**5**. doi:10.3389/fimmu.2014.00491

76. Chang Z-L. Recent development of the mononuclear phagocyte system: in memory of Metchnikoff and Ehrlich on the 100th Anniversary of the 1908 Nobel Prize in Physiology or Medicine. *Biol Cell* 2009;**101**:709–721.

77. Stefater JA, Ren S, Lang RA, Duffield JS. Metchnikoff's policemen: Macrophages in development, homeostasis and regeneration. Trends Mol. Med. 2011;**17**:743–752.

78. Tauber AI. Metchnikoff and the phagocytosis theory. Nat. Rev. Mol. Cell Biol. 2003;**4**:897–901.

79. Aschoff L. Das reticulo-endotheliale System. In: *Ergebnisse der inneren Medizin und Kinderheilkunde*. Springer 1924: 1–118.

80. Wake K, Kawai Y, Smedsrød B. Re-evaluation of the reticulo-endothelial system. *Ital J Anat Embryol* 2001;**106**:261–269.

81. van Furth R, Cohn ZA, Hirsch JG, Humphrey JH, Spector WG, Langevoort HL. The mononuclear phagocyte system: a new classification of macrophages, monocytes, and their precursor cells. *Bull World Health Organ* 1972;**46**:845–852.

82. Kelly A, Grabiec AM, Travis MA. Culture of Human Monocyte-Derived Macrophages BT - Macrophages: Methods and Protocols. In: Rousselet G, editor. *Methods in Molecular Biology*. New York, NY: Springer New York 2018: 1–11.

83. Murray PJ, Wynn TA. Protective and pathogenic functions of macrophage subsets. *Nat Rev Immunol* Published Online First: 2011. doi:10.1038/nri3073

84. Ginhoux F, Guilliams M. Tissue-Resident Macrophage Ontogeny and Homeostasis. *Immunity* 2016;**44**:439–449.

85. Jakubzick C V, Randolph GJ, Henson PM. Monocyte differentiation and antigen-presenting functions. *Nat Rev Immunol* 2017;**17**:349–362.

86. Geissmann F, Manz MG, Jung S, Sieweke MH, Merad M, Ley K. Development of monocytes, macrophages, and dendritic cells. Science (80-.). 2010;**327**:656–661.

87. Coillard A, Segura E. In vivo Differentiation of Human Monocytes . Front. Immunol. . 2019;**10**:1907.

88. Kapellos TS, Bonaguro L, Gemünd I, Reusch N, Saglam A, Hinkley ER et al. Human monocyte subsets and phenotypes in major chronic inflammatory diseases. Front. Immunol. 2019;**10**:2035.

89. Gren ST, Rasmussen TB, Janciauskiene S, Hakansson K, Gerwien JG, Grip O. A single-cell gene-expression profile reveals inter-cellular heterogeneity within human monocyte subsets. *PLoS One*

2015;**10**. doi:10.1371/journal.pone.0144351

90. Yona S, Kim K-W, Wolf Y, Mildner A, Varol D, Breker M et al. Fate mapping reveals origins and dynamics of monocytes and tissue macrophages under homeostasis. *Immunity* 2013;**38**:79–91.

91. Sieweke MH, Allen JE. Beyond stem cells: Self-renewal of differentiated macrophages. Science (80-.). 2013;**342**. doi:10.1126/science.1242974

92. Ginhoux F, Jung S. Monocytes and macrophages: developmental pathways and tissue homeostasis. *Nat Rev Immunol* 2014;**14**:392–404.

93. Chawla A. Control of macrophage activation and function by PPARs. Circ. Res. 2010;**106**:1559–1569.

94. Aderem A, Underhill DM. Mechanisms of phagocytosis in macrophages. Annu. Rev. Immunol. 1999;**17**:593–623.

95. Wood W. Clearance of apoptotic debris in PU.1 KO embryos. 2000https://dev.biologists.org/content/127/24/5245.short (accessed 2 Nov2020).

96. Wood W, Turmaine M, Weber R, Camp V, Maki RA, McKercher SR et al. Mesenchymal cells engulf and clear apoptotic footplate cells in macrophageless PU.1 null mouse embryos. *Development* 2000;**127**:5245 LP – 5252.

97. Tang D, Kang R, Coyne CB, Zeh HJ, Lotze MT. PAMPs and DAMPs: Signal 0s that spur autophagy and immunity. *Immunol Rev* 2012;**249**:158–175.

98. Amarante-Mendes GP, Adjemian S, Branco LM, Zanetti LC, Weinlich R, Bortoluci KR. Pattern recognition receptors and the host cell death molecular machinery. Front. Immunol. 2018;**9**:2379.

99. Zaru R. Pattern recognition receptors ligands Category: Receptors and Molecules. Br. Soc. Immunol. 2020;:1–2.

100. Poltorak A, He X, Smirnova I, Liu MY, Van Huffel C, Du X et al. Defective LPS signaling in C3H/HeJ and C57BL/10ScCr mice: Mutations in Tlr4 gene. *Science (80-)* 1998;**282**:2085–2088.

101. Aderem A. Phagocytosis and the Inflammatory Response. *J Infect Dis* 2003;**187**:S340–S345.

102. Mann ER, Li X. Intestinal antigen-presenting cells in mucosal immune homeostasis: Crosstalk between dendritic cells, macrophages and B-cells. World J. Gastroenterol. 2014;**20**:9653–9664.

103. Unanue ER. Antigen-Presenting Function of the Macrophage. *Annu Rev Immunol* 1984;**2**:395–428.

104. Kambayashi T, Laufer TM. Atypical MHC class II-expressing antigen-presenting cells: Can anything replace a dendritic cell? Nat. Rev. Immunol. 2014;**14**:719–730.

105. Barker RN, Erwig LP, Hill KSK, Devine A, Pearce WP, Rees AJ. Antigen presentation by macrophages is enhanced by the uptake of necrotic, but not apoptotic, cells. *Clin Exp Immunol* 2002;**127**:220–225.

106. Unanue ER. Antigen Presentation Via MHC Class II Molecules. In: *Encyclopedia of Immunology*. Elsevier 1998: 194–198.

107. Waithman J, Moffat JM, Patterson NL, van Beek AE, Mintern JD. Antigen Presentation. In: *Reference Module in Biomedical Sciences*. Elsevier 2014 doi:10.1016/B978-0-12-801238-3.00118-5

108. Benveniste E. Chapter 00175 - Cytokines | Elsevier Enhanced Reader. In: *Elsevier Inc*. 2014: 921–925.

109. Cavaillon JM. Cytokines and macrophages. *Biomed Pharmacother* 1994;**48**:445–453.

110. Müller E, Speth M, Christopoulos PF, Lunde A, Avdagic A, Øynebråten I et al. Both type I and type II interferons can activate antitumor M1 macrophages when combined with TLR stimulation. *Front Immunol* 2018;**9**. doi:10.3389/fimmu.2018.02520

111. Müller E, Christopoulos PF, Halder S, Lunde A, Beraki K, Speth M et al. Toll-like receptor ligands and interferon-γ synergize for induction of antitumor M1 macrophages. *Front Immunol* 2017;**8**:1383.

112. Corthay A, Skovseth DK, Lundin KU, Røsjø E, Omholt H, Hofgaard PO et al. Primary antitumor immune response mediated by CD4+ T cells. *Immunity* 2005;**22**:371–383.

113. Mantovani A, Sica A, Sozzani S, Allavena P, Vecchi A, Locati M. The chemokine system in diverse forms of macrophage activation and polarization. *Trends Immunol* 2004;**25**:677–686.

114. Contassot E, Beer HD, French LE. Interleukin-1, inflammasomes, autoinflammation and the skin. Swiss Med. Wkly. 2012;**142**. doi:10.4414/smw.2012.13590

115. Dickerson EB, Akhtar N, Steinberg H, Wang ZY, Lindstrom MJ, Padilla ML et al. Enhancement of the antiangiogenic activity of interleukin-12 by peptide targeted delivery of the cytokine to α vβ 3 integrin. *Mol Cancer Res* 2004;**2**:663–673.

116. Zheng H, Ban Y, Wei F, Ma X. Regulation of interleukin-12 production in antigen-presenting cells. In: *Advances in Experimental Medicine and Biology*. Springer New York LLC 2016: 117–138.

117. Oswald IP, Wynn TA, Sher A, James SL. Interleukin 10 inhibits macrophage microbicidal activity by blocking the endogenous production of tumor necrosis factor α required as a costimulatory factor for interferon γ-induced activation. *Proc Natl Acad Sci U S A* 1992;**89**:8676–8680.

118. Varzaneh FN, Keller B, Unger S, Aghamohammadi A, Warnatz K, Rezaei N. Cytokines in common variable immunodeficiency as signs of immune dysregulation and potential therapeutic targets - A review of the current knowledge. J. Clin. Immunol. 2014;**34**:524–543.

119. Kubiczkova L, Sedlarikova L, Hajek R, Sevcikova S. TGF-β - an excellent servant but a bad master. J. Transl. Med. 2012;**10**:1–24.

120. Travis MA, Sheppard D. TGF-β activation and function in immunity. Annu. Rev. Immunol. 2014;**32**:51–82.

121. Ushach I, Zlotnik A. Biological role of granulocyte macrophage colony-stimulating factor (GM-CSF) and macrophage colony-stimulating factor (M-CSF) on cells of the myeloid lineage. *J Leukoc Biol* 2016;**100**:481–489.

122. Egea L, Hirata Y, Kagnoff MF. GM-CSF: A role in immune and inflammatory reactions in the intestine. Expert Rev. Gastroenterol. Hepatol. 2010;**4**:723–731.

123. Trus E, Basta S, Gee K. Who's in charge here? Macrophage colony stimulating factor and granulocyte macrophage colony stimulating factor: Competing factors in macrophage polarization. *Cytokine* 2020;**127**:1–6.

124. Fleetwood AJ, Achuthan A, Hamilton JA. Colony Stimulating Factors (CSFs). In: *Encyclopedia of*

Immunobiology. Elsevier Inc. 2016: 586–596.

125. Willman CL, Stewart CC, Miller V, Yi TL, Tomasi TB. Regulation of MHC class II gene expression in macrophages by hematopoietic colony-stimulating factors (CSF). Induction by granulocyte/macrophage CSF and inhibition by CSF-1. *J Exp Med* 1989;**170**:1559–1567.

126. Wiktor-Jedrzejczak W, Bartocci A, Ferrante AW, Ahmed-Ansari A, Sell KW, Pollard JW et al. Total absence of colony-stimulating factor 1 in the macrophage-deficient osteopetrotic (op/op) mouse. *Proc Natl Acad Sci* 1990;**87**:4828–4832.

127. Jones C V, Ricardo SD. Macrophages and CSF-1: implications for development and beyond. *Organogenesis* 2013;**9**:249–260.

128. Martinez FO, Gordon S. The M1 and M2 paradigm of macrophage activation: time for reassessment. *F1000Prime Rep* 2014;**6**.

129. Oo YH, Shetty S, Adams DH. The role of chemokines in the recruitment of lymphocytes to the liver. Dig. Dis. 2010;**28**:31–44.

130. Rot A, von Andrian UH. Chemokines in innate and adaptive host defense: basic chemokinese grammar for immune cells. *Annu Rev Immunol* 2004;**22**:891–928.

131. Unanue ER, Beller DI, Calderon J, Kiely JM, Stadecker MJ. Regulation of immunity and inflammation by mediators from macrophages. Am. J. Pathol. 1976;**85**:465–478.

132. Addison CL, Arenberg DA, Morris SB, Xue YY, Burdick MD, Mulligan MS et al. The CXC chemokine, monokine induced by interferon-γ, inhibits non-small cell lung carcinoma tumor growth and metastasis. *Hum Gene Ther* 2000;**11**:247–261.

133. Gouwy M, Struyf S, Catusse J, Proost P, Van Damme J. Synergy between proinflammatory ligands of G protein-coupled receptors in neutrophil activation and migration. *J Leukoc Biol* 2004;**76**:185–194.

134. Harada A, Sekido N, Akahoshi T, Wada T, Mukaida N, Matsushima K. Essential involvement of interleukin-8 (IL-8) in acute inflammation. In: *Journal of Leukocyte Biology*. Federation of American Societies for Experimental Biology 1994: 559–564.

135. Van Damme J, Struyf S, Opdenakker G. Chemokine-protease interactions in cancer. *Semin Cancer Biol* 2004;**14**:201–208.

136. Gijsbers K, Van Assche G, Joossens S, Struyf S, Proost P, Rutgeerts P et al. CXCR1-binding chemokines in inflammatory bowel diseases: Down-regulated IL-8/CXCL8 production by leukocytes in Crohn's disease and selective GCP-2/CXCL6 expression in inflamed intestinal tissue. *Eur J Immunol* 2004;**34**:1992–2000.

137. Liu M, Guo S, Hibbert JM, Jain V, Singh N, Wilson NO et al. CXCL10/IP-10 in infectious diseases pathogenesis and potential therapeutic implications. Cytokine Growth Factor Rev. 2011;**22**:121–130.

138. Haabeth OAW, Lorvik KB, Hammarström C, Donaldson IM, Haraldsen G, Bogen B et al. Inflammation driven by tumour-specific Th1 cells protects against B-cell cancer. *Nat Commun* 2011;**2**. doi:10.1038/ncomms1239

139. Mosser DM, Edwards JP. Exploring the full spectrum of macrophage activation. Nat. Rev. Immunol. 2008;**8**:958–969.

140. Murray PJ, Allen JE, Biswas SK, Fisher EA, Gilroy DW, Goerdt S et al. Macrophage Activation and Polarization: Nomenclature and Experimental Guidelines. Immunity. 2014;**41**:14–20.

141. Hamilton TA. Macrophage activation. *Contemp Top Immunobiol* 1984;**13**:1–262.

142. Murray PJ. Macrophage Polarization. Annu. Rev. Physiol. 2017;**79**:541–566.

143. Adams DO. Macrophages as destructive cells in host defence. *Inflamm Basic Princ Clin Correl* 1992;:637–662.

144. Mackaness GB. Cellular resistance to infection. *J Exp Med* 1962;**116**:381–406.

145. Nathan CF, Murray HW, Wiebe ME, Rubin BY. Identification of interferon-gamma as the lymphokine that activates human macrophage oxidative metabolism and antimicrobial activity. *J Exp Med* 1983;**158**:670—689.

146. Liu Y-C, Zou X-B, Chai Y-F, Yao Y-M. Macrophage Polarization in Inflammatory Diseases. *Int J Biol Sci* 2014;**10**. doi:10.7150/ijbs.8879

147. Stein M, Keshav S, Harris N, Gordon S. Interleukin 4 Potently Enhances Murine Macrophage Mannose Receptor Activity: A Marker of Alternative Immunologic Macrophage Activation. *J Exp Med 176(1), 287-292* 1992;**1**:287–292.

148. Murray PJ, Allen JE, Biswas SK, Fisher EA, Gilroy DW, Goerdt S et al. Macrophage Activation and Polarization: Nomenclature and Experimental Guidelines. Immunity. 2014;**41**:14–20.

149. Mills CD, Kincaid K, Alt JM, Heilman MJ, Hill AM. M-1/M-2 Macrophages and the Th1/Th2 Paradigm. *J Immunol* 2000;**164**:6166–6173.

150. Gao C-H, Dong H-L, Tai L, Gao X-M. Lactoferrin-Containing Immunocomplexes Drive the Conversion of Human Macrophages from M2- into M1-like Phenotype. *Front Immunol* 2018;**9**:23.

151. Locati M, Curtale G, Mantovani A. Diversity, Mechanisms, and Significance of Macrophage Plasticity. *Annu Rev Pathol Mech Dis* 2020;**15**:123–147.

152. Jablonski KA, Amici SA, Webb LM, Ruiz-Rosado J de D, Popovich PG, Partida-Sanchez S et al. Novel Markers to Delineate Murine M1 and M2 Macrophages. *PLoS One* 2015;**10**:e0145342.

153. Biswas SK, Mantovani A. Macrophage plasticity and interaction with lymphocyte subsets: Cancer as a paradigm. Nat. Immunol. 2010;**11**:889–896.

154. Roszer T. Understanding the mysterious M2 macrophage through activation markers and effector mechanisms. Mediators Inflamm. 2015;**2015**. doi:10.1155/2015/816460

155. El Kasmi KC, Qualls JE, Pesce JT, Smith AM, Thompson RW, Henao-Tamayo M et al. Toll-like receptor–induced arginase 1 in macrophages thwarts effective immunity against intracellular pathogens. *Nat Immunol* 2008;**9**:1399–1406.

156. Antonios JK, Yao Z, Li C, Rao AJ, Goodman SB. Macrophage polarization in response to wear particles in vitro. *Cell Mol Immunol* 2013;**10**:471–482.

157. Gong D, Shi W, Yi S ju, Chen H, Groffen J, Heisterkamp N. TGFβ signaling plays a critical role in promoting alternative macrophage activation. *BMC Immunol* 2012;**13**:31.

158. Chávez-Galán L, Olleros ML, Vesin D, Garcia I. Much more than M1 and M2 macrophages, there are also CD169+ and TCR+ macrophages. Front. Immunol. 2015;**6**:263.

159. Martinez FO, Helming L, Gordon S. Alternative activation of macrophages: An immunologic functional perspective. Annu. Rev. Immunol. 2009;**27**:451–483.

160. Chang CI, Liao JC, Kuo L. Arginase modulates nitric oxide production in activated macrophages. *Am J Physiol - Hear Circ Physiol* 1998;**274**. doi:10.1152/ajpheart.1998.274.1.h342

161. Mantovani A, Sozzani S, Locati M, Allavena P, Sica A. Macrophage polarization: Tumor-associated macrophages as a paradigm for polarized M2 mononuclear phagocytes. Trends Immunol. 2002;**23**:549–555.

162. Joshi S, Singh AR, Zulcic M, Bao L, Messer K, Ideker T et al. Rac2 controls tumor growth, metastasis and M1-M2 macrophage differentiation in vivo. *PLoS One* 2014;**9**:e95893.

163. Orecchioni M, Ghosheh Y, Pramod AB, Ley K. Macrophage polarization: Different gene signatures in M1(Lps+) vs. Classically and M2(LPS-) vs. Alternatively activated macrophages. Front. Immunol. 2019;**10**:1084.

164. Fleetwood AJ, Lawrence T, Hamilton JA, Cook AD. Granulocyte-macrophage colony-stimulating factor (CSF) and macrophage CSF-dependent macrophage phenotypes display differences in cytokine profiles and transcription factor activities: implications for CSF blockade in inflammation. *J Immunol* 2007;**178**:5245–5252.

165. Fleetwood AJ, Dinh H, Cook AD, Hertzog PJ, Hamilton JA. GM-CSF-and M-CSF-dependent macrophage phenotypes display differential dependence on type I interferon signaling. *J Leukoc Biol* 2009;**86**:411–421.

166. Jayasingam SD, Citartan M, Thang TH, Mat Zin AA, Ang KC, Ch'ng ES. Evaluating the Polarization of Tumor-Associated Macrophages Into M1 and M2 Phenotypes in Human Cancer Tissue: Technicalities and Challenges in Routine Clinical Practice. Front. Oncol. 2020;**9**:1512.

167. Solinas G, Germano G, Mantovani A, Allavena P. Tumor-associated macrophages (TAM) as major players of the cancer-related inflammation. *J Leukoc Biol* 2009;**86**:1065–1073.

168. Zhou J, Tang Z, Gao S, Li C, Feng Y, Zhou X. Tumor-Associated Macrophages: Recent Insights and Therapies. Front. Oncol. 2020;**10**:188.

169. Vitale I, Manic G, Coussens LM, Kroemer G, Galluzzi L. Macrophages and Metabolism in the Tumor Microenvironment. Cell Metab. 2019;**30**:36–50.

170. Dai F, Liu L, Che G, Yu N, Pu Q, Zhang S et al. The number and microlocalization of tumor-associated immune cells are associated with patient's survival time in non-small cell lung cancer. *BMC Cancer* 2010;**10**:220.

171. Frafjord A, Skarshaug R, Hammarström C, Stankovic B, Dorg LT, Aamodt H et al. Antibody combinations for optimized staining of macrophages in human lung tumours. *Scand J Immunol* 2020;**92**. doi:10.1111/sji.12889

172. Kim D-W, Min HS, Lee K-H, Kim YJ, Oh D-Y, Jeon YK et al. High tumour islet macrophage infiltration correlates with improved patient survival but not with EGFR mutations, gene copy number or protein expression in resected non-small cell lung cancer. *Br J Cancer* 2008;**98**:1118–1124.

173. Lin EY, Pollard JW. Tumor-associated macrophages press the angiogenic switch in breast cancer. Cancer Res. 2007;**67**:5064–5066.

174. Qian BZ, Pollard JW. Macrophage Diversity Enhances Tumor Progression and Metastasis. Cell. 2010;**141**:39–51.

175. Lamagna C, Aurrand-Lions M, Imhof BA. Dual role of macrophages in tumor growth and angiogenesis. *J Leukoc Biol* 2006;**80**:705–713.

176. Yang Q, Guo N, Zhou Y, Chen J, Wei Q, Han M. The role of tumor-associated macrophages (TAMs) in tumor progression and relevant advance in targeted therapy. Acta Pharm. Sin. B. 2020. doi:10.1016/j.apsb.2020.04.004

177. Loyher PL, Hamon P, Laviron M, Meghraoui-Kheddar A, Goncalves E, Deng Z et al. Macrophages of distinct origins contribute to tumor development in the lung. *J Exp Med* 2018;**215**:1–18.

178. Chen Y, Song Y, Du W, Gong L, Chang H, Zou Z. Tumor-associated macrophages: An accomplice in solid tumor progression. J. Biomed. Sci. 2019;**26**. doi:10.1186/s12929-019-0568-z

179. Cassetta L, Pollard JW. Targeting macrophages: therapeutic approaches in cancer. *Nat Rev Drug Discov* 2018;**17**:887–904.

180. Pettenati C, Ingersoll MA. Mechanisms of BCG immunotherapy and its outlook for bladder cancer. *Nat Rev Urol* 2018;**15**:615–625.

181. Redelman-Sidi G, Glickman MS, Bochner BH. The mechanism of action of BCG therapy for bladder cancer—a current perspective. *Nat Rev Urol* 2014;**11**:153.

182. Alexandroff AB, Jackson AM, O'Donnell MA, James K. BCG immunotherapy of bladder cancer: 20 years on. *Lancet* 1999;**353**:1689–1694.

183. Movahedi K, Laoui D, Gysemans C, Baeten M, Stangé G, Van Bossche J Den et al. Different tumor microenvironments contain functionally distinct subsets of macrophages derived from Ly6C(high) monocytes. *Cancer Res* 2010;**70**:5728–5739.

184. Jeong H, Kim S, Hong BJ, Lee CJ, Kim YE, Bok S et al. Tumor-associated macrophages enhance tumor hypoxia and aerobic glycolysis. *Cancer Res* 2019;**79**:795–806.

185. Chevrier S, Levine JH, Zanotelli VRT, Silina K, Schulz D, Bacac M et al. An Immune Atlas of Clear Cell Renal Cell Carcinoma. *Cell* 2017;**169**:736-749.e18.

186. Pathria P, Louis TL, Varner JA. Targeting Tumor-Associated Macrophages in Cancer. Trends Immunol. 2019;**40**:310–327.

187. Kozloski GA. Macrophage Markers. *Mater Methods* 2019;**9**. doi:10.13070/mm.en.9.2758

188. Ferenbach D, Hughes J. Macrophages and dendritic cells: What is the difference? Kidney Int. 2008;**74**:5–7.

189. Davis MJ, Tsang TM, Qiu Y, Dayrit JK, Freij JB, Huffnagle GB et al. Macrophage M1/M2 polarization dynamically adapts to changes in cytokine microenvironments in Cryptococcus neoformans infection. *MBio* 2013;**4**. doi:10.1128/mBio.00264-13

190. Mosser DM. The many faces of macrophage activation. *J Leukoc Biol* 2003;**73**:209–212.

191. Martinez FO, Gordon S. The M1 and M2 paradigm of macrophage activation: Time for reassessment. *F1000Prime Rep* 2014;**6**. doi:10.12703/P6-13

192. Binesh A, Devaraj SN, Devaraj H. Expression of chemokines in macrophage polarization and downregulation of NFκB in aorta allow macrophage polarization by diosgenin in atherosclerosis. *J Biochem Mol Toxicol* 2020;**34**. doi:10.1002/jbt.22422

193. Xuan W, Qu Q, Zheng B, Xiong S, Fan G-H. The chemotaxis of M1 and M2 macrophages is regulated by different chemokines. *J Leukoc Biol* 2015;**97**:61–69.

194. Darnell JE, Kerr IM, Stark GR. Jak-STAT pathways and transcriptional activation in response to IFNs and other extracellular signaling proteins. *Science (80-)* 1994;**264**:1415–1421.

195. Tarique AA, Logan J, Thomas E, Holt PG, Sly PD, Fantino E. Phenotypic,functional,and plasticity features of classical and alternatively activated human macrophages. *Am J Respir Cell Mol Biol* 2015;**53**:676–688.

196. Mia S, Warnecke A, Zhang XM, Malmström V, Harris RA. An optimized protocol for human M2 macrophages using M-CSF and IL-4/IL-10/TGF-β yields a dominant immunosuppressive phenotype. *Scand J Immunol* 2014;**79**:305–314.

197. Jaguin M, Houlbert N, Fardel O, Lecureur V. Polarization profiles of human M-CSF-generated macrophages and comparison of M1-markers in classically activated macrophages from GM-CSF and M-CSF origin. *Cell Immunol* 2013;**281**:51–61.

198. Ambarus CA, Krausz S, van Eijk M, Hamann J, Radstake TRDJ, Reedquist KA et al. Systematic validation of specific phenotypic markers for in vitro polarized human macrophages. *J Immunol Methods* 2012;**375**:196–206.

199. Stout RD, Jiang C, Matta B, Tietzel I, Watkins SK, Suttles J. Macrophages Sequentially Change Their Functional Phenotype in Response to Changes in Microenvironmental Influences. *J Immunol* 2005;**175**:342–349.

200. Colin S, Chinetti-Gbaguidi G, Staels B. Macrophage phenotypes in atherosclerosis. *Immunol Rev* 2014;**262**:153–166.

201. Grinberg S, Hasko G, Wu D, Leibovich SJ. Suppression of PLCβ2 by endotoxin plays a role in the adenosine A2A receptor-mediated switch of macrophages from an inflammatory to an angiogenic phenotype. *Am J Pathol* 2009;**175**:2439–2453.

202. Ferrante CJ, Leibovich SJ. Regulation of macrophage polarization and wound healing. *Adv wound care* 2012;**1**:10–16.

203. Ferrante CJ, Pinhal-Enfield G, Elson G, Cronstein BN, Hasko G, Outram S et al. The adenosine-dependent angiogenic switch of macrophages to an M2-like phenotype is independent of interleukin-4 receptor alpha (IL-4Rα) signaling. *Inflammation* 2013;**36**:921–931.

204. Chan GCF, Chan WK, Sze DMY. The effects of beta-glucan on human immune and cancer cells. J. Hematol. Oncol. 2009;**2**:25.

205. Zhang M, Chun L, Sandoval V, Graor H, Myers J, Nthale J et al. Systemic administration of β-glucan of 200 kDa modulates melanoma microenvironment and suppresses metastatic cancer. *Oncoimmunology* 2018;**7**:e1387347.

206. Yan J, Allendorf DJ, Brandley B. Yeast whole glucan particle (WGP) β-glucan in conjunction with antitumour monoclonal antibodies to treat cancer. Expert Opin. Biol. Ther. 2005;**5**:691–702.

207. Bose N, Chan ASH, Guerrero F, Maristany C, Walsh R, Ertelt K et al. Binding of Soluble Yeast β-Glucan to Human Neutrophils and Monocytes is Complement-Dependent . Front. Immunol. . 2013;**4**:230.

208. Wold CW, Kjeldsen C, Corthay A, Rise F, Christensen BE, Duus JØ et al. Structural characterization of bioactive heteropolysaccharides from the medicinal fungus Inonotus obliquus (Chaga). *Carbohydr Polym* 2018;**185**:27–40.

209. Géry A, Dubreule C, André V, Rioult J-P, Bouchart V, Heutte N et al. Chaga (Inonotus obliquus), a Future Potential Medicinal Fungus in Oncology? A Chemical Study and a Comparison of the Cytotoxicity Against Human Lung Adenocarcinoma Cells (A549) and Human Bronchial Epithelial Cells (BEAS-2B). *Integr Cancer Ther* 2018;**17**:832–843.

210. Song FQ, Liu Y, Kong XS, Chang W, Song G. Progress on understanding the anticancer mechanisms of medicinal mushroom: Inonotus obliquus. Asian Pacific J. Cancer Prev. 2013;**14**. doi:10.7314/APJCP.2013.14.3.1571

211. Arata S, Watanabe J, Maeda M, Yamamoto M, Matsuhashi H, Mochizuki M et al. Continuous intake of the Chaga mushroom (Inonotus obliquus) aqueous extract suppresses cancer progression and maintains body temperature in mice. *Heliyon* 2016;**2**. doi:10.1016/j.heliyon.2016.e00111

212. Ham SS, Kim SH, Moon SY, Chung MJ, Cui CB, Han EK et al. Antimutagenic effects of subfractions of Chaga mushroom (Inonotus obliquus) extract. *Mutat Res - Genet Toxicol Environ Mutagen* 2009;**672**:55–59.

213. Youn MJ, Kim JK, Park SY, Kim Y, Kim SJ, Lee JS et al. Chaga mushroom (Inonotus obliquus) induces Go/G1 arrest and apoptosis in human hepatoma HepG2 cells. *World J Gastroenterol* 2008;**14**:511–517.

214. Kim YO, Park HW, Kim JH, Lee JY, Moon SH, Shin CS. Anti-cancer effect and structural characterization of endo-polysaccharide from cultivated mycelia of Inonotus obliquus. *Life Sci* 2006;**79**:72–80.

215. Van Q, Nayak BN, Reimer M, Jones PJH, Fulcher RG, Rempel CB. Anti-inflammatory effect of Inonotus obliquus, Polygala senega L., and Viburnum trilobum in a cell screening assay. *J Ethnopharmacol* 2009;**125**:487–493.

216. Najafzadeh M, Reynolds PD, Baumgartner A, Jerwood D, Anderson D. Chaga mushroom extract inhibits oxidative DNA damage in lymphocytes of patients with inflammatory bowel disease. *BioFactors* 2007;**31**:191–200.

217. Won DP, Lee JS, Kwon DS, Lee KE, Shin WC, Hong EK. Immunostimulating activity by polysaccharides isolated from fruiting body of Inonotus obliquus. *Mol Cells* 2011;**31**:165–173.

218. Aiken CD and SJ. KOVA ® GLASSTIC ® SLIDE 10 WITH GRIDS. In: *Urologie*. 1983: 79-undefined.

219. Louis KS, Siegel AC. Cell Viability Analysis Using Trypan Blue: Manual and Automated Methods. In: Stoddart MJ, editor. *Methods in Molecular Biology*. New York: Springer Science 2011: 7–12.

220. Tomayko MM, Reynolds CP. Determination of subcutaneous tumor size in athymic (nude) mice. *Cancer Chemother Pharmacol* 1989;**24**:148–154.

221. Pickl WF, Majdic O, Kohl P, Stöckl J, Riedl E, Scheinecker C et al. Molecular and functional characteristics of dendritic cells generated from highly purified CD14+ peripheral blood monocytes. *J Immunol* 1996;**157**:3850–3859.

222. Gibon E, Loi F, Córdova LA, Pajarinen J, Lin T, Lu L et al. Aging Affects Bone Marrow Macrophage Polarization: Relevance to Bone Healing. *Regen Eng Transl Med* 2016;**2**:98–104.

223. Guilliams M, Ginhoux F, Jakubzick C, Naik SH, Onai N, Schraml BU et al. Dendritic cells, monocytes and macrophages: a unified nomenclature based on ontogeny. *Nat Rev Immunol* 2014;**14**:571–578.

224. Müller E, Christopoulos PF, Halder S, Lunde A, Beraki K, Speth M et al. Toll-like receptor ligands and interferon-γ synergize for induction of antitumor M1 macrophages. *Front Immunol* 2017;**8**:1383.

225. Smyth CM. Differential subcellular localization of CD86 in human PBMC-derived macrophages and DCs, and ultrastructural characterization by immuno-electron microscopy. *Int Immunol* 2004;**17**:123–132.

226. Carswell EA, Old LJ, Kassel RL, Green S, Fiore N, Williamson B. An endotoxin induced serum factor that cuases necrosis of tumors. *Proc Natl Acad Sci U S A* 1975;**72**:3666–3670.

227. Pennica D, Nedwin GE, Hayflick JS, Seeburg PH, Derynck R, Palladino MA et al. Human tumour necrosis factor: precursor structure, expression and homology to lymphotoxin. *Nature* 1984;**312**:724–729.

228. Wang KS, Frank DA, Ritz J. Interleukin-2 enhances the response of natural killer cells to interleukin-12 through up-regulation of the interleukin-12 receptor and STAT4. *Blood* 2000;**95**:3183–3190.

229. Kelly A, Grabiec AM, Travis MA. Culture of human monocyte-derived macrophages. In: *Methods in Molecular Biology*. Humana Press Inc. 2018: 1–11.

230. Erbel C, Rupp G, Helmes CM, Tyka M, Linden F, Doesch AO et al. An in vitro model to study heterogeneity of human macrophage differentiation and polarization. *J Vis Exp* 2013;:50332.

231. Davies JQ, Gordon S. Isolation and culture of human macrophages. *Methods Mol Biol* 2005;**290**:105–116.

232. Nielsen MC, Andersen MN, Møller HJ. Monocyte isolation techniques significantly impact the phenotype of both isolated monocytes and derived macrophages *in vitro*. *Immunology* 2020;**159**:63–74.

233. Delirezh N, Shojaeefar E, Parvin P, Asadi B. Comparison the effects of two monocyte isolation methods, plastic adherence and magnetic activated cell sorting methods, on phagocytic activity of generated dendritic cells. *Cell J* 2013;**15**:218–223.

234. Bhattacharjee J, Das B, Mishra A, Sahay P, Upadhyay P. Monocytes isolated by positive and negative magnetic sorting techniques show different molecular characteristics and immunophenotypic behaviour. *F1000Research* 2018;**6**. doi:10.12688/f1000research.12802.3

235. Miltenyi S, Müller W, Weichel W, Radbruch A. High gradient magnetic cell separation with MACS. *Cytometry* 1990;**11**:231–238.

236. Contents 1. Description 1.1 Principle of the MACS® Separation 1.2 Background information 1.3 Applications 1.4 Reagent and instrument requirements 2. Protocol 2.1 Sample preparation 2.2 Magnetic labeling 2.3 Magnetic separation 3. Example of a separation using the CD14 MicroBeads 4. References. www.miltenyibiotec.com/ (accessed 21 Jan2021).

237. Guha M, Mackman N. LPS induction of gene expression in human monocytes. *Cell Signal* 2001;**13**:85–94.

238. Kim D, Kim JY. Anti-CD14 antibody reduces LPS responsiveness via TLR4 internalization in human monocytes. *Mol Immunol* 2014;**57**:210–215.

239. Lescoat A, Ballerie A, Augagneur Y, Morzadec C, Vernhet L, Fardel O et al. Distinct properties of human M-CSF and GM-CSF monocyte-derived macrophages to simulate pathological lung conditions in vitro: Application to systemic and inflammatory disorders with pulmonary involvement. *Int J Mol Sci* 2018;**19**. doi:10.3390/ijms19030894

240. Gao J, Scheenstra MR, van Dijk A, Veldhuizen EJA, Haagsman HP. A new and efficient culture method for porcine bone marrow-derived M1- and M2-polarized macrophages. *Vet Immunol Immunopathol* 2018;**200**:7–15.

241. Rimaniol A-C, Haïk S, Martin M, Le Grand R, Boussin FD, Dereuddre-Bosquet N et al. Na + -Dependent High-Affinity Glutamate Transport in Macrophages . *J Immunol* 2000;**164**:5430–5438.

242. Lukic A, Larssen P, Fauland A, Samuelsson B, Wheelock CE, Gabrielsson S et al. GM-CSF– and M-CSF–primed macrophages present similar resolving but distinct inflammatory lipid mediator signatures. *FASEB J* 2017;**31**:4370–4381.

243. Hashimoto SI, Suzuki T, Dong HY, Yamazaki N, Matsushima K. Serial analysis of gene expression in human monocytes and macrophages. *Blood* 1999;**94**:837–844.

244. Marti LC, Bacal NS, Bento LC, Rocha FA. Phenotypic Markers and Functional Regulators of Myelomonocytic Cells. In: *Biology of Myelomonocytic Cells*. InTech 2017 doi:10.5772/67324

245. Brunner D, Frank J, Appl H, Schöffl H, Pfaller W, Gstraunthaler G. Serum-free cell culture: the serum-free media interactive online database. *ALTEX* 2010;**27**:53–62.

246. van der Valk J, Bieback K, Buta C, Cochrane B, Dirks WG, Fu J et al. Fetal Bovine Serum (FBS): Past - Present - Future. *ALTEX* 2018;**35**:99–118.

247. Vojgani Y, Shirazi A, Zarei S, Yeganeh O, Jeddi-Tehrani M. Comparison of efficacies of fetal bovine sera from different suppliers in cell culture experiments. doi:10.1007/s00580-017-2622-0

248. Fang CY, Wu CC, Fang CL, Chen WY, Chen CL. Long-term growth comparison studies of FBS and FBS alternatives in six head and neck cell lines. *PLoS One* 2017;**12**. doi:10.1371/journal.pone.0178960

249. Leporatti S, Gerth A, Köhler G, Kohlstrunk B, Hauschildt S, Donath E. Elasticity and adhesion of resting and lipopolysaccharide-stimulated macrophages. *FEBS Lett* 2006;**580**:450–454.

250. Malheiro V, Elbs-Glatz Y, Obarzanek-Fojt M, Maniura-Weber K, Bruinink A. Harvesting pre-polarized macrophages using thermo-responsive substrates. *Sci Rep* 2017;**7**:42495.

251. Zarif JC, Hernandez JR, Verdone JE, Campbell SP, Drake CG, Pienta KJ. A phased strategy to differentiate human CD14+ monocytes into classically and alternatively activated macrophages and

dendritic cells. *Biotechniques* 2016;**61**:33–41.

252. Cho HJ, Shashkin P, Gleissner CA, Dunson D, Jain N, Lee JK et al. Induction of dendritic cell-like phenotype in macrophages during foam cell formation. *Physiol Genomics* 2007;**29**:149–160.

253. Wentworth JM, Naselli G, Brown WA, Doyle L, Phipson B, Smyth GK et al. Pro-Inflammatory CD11c⁺CD206⁺ Adipose Tissue Macrophages Are Associated With Insulin Resistance in Human Obesity. *Diabetes* 2010;**59**:1648 LP – 1656.

254. Lavnikova N, Drapier JC, Laskin DL. A single exogenous stimulus activates resident rat macrophages for nitric oxide production and tumor cytotoxicity. *J Leukoc Biol* 1993;**54**:322–328.

255. Meng F, Lowell CA. Lipopolysaccharide (LPS)-induced macrophage activation and signal transduction in the absence of Src-family kinases Hck, Fgr, and Lyn. *J Exp Med* 1997;**185**:1661–1670.

256. Lu YC, Yeh WC, Ohashi PS. LPS/TLR4 signal transduction pathway. Cytokine. 2008;**42**:145–151.

257. Pålsson-McDermott EM, O'Neill LAJ. Signal transduction by the lipopolysaccharide receptor, Toll-like receptor-4. Immunology. 2004;**113**:153–162.

258. Wold CW, Christopoulos PF, Arias MA, Dzovor DE, Øynebråten I, Corthay A et al. Polysaccharides from the fungus Inonotus obliquus activate macrophages into a tumoricidal phenotype via interaction with TLR2, TLR4 and Dectin-1a. *bioRxiv* 2020;:2020.11.11.378356.

259. Tugues S, Burkhard SH, Ohs I, Vrohlings M, Nussbaum K, vom Berg J et al. New insights into IL-12-mediated tumor suppression. *Cell Death Differ* 2015;**22**:237–246.

260. Perussia B, Chan SH, D'andrea A, Tsuji K, Santoli D, Pospisil M et al. Natural killer (NK) cell stimulatory factor or IL-12 has differential effects on the proliferation of TCR-alpha beta+, TCR-gamma delta+ T lymphocytes, and NK cells. *J Immunol* 1992;**149**:3495–3502.

261. Ley K. M1 Means Kill; M2 Means Heal. *J Immunol* 2017;**199**:2191 LP – 2193.

262. Nywening TM, Wang-Gillam A, Sanford DE, Belt BA, Panni RZ, Cusworth BM et al. Targeting tumour-associated macrophages with CCR2 inhibition in combination with FOLFIRINOX in patients with borderline resectable and locally advanced pancreatic cancer: a single-centre, open-label, dose-finding, non-randomised, phase 1b trial. *Lancet Oncol* 2016;**17**:651–662.

263. Ben-Sasson SZ, Hu-Li J, Quiel J, Cauchetaux S, Ratner M, Shapira I et al. IL-1 acts directly on CD4 T cells to enhance their antigen-driven expansion and differentiation. *Proc Natl Acad Sci U S A* 2009;**106**:7119–7124.

264. Netea MG, Giamarellos-Bourboulis EJ, Domínguez-Andrés J, Curtis N, van Crevel R, van de Veerdonk FL et al. Trained Immunity: a Tool for Reducing Susceptibility to and the Severity of SARS-CoV-2 Infection. *Cell* 2020;**181**:969–977.

265. Lérias JR, de Sousa E, Paraschoudi G, Martins J, Condeço C, Figueiredo N et al. Trained Immunity for Personalized Cancer Immunotherapy: Current Knowledge and Future Opportunities. *Front Microbiol* 2019;**10**:2924.

266. Netea MG, Domínguez-Andrés J, Barreiro LB, Chavakis T, Divangahi M, Fuchs E et al. Defining trained immunity and its role in health and disease. *Nat Rev Immunol* 2020;**20**:375–388.

7. SUPPLEMENTARY

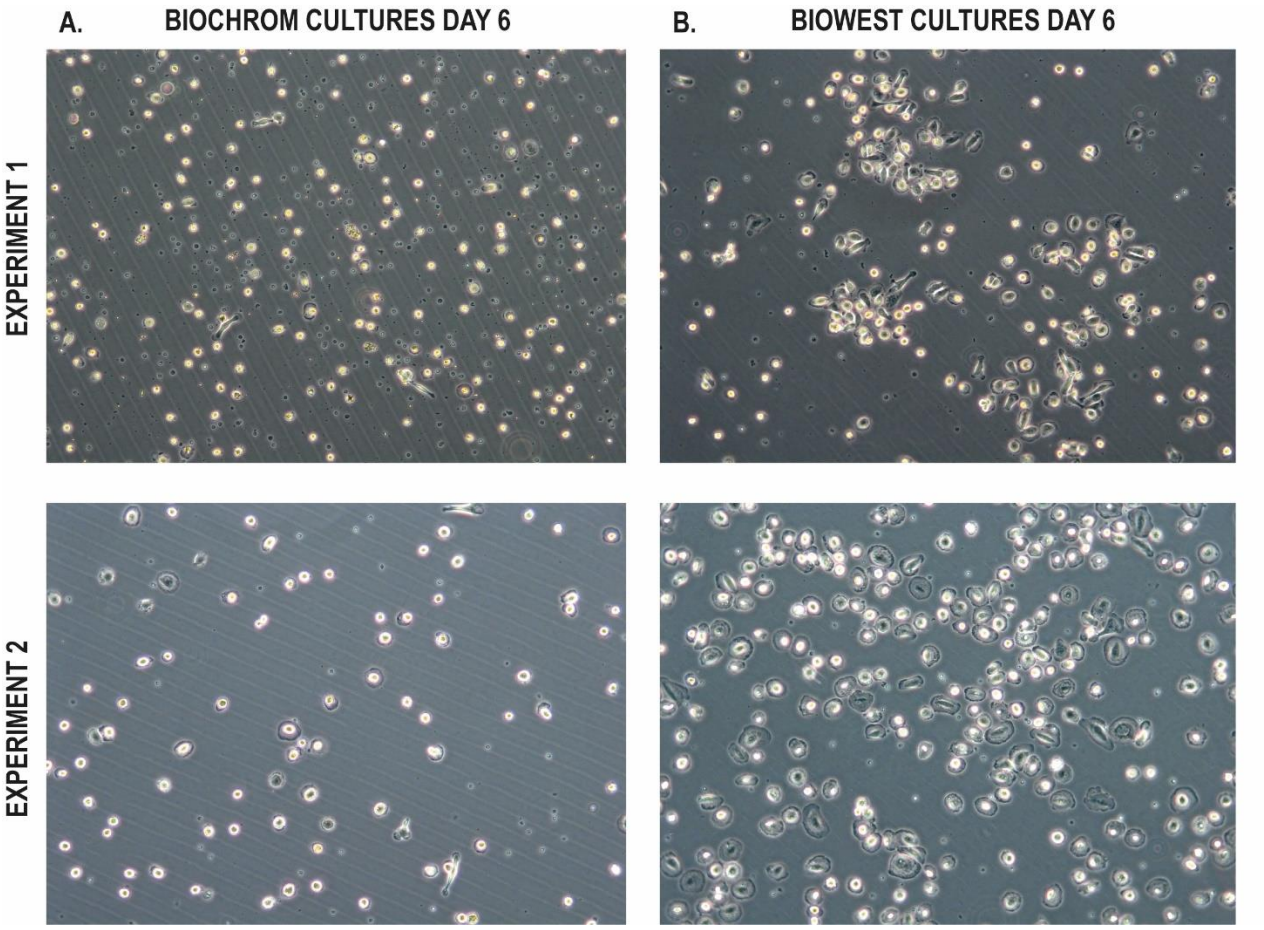

Supplementary Figure 1. Comparison of the effect of sera from different suppliers on macrophage differentiation.

Photographs show cultures of differentiated MoDMs on day 6. CD14+ monocytes were seeded at 3.0 x10^6/ 10 mL growth medium containing RPMI 1640 w/L-Glutamine +10% FBS +1% Pen/Strep. The FBS were obtained from two suppliers: ***(A)*** *Biochrom and* ***(B)*** *BioWest. The experiment was performed twice, and cells in experiments 1 (top row) and 2 (bottom row) were obtained from different donors. Images were taken on day 6 before harvesting; original magnification at x 60.*

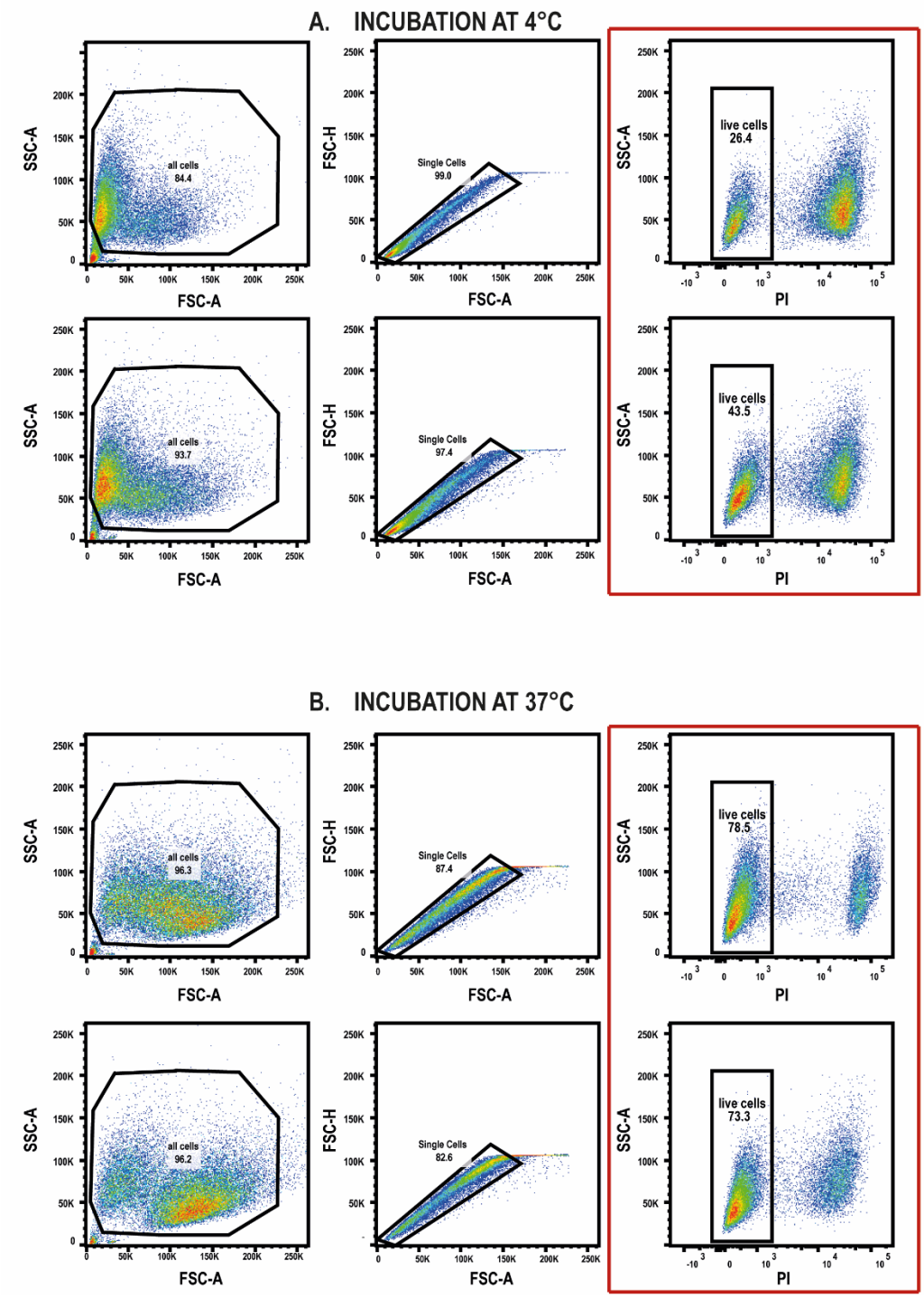

Supplementary Figure 2. Effect of different detachment techniques on MoDMs yield and viability. *Mature MoDMs were harvested on culture day 6 by incubation with detachment buffer at either 4 °C or 37 °C. Harvested cells were analysed for viability through flow cytometry; staining was done with propidium iodide (PI). All cells were gated using FSC vs SSC parameters, followed by single cell gating with FSC-A vs FSC-H. Live cells (Red rectangle) were gated by exlcuding all events positive for the PI stain. Two identical cultures were compared under each condition with an average of* ***(A)*** *35% viable cells obtained during incubation at 4 °C as opposed to* ***(B)*** *76% when incubated at 37 °C.*

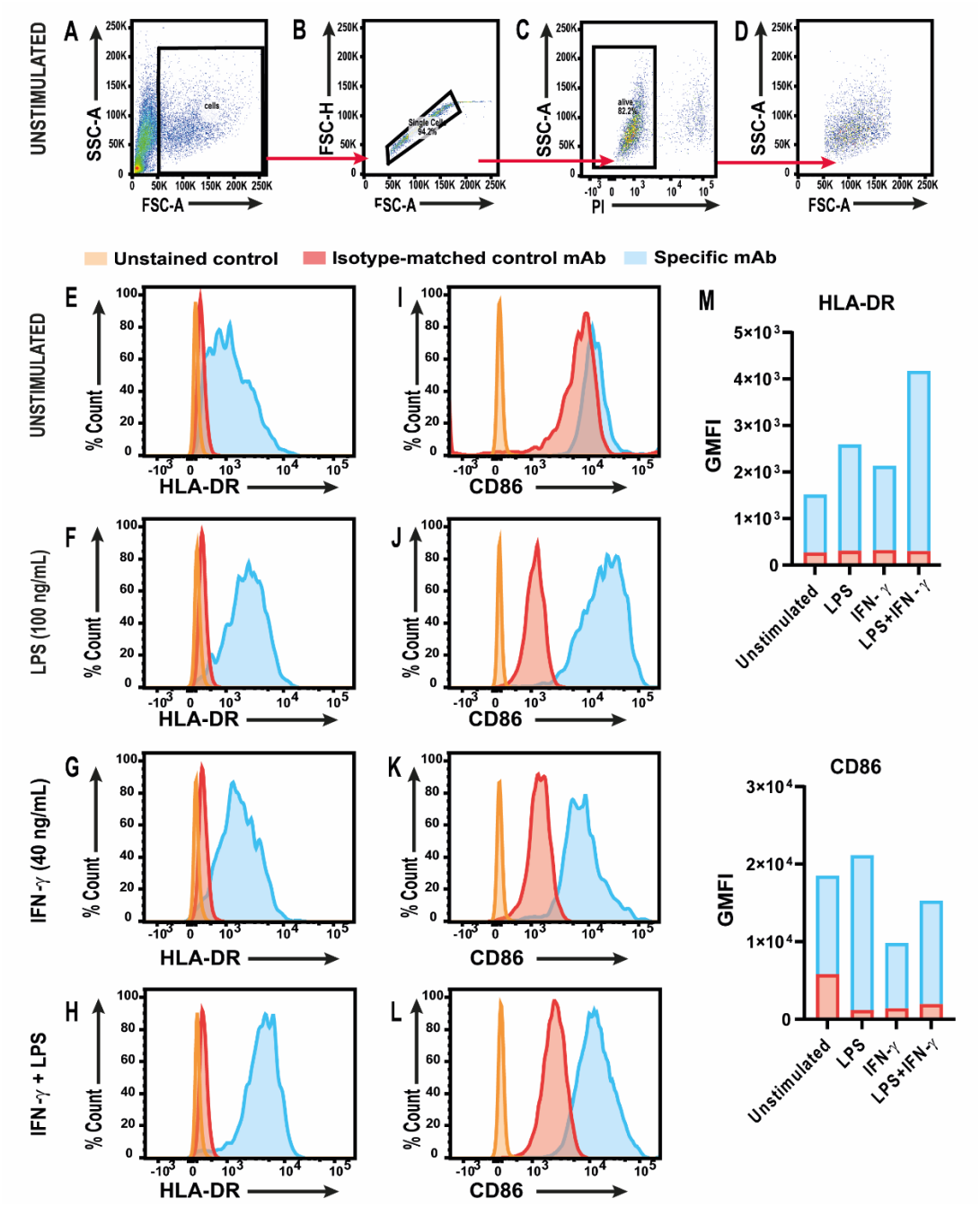

Supplementary Figure 3. Flow cytometric analysis of M1 polarized macrophages.
*In vitro GM-CSF differentiated macrophages induce activation markers after overnight stimulation with 100 ng/mL LPS only (from E. coli K12), 40 ng/mL IFN-γ only or LPS+ IFN-γ at stated concentrations. (**A**) Size exclusion gate used to select cells above 50K on FSC scale. (**B**) Single cells were identified using FSC-A and FSC-H parameters and (**C**) dead cells stained with propidium iodide (PI) were excluded. (**D**) Resulting population was identified as live, fully differentiated MoDMs and used for the analysis. Unstimulated macrophages were used as control and identical gates were set for macrophages activated with either LPS or IFN-γ only, or LPS+IFN-γ (not shown). Histograms showing expression of established classically activated macrophage markers: HLA-DR **(E)**, **(F)**, **(G)**, **(H)** and CD86 **(I)**, **(J)**, **(K)**, **(L)** in unstimulated, LPS, IFN-γ, and LPS+ IFN-γ treated MoDMs, respectively. **(M)** The GMFI for all conditions were compared to confirm results obtained.*

Supplementary Table 1. Comparison of serum-coated tubes vs. plain tubes during harvesting of MoDMs.

Cell counting comparing MoDMs harvested into serum-coated falcon tubes vs. non-coated tubes after centrifugation at x 400g, 4°C for 7 min. Cell pellets were resuspended in 1 mL residual medium after centrifugation and counting was performed manually, using KOVA Glasstic® microscopic slide. Trypan was used to exclude dead cells. Table show average counts from three independent experiments.

Parameter	Serum-coated tubes	Plain tubes
Live cells	4.3×10^6	1.2×10^6
Dead cells	5.0×10^5	7.6×10^5
Total	4.8×10^6	1.9×10^6
Viability	**90%**	**62%**

8. ANNEX - MANUSCRIPT

Polysaccharides from the fungus *Inonotus obliquus* activate macrophages into a tumoricidal phenotype via interaction with TLR2, TLR4, and Dectin-1a

Wold CW[a], Christopoulos PF[b], Arias MA[c], Dzovor DE[b], Øynebråten I[b], Corthay A[bd]*, Inngjerdingen KT[a]*

[a] Section for Pharmaceutical Chemistry, Department of Pharmacy, University of Oslo, Norway

[b] Tumor Immunology Lab, Department of Pathology, Rikshospitalet, Oslo University Hospital, Oslo, Norway

[c] Centro de Investigación Biomédica de Aragón (CIBA), University of Zaragoza, Spain

[d] Hybrid Technology Hub – Centre of Excellence, Institute of Basic Medical Sciences, University of Oslo, Oslo, Norway.

* These authors contributed equally

Abstract

Tumor-associated macrophages (TAMs) may both promote and suppress tumor development, and molecules that can polarize these cells into a tumoricidal phenotype are of great immunotherapeutical interest. Fungal β-glucans have been suggested for triggering the antitumor activity of TAMs, but particulate β-glucans have limitations due to their large size and poor water-solubility. Here, we used water-soluble polysaccharides isolated from the medicinal fungus *Inonotus obliquus* in order to activate mouse and human macrophages. We show that two different fractions of acidic polysaccharides from *I. obliquus* bind Toll-like receptor (TLR) 2, TLR4, and Dectin-1a and induce an M1 antitumor macrophage phenotype, associated with *in vitro* tumoricidal activity and secretion of the pro-inflammatory cytokines interleukin (IL)-6, tumor necrosis factor (TNF)-α and the Th1 polarizing cytokine IL-12p70. Polysaccharide-activated macrophages efficiently prevented tumor development in mice upon co-injection with cancer cells. Our data reveal that polysaccharides from *I. obliquus* have a unique potential for activating macrophages, through simultaneous triggering of multiple receptors, which could lead to a new strategy for cancer immunotherapy.

Abbreviations. TAM, Tumor-Associated Macrophage; TLR, Toll-Like Receptor; IL, Interleukin; TNF-α, Tumor Necrosis Factor α; IFN-γ, Interferon γ; NO, Nitric Oxide; PRR, Pattern Recognition Receptor; GalA, (1→4)-α-Galacturonic Acid; GS-MS, Gas Chromatography – Mass Spectrometry; NMR, Nuclear Magnetic Resonance; BMDMs, Bone Marrow-Derived Macrophages; iNOS, inducible Nitric Oxide Synthase; LLC cells, Lewis Lung Carcinoma cells; PMB, Polymyxin B; LPS, Lipopolysaccharide; ZymC, Zymosan Crude; ZymP, Zymosan Purified; SEAP, Secreted Embryonic Alkaline Phosphatase; CM, Conditioned Medium; M-CSF, Macrophage Colony-Stimulating Factor.

Introduction

Cancer is a leading cause of mortality worldwide. The ability of our immune system to combat this complex and heterogeneous disease is well documented and has been demonstrated by the success of immune checkpoint inhibitors that activate T cells to eliminate cancer tamas. Depending on molecular cues from the tumor microenvironment, there is emerging evidence that certain immune cells such as macrophages can display both anti- and pro-tumorigenic phenotypes [3-5]. For example, tumor-associated macrophages (TAMs) can be pro-tumorigenic by promoting angiogenesis and by dampening the general immune response against the tumor. In these cases, there is often a correlation between high TAM density and poor survival of cancer patients [6,7]. As such, TAMs are attractive targets for novel anti-tumor immunotherapy drugs, evident by the increasing number of ongoing clinical trials against solid tumors using macrophage-targeting agents [4]. Activation of macrophages might induce anti-tumor responses by several distinct mechanisms. Polarization of macrophages into an anti-tumor "M1" phenotype by stimulation with toll-like receptor (TLR) ligands and interferon γ (IFN-γ) causes upregulation of nitric oxide (NO) and cytokines like tumor necrosis factor alpha α (TNF-α) [8], leading to direct killing of cancer cells [8]. Further, chemokines such as CXCL9 and CXCL10 produced by activated TAMs are shown to be important for $CD8^+$ T cell infiltration into tumors [9,10]. Finally, macrophage activation could lead to increased uptake of tumor neoantigens with subsequent presentation of the antigens to T cells, in addition to activation of NK cells [4,7,11].

Fungal polysaccharides, especially β-glucans, have recently emerged as promising candidates for macrophage polarization into an M1 phenotype, due to their non-toxic nature and their potential to bind pattern recognition receptors (PRRs) such as Dectin-1 [12-14]. Fungal β-glucans are

polymers consisting of glucose in a β-anomeric configuration with (1→3) and/or (1→6) glycosidic linkages between the monomers. Particulate, large-sized (1→3)/(1→6)-β-glucans are able to elicit strong immune responses by binding to the C-type lectin receptor Dectin-1 found on macrophages and dendritic cells [15]. However, there is conflicting evidence in the literature regarding fungal β-glucans, often because alleged β-glucans are not actually pure β-glucans but rather a mix of various polysaccharides, proteins and lipoproteins. For example, when the TLR2/Dectin-1 agonist zymosan – a cell wall preparation of *Saccharomyces cerevisiae* rich in β-glucans – was treated with various solvents to purify the β-glucan part, the TLR2 binding capability was lost whereas the affinity for Dectin-1 was fully retained [16]. The TLR2 binding capability of zymosan has been attributed to other fungal compounds, and it now appears evident that smaller-sized, water-soluble polysaccharides are able to bind to and activate TLR2 [17,18].

Inonotus obliquus, a white-rot fungus found on birch trees in the northern hemisphere, is a promising source of bioactive compounds, and several authors have described immunomodulating polysaccharides from this fungus [19,20]. However, systematic characterization of the immunological properties of *I. obliquus* polysaccharides is lacking. Further, the immune receptors responsible for the activity have not yet been established. One study indicated that a crude polysaccharide extract from *I. obliquus* induced TLR2 signaling, but the extract was not chemically characterized [21]. We have previously isolated polysaccharides from the water- and alkali extracts from interior and exterior parts of *I. obliquus* [22]. We found that the water-extracted polysaccharides were complex and highly branched, and in addition to (1→3/1→6)-β-glucose (Glc) they contained several types of sugars, such as (1→6)-α-galactose (Gal), (1→4)-α-galacturonic acid (GalA), (1→3)-α-mannose (Man) and (1→4)-β-xylose (Xyl). The alkali-extracted polysaccharides had a simpler structural motif that resembled the classical β-glucans found in other fungi. The polysaccharides were screened using the Griess assay to measure NO production by the macrophage cell line J774A.1 and the dendritic cell line D2SC/1. Six polysaccharides were deemed promising for further testing, and these form the basis of the studies presented herein, in which we performed an extensive immunological characterization of the isolated and purified polysaccharides from *I. obliquus*. We show that two of the water-extracted, acidic polysaccharide fractions, denominated AcF1 and AcF3, induce potent production of NO, TNF-α, IL-6 and IL12-p70 in macrophages via TLR2, TLR4, and Dectin-1, which was associated with a strong *in vitro* and *in vivo* tumoricidal activity. The ability of these

polysaccharides to activate multiple receptors using “one molecule” has not previously been demonstrated and could open new avenues for cancer immunotherapy.

Results

Polysaccharides from *I. obliquus* synergize with IFN-γ to induce nitric oxide production by macrophages in a dose-dependent manner

The main structural and chemical characteristics of the *I. obliquus* polysaccharides used in this study are summarized in Figure 1a. Based on their structural motifs and molecular weight, the polysaccharides could be allocated to three main structural types, defined by their water-solubility and their absence (neutral) or presence (acidic) of galacturonic acid. Simplified structural models of the polysaccharides are shown in Figure 1b. The models represent probable polymer compositions based on gas chromatography - mass spectrometry (GS-MS) data and nuclear magnetic resonance (NMR) spectroscopy, but the illustrations do not necessarily reflect the structural complexity or the accurate relationship between the monomers. For detailed characteristics of the polysaccharides, see Wold et al. (2018) [22]. While the water-soluble polysaccharides consisted of many types of monomers, the particulate and high molecular weight polysaccharide A1 consisted predominantly of (1→3)/(1→6)-β-glucose, thus resembling the classical immunogenic β-glucan structure described in the literature [15].

Figure 1

a

Polysaccharide fraction	Abbreviation	Molecular weight (kDa)	Water-solubility	Type	Main monomeric units
I. obliquus interior part, water-soluble, neutral	IWN	60	Yes	Neutral	(1→3/1→6)-β-Glc (1→6)-α-Gal
I. obliquus exterior part, water-soluble, neutral	EWN	73	Yes	Neutral	(1→3/1→6)-β-Glc (1→6)-α-Gal
I. obliquus interior part, water-soluble, acidic fraction 1	AcF1	28	Yes	Acidic	(1→3/1→6)-β-Glc (1→6)-α-Gal (1→4)-α-GalA
I. obliquus interior part, water-soluble, acidic fraction 2	AcF2	14	Yes	Acidic	(1→3/1→6)-β-Glc (1→6)-α-Gal (1→4)-α-GalA (1→4)-β-Xyl
I. obliquus interior part, water-soluble, acidic fraction 3	AcF3	10	Yes	Acidic	(1→3/1→6)-β-Glc (1→6)-α-Gal (1→4)-α-GalA (1→4)-β-Xyl
I. obliquus interior part, alkali-extracted, neutral	A1	>450	No (particulate)	Neutral	(1→3/1→6)-β-Glc (1→4)-β-Xyl

b

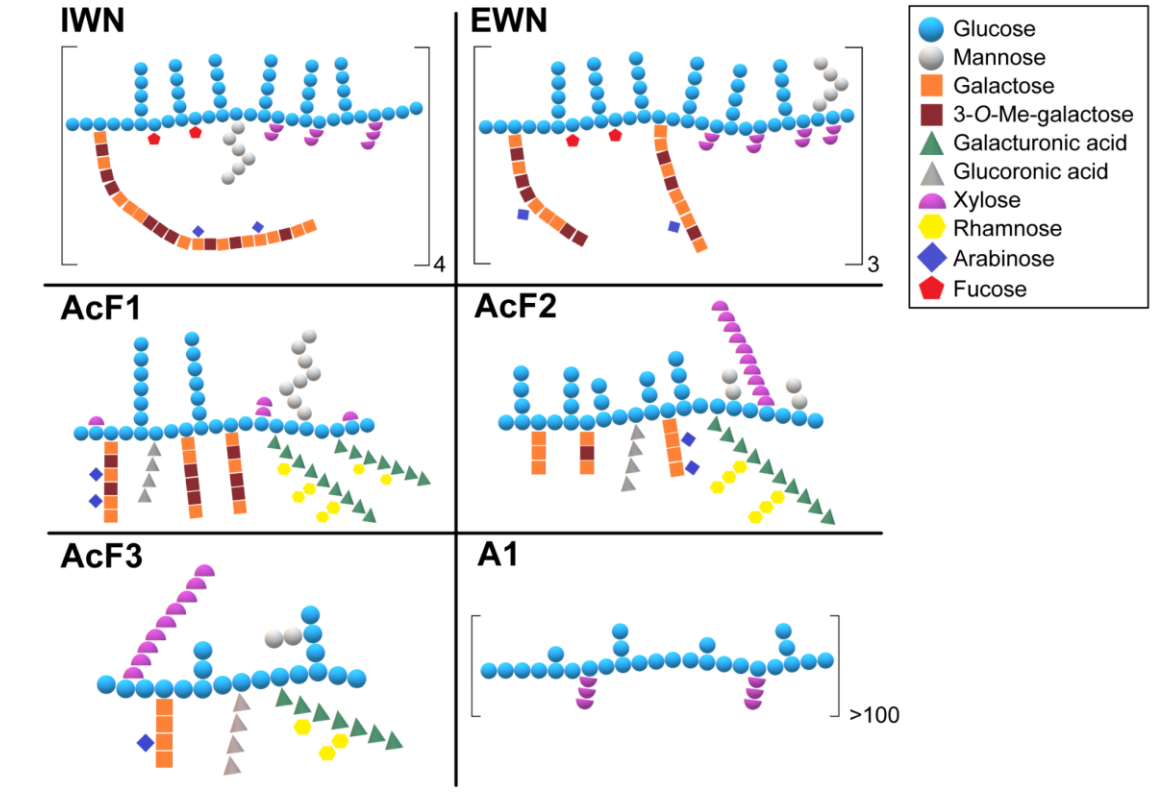

Figure 1. Characteristics of the polysaccharides isolated from *I. obliquus* used in this study. **a**) An overview of names, abbreviations and the most important chemical characteristics of the polysaccharides, including molecular

weight, water solubility and main monomeric units. **b**) Tentative structures of the polysaccharides based on GC, GC-MS and NMR spectroscopic data. The drawings are theoretical, and do not necessarily reflect the three-dimensional shape of the polymers or the accuracy of the linkages between the different monomers. IWN and EWN are neutral polymers, with β-glucose and α-galactose being the main monomeric units. AcF1, AcF2 and AcF3 are acidic polysaccharides with β-glucose as the main monomeric unit, with varying amounts of α-galacturonic acid, α-galactose and other monomers. A1 is an alkali-extracted polysaccharide with much higher molecular weight than the rest, and consists almost exclusively of β-glucose, in addition to minor amounts of β-xylose.

The polysaccharides were analyzed for their ability to induce NO production by macrophages, as NO is an important marker of an M1 macrophage phenotype [7]. Bone marrow-derived mouse macrophages (BMDMs) were generated from C57BL/6NRj mice and were incubated with polysaccharides alone or in combination with IFN-γ. The Griess assay was then used to measure NO in the cell supernatants. IFN-γ is known to synergize with TLR ligands to induce a tumoricidal macrophage phenotype [8], and all six *I. obliquus* polysaccharides were capable of activating macrophages to secrete NO in a dose-dependent manner when used in combination with IFN-γ (Figure 2a). Most of the polysaccharides required co-treatment with IFN-γ to activate the macrophages. However, AcF1 in the absence of IFN-γ, was able to statistically significantly increase the NO production, and AcF3 alone showed a trend toward increased NO production compared to the untreated control BMDMs. Notably, AcF1 and AcF3 were also more potent than the rest when used in combination with IFN-γ.

Next, we investigated the ability of the polysaccharides to induce mRNA production of inducible nitric oxide synthase (iNOS) which is the enzyme that catalyzes the production of NO from L-arginine [23]. Figure 2b shows iNOS mRNA levels compared to the housekeeping gene 18S rRNA in BMDMs which had been treated with polysaccharides at 100 µg/mL with or without IFN-γ. Compared to macrophages treated with IFN-γ only, the iNOS mRNA levels were statistically significantly upregulated in macrophages treated with EWN, AcF1, AcF2 or AcF3 in combination with IFN-γ (Figure 2b). Moreover, although not significant, AcF1 and AcF3 alone showed a tendency towards increased iNOS mRNA levels beyond the level observed in untreated BMDMs. The results correlated with the nitrite levels seen in Figure 2a, and confirm that the polysaccharides synergize with IFN-γ to activate mouse macrophages to produce NO.

Figure 2

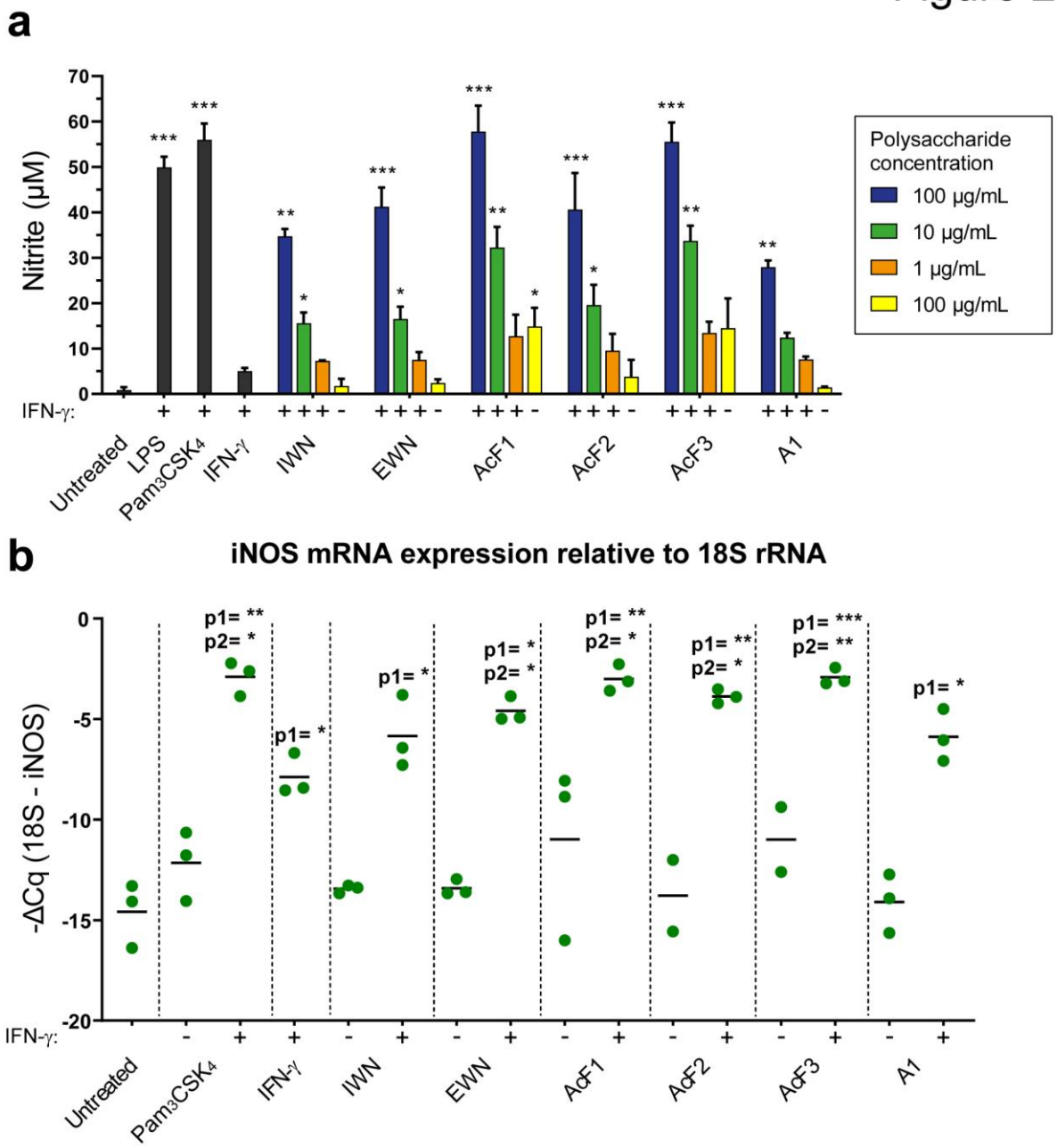

Figure 2. Polysaccharides from *I. obliquus* synergize with IFN-γ to induce NO production by mouse macrophages. **a)** Bone marrow-derived macrophages (BMDMs) were incubated for 24 h with polysaccharides at different concentrations (1, 10 and 100 µg/mL) with IFN-γ (20 ng/mL), or at 100 µg/mL alone, before nitrite levels in the supernatants were quantified using the Griess assay. Lipopolysaccharide (LPS) from *E. coli* (100 ng/mL) and Pam_3CSK_4 (100 ng/mL) together with IFN-γ (20 ng/mL) were used as positive controls. Three independent experiments were performed, and the pooled data are shown as means ± SD. Statistical significance was calculated using one-way ANOVA followed by Dunn's multiple comparison test, with single comparisons against the untreated control. *** = $p < 0.001$, ** = $p < 0.01$, * = $p < 0.05$. **b)** BMDMs were incubated for 24 h with polysaccharides (100

μg/mL) with or without IFN-γ (20 ng/mL), before cells were harvested, mRNA was isolated and iNOS mRNA and 18S rRNA were quantified using RT-qPCR. Pam_3CSK_4 (100 ng/mL) and IFN-γ (20 ng/mL) alone or in combination were used as controls. Each dot in the graph represents the mean value of technical triplicates from one experiment. The black lines indicate means for two or three independent experiments. Statistical significance was calculated using one-way ANOVA followed by Dunn's multiple comparison test, with single comparisons against either untreated macrophages (p1) or against the IFN-γ-treated macrophages (p2). *** = $p < 0.001$, ** = $p < 0.01$, * = $p < 0.05$

Water-soluble *I. obliquus* polysaccharides synergize with IFN-γ to make macrophages inhibit cancer cell growth *in vitro*

To investigate the potential of the *I. obliquus* polysaccharides to inhibit cancer cell growth, an *in vitro* growth inhibition assay was conducted by co-culturing BMDMs with Lewis lung carcinoma (LLC) cells. As described in Figure 3a, the macrophages were first treated with the DNA crosslinker mitomycin C to prevent their proliferation. Next, BMDMs were incubated with the polysaccharides in the absence or presence of IFN-γ for 24 h before LLC cells were added using three different ratios between macrophages and LLC cells (20:1, 10:1, and 1:1). Ultimately, proliferation of the cancer cells was measured after the addition of radiolabeled thymidine, which is an indirect way of measuring macrophage-mediated cytostatic and/or cytotoxic effects on the cancer cells. Several of the polysaccharides were able to activate the macrophages to inhibit cancer cell proliferation (Figure 3b), and this activation correlated with NO levels in the cell supernatants (Figure 3c). All polysaccharides, except the particulate β-glucan fraction A1, gave a dose-dependent inhibitory effect on cancer cell proliferation, with the most prominent effect seen from AcF1 and AcF3 in combination with IFN-γ. The growth inhibition was almost equally effective at ratio 10:1 and 20:1 of BMDM:LLC. However, at lower concentrations of the polysaccharides: 10 and 1 μg/ml of AcF1 and 1 μg/ml of AcF3 the ratio 20:1 showed a trend towards being more effective than 10:1. Also in this assay, AcF3 showed a tendency of being effective alone, in the absence of IFN-γ (ratio 20:1). At BMDM:LLC 1:1 ratio, the cancer cell proliferation was only marginally inhibited (data not shown). The results demonstrate the ability of the water-soluble *I. obliquus* polysaccharides to activate macrophages into a tumoricidal phenotype, in particular the acidic fractions AcF1, AcF2 and AcF3. Further, the concentrations of NO correlated strongly with the cancer cell growth inhibition, suggesting that NO could be important for the inhibitory effect.

Figure 3

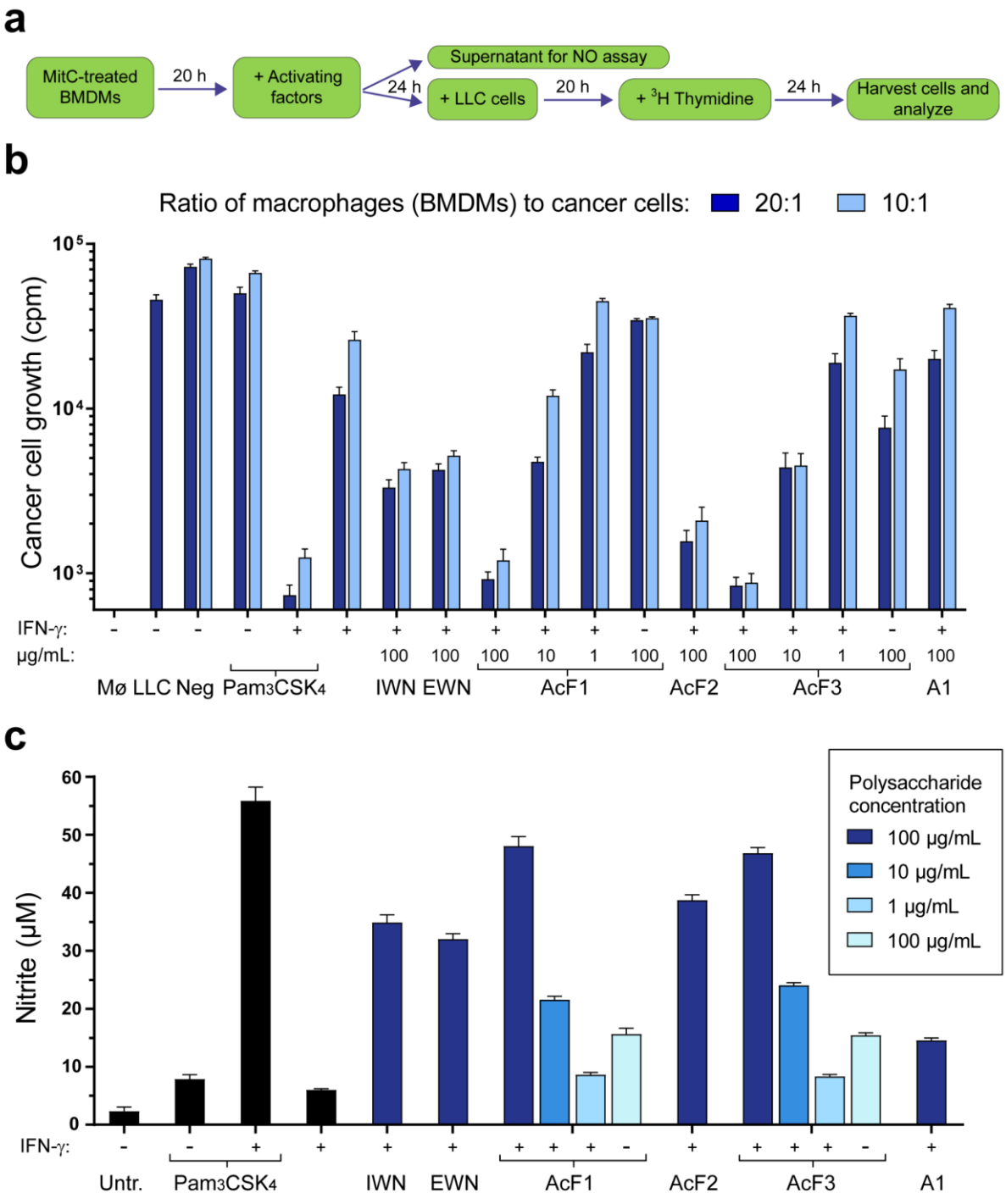

Figure 3. Polysaccharides from *I. obliquus* in combination with IFN-γ inhibit cancer cell growth by activating macrophages. **a**) The experimental setup: mouse macrophages (BMDMs, 6 x 10^4 cells/well or 3 x 10^4 cells/well for 20:1 and 10:1 ratios, respectively) were incubated with mitomycin C for 2 h, and then cultivated for 20 h before treatment with polysaccharides ± IFN-γ for 24 h. Then, 100 μL cell medium was removed and analyzed for NO before Lewis lung carcinoma (LLC) cells (3 x 10^3 cells/well) were added to the wells containing macrophages,

giving two different ratios between macrophages and cancer cells (20:1 and 10:1). After 20 h, radiolabeled thymidine was added and the co-cultures were incubated for another 24 h before inhibition of cancer cell growth was measured. **b)** NO concentrations in the macrophage cell medium were measured using the Griess assay. The polysaccharide concentration was 100 µg/mL except for AcF1 and AcF3, which were tested in concentrations 1, 10 and 100 µg/mL. All samples were tested alone and in combination with IFN-γ (20 ng/mL). Pam_3CSK_4 (100 ng/mL) and IFN-γ (20 ng/mL) were used as controls. **c)** Cancer cell growth inhibition was measured using radiolabeled thymidine, expressed as radioactive counts per minute (cpm). The polysaccharide concentration was 100 µg/mL except for AcF1 and AcF3, which were tested in concentrations 1, 10 and 100 µg/mL. All samples were tested alone and in combination with IFN-γ (20 ng/mL). Pam_3CSK_4 (100 ng/mL) and IFN-γ (20 ng/mL) were used as controls. Macrophages (Mø) and LLC cells were also tested in single culture, and the untreated, negative control consisted of co-cultured, non-activated BMDMs and LLC cells. Three independent experiments were performed, and a representative experiment is shown using average values ± SD from technical triplicates.

AcF1, AcF2, and AcF3 activate macrophages to inhibit cancer cell growth independently of TLR4

Bacterial lipopolysaccharide (LPS) is a common contaminant when working with compounds of natural origin [24]. Therefore, we wanted to rule out that macrophage activation by the *I. obliquus* polysaccharide fractions was due to LPS contamination. First, we performed an experiment using the LPS inhibitor polymyxin B (PMB), which neutralizes LPS by binding to its Lipid A moiety and thereby blocking LPS-mediated activation [25]. NO-production following incubation with PMB-pre-treated LPS (10 ng/mL) was entirely inhibited in the absence of IFN-γ, and upon co-incubation with IFN-γ close to completely abolished (Figure S1). In contrast, PMB pre-treatment did not influence the activity of AcF1, AcF2, AcF3 or A1, but reduced the activity of IWN and EWN slightly. Because PMB was able to inhibit 10 ng/mL LPS, and all the polysaccharides in concentration 100 µg/mL contained less than 1.4 ng/mL LPS according to a previously conducted GC-MS analysis [22], any potential LPS contamination in our samples should be completely blocked by PMB. Therefore, we conclude that it is very unlikely that the observed activity of the polysaccharide fractions AcF1, AcF2, AcF3 or A1 was due to LPS contamination.

To verify that the activity was mediated by the polysaccharides and not LPS contamination, BMDMs were generated from TLR4 knockout (KO) mice ($TLR4^{-/-}$), since TLR4 is the receptor for LPS [26]. The activation of TLR4 KO and wild type (WT) mouse macrophages was then compared after treatment with control ligands, or *I. obliquus* polysaccharides in combination with IFN-γ (Figure 4a). LPS from both *E. coli* (LPS-EK) and *Salmonella minnesota* (LPS-SM)

(negative controls) were incapable of activating TLR4 KO macrophages to produce NO. In contrast, Pam_3CSK_4 (TLR2 agonist) and zymosan crude (ZymC, TLR2/Dectin-1 agonist) (positive controls) as well as AcF1 and AcF3 generated similar NO levels in TLR4 KO and WT BMDMs. The results show that AcF1 and AcF3 were able to activate macrophages in a TLR4-independent manner, which also excluded possible contamination with LPS. IWN, EWN, and AcF2 on the other hand, had statistically significantly lower activity in the knockout cells. Therefore, it cannot be excluded that LPS contamination is contributing to the activity of IWN, EWN, and AcF2. However, activity was observed from these polysaccharide fractions in the TLR4 KO cells as well, suggesting that LPS contamination was not the only reason for the macrophages activation.

The NO concentrations induced by the polysaccharides correlated well with cancer cell growth inhibition (Figure 4a, b): AcF1 and AcF3 were the most active polysaccharide fractions in the growth inhibition assay, with no significant differences in activity between TLR4 KO and WT macrophages (Figure 4b). Interestingly, zymosan purified (ZymP, Dectin-1 agonist) significantly increased the inhibition of cancer cell growth when using TLR4 KO cells compared to WT cells, although the NO production was similar using the two cell types. The results presented in Figure 4b show a macrophage to cancer cell ratio of 10:1, which gave similar results as the 20:1 ratio, whereas at a 1:1 ratio the inhibitory effect was lost (data not shown). The results are in agreement with the results presented in Figure S1 and demonstrate the ability of the polysaccharides AcF1 and AcF3 to activate macrophages into a tumoricidal phenotype independently of TLR4 and thereby of any putative LPS contamination.

Figure 4

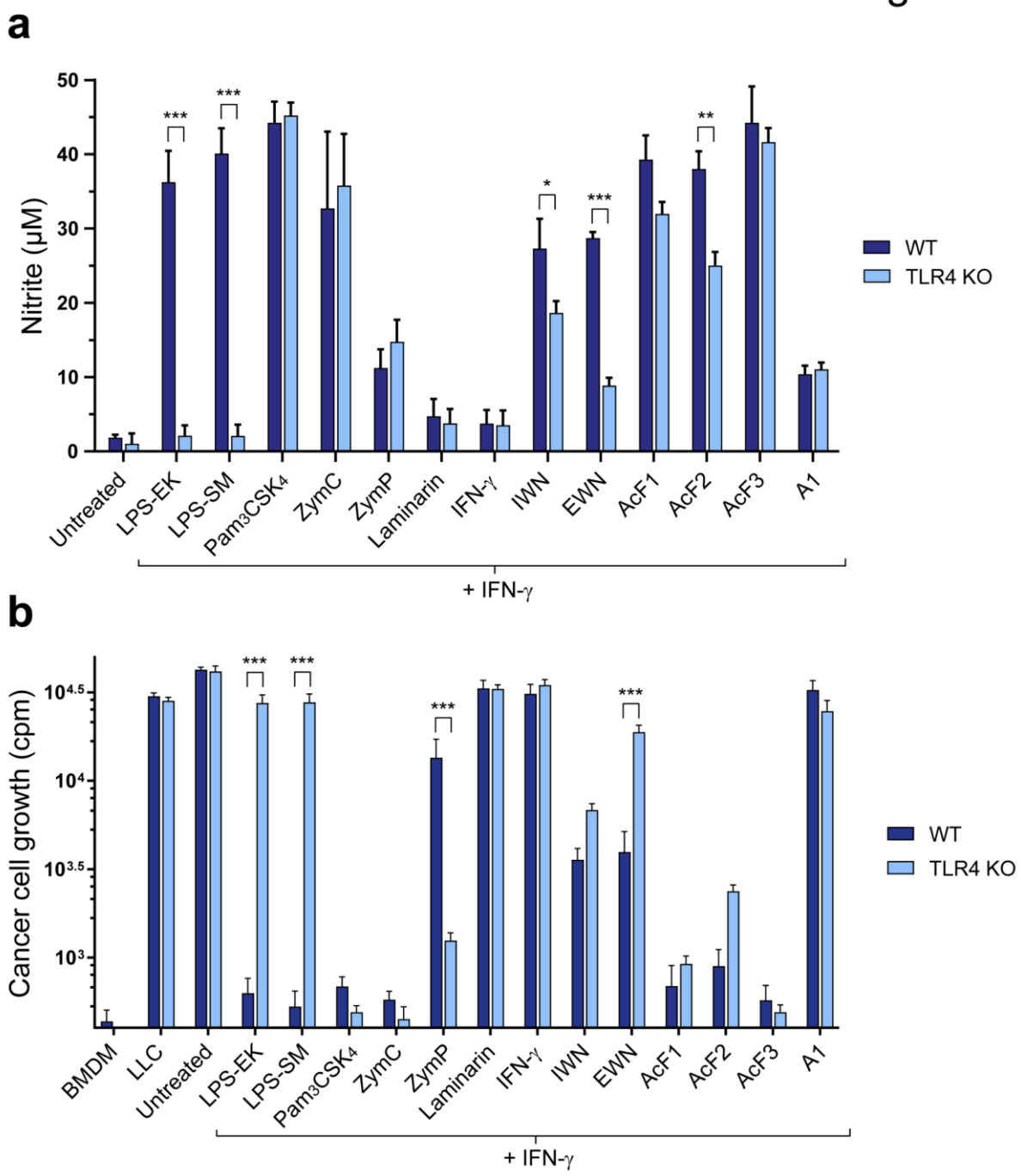

Figure 4. Polysaccharides from *I. obliquus* synergize with IFN-γ to produce NO in wild type (WT) and TLR4 KO macrophages (BMDMs), with subsequent growth inhibition of Lewis lung carcinoma (LLC) cells. BMDMs were incubated with mitomycin C for 2 h, before treatment with polysaccharides and IFN-γ (20 ng/mL) for 24 h. The *I. obliquus* polysaccharide concentration was 100 μg/mL. LPS-EK, LPS-SM, Pam_3CSK_4 (all 100 ng/mL), zymosan crude (ZymC), zymosan purified (ZymP) and laminarin (all 100 μg/mL) together with IFN-γ were used as controls. **a**) NO in the cell supernatants was quantified using the Griess assay, prior to the growth inhibition assay. **b**) Growth

inhibition of LLC cells by activation of macrophages. LLC cells (3 x 10^3/well) were added to stimulated BMDMs (3 x 10^4 cells/well) in ratio 10:1 (BMDM:LLC). After 20 h, radiolabeled thymidine was added and the cells were incubated for 24 h before inhibition of cancer cell growth was measured by radioactive counts per minute (cpm). Three independent experiments were performed, and average values ± SD are shown. Statistical significance indicates the difference between WT and TLR4 KO cells, and was calculated using two-way ANOVA followed by Sidak's multiple comparison test, *** = $p < 0.001$, ** = $p < 0.01$, * = $p < 0.05$.

Several of the polysaccharides induce secretion of the pro-inflammatory cytokines IL-6, TNF-α, and IL-12p70 by mouse and human macrophages

To investigate whether the polysaccharides from *I. obliquus* could activate macrophages to secrete pro-inflammatory cytokines, mouse and human macrophages were stimulated with the polysaccharides with and without IFN-γ for 24 h. In mouse BMDMs, AcF1, AcF2, and AcF3 statistically significantly induced secretion of IL-6 (Figure 5a) and TNF-α (Figure 5b) in the presence of IFN-γ. Notably, AcF3 induced 5-10 fold more IL-6 and TNF-α than AcF1 and AcF2. Moreover, AcF3 alone was able to significantly increase the levels of IL-6 and TNF-α. In human monocyte-derived macrophages, AcF1 and AcF3 induced secretion of IL-6 (Figure 5c), TNF-α (Figure 5d), and IL-12p70 (Figure 5e) at levels comparable to the positive controls LPS-EK and Pam_3CSK_4. Co-incubation with IFN-γ showed minor or no effect on the secretion of IL-6 mediated by the polysaccharides. Slightly different results were observed for TNF-α, although TNF-α secretion induced by AcF1 and AcF3 was independent on IFN-γ. The polysaccharides synergized with IFN-γ in secretion of IL-12p70, yet AcF3 alone induced some IL-12p70 secretion at levels 3-4 fold lower than the combination AcF3+ IFN-γ. Interestingly, all *I. obliquus* polysaccharides seemed to be more active on human cells than on mouse cells, especially when compared to Pam_3CSK_4. The results demonstrate the pro-inflammatory potential of the *I. obliquus* polysaccharides, with AcF3 being the most potent fraction, activating macrophages to secrete high levels of IL-6, TNF-α, and IL-12p70.

Figure 5

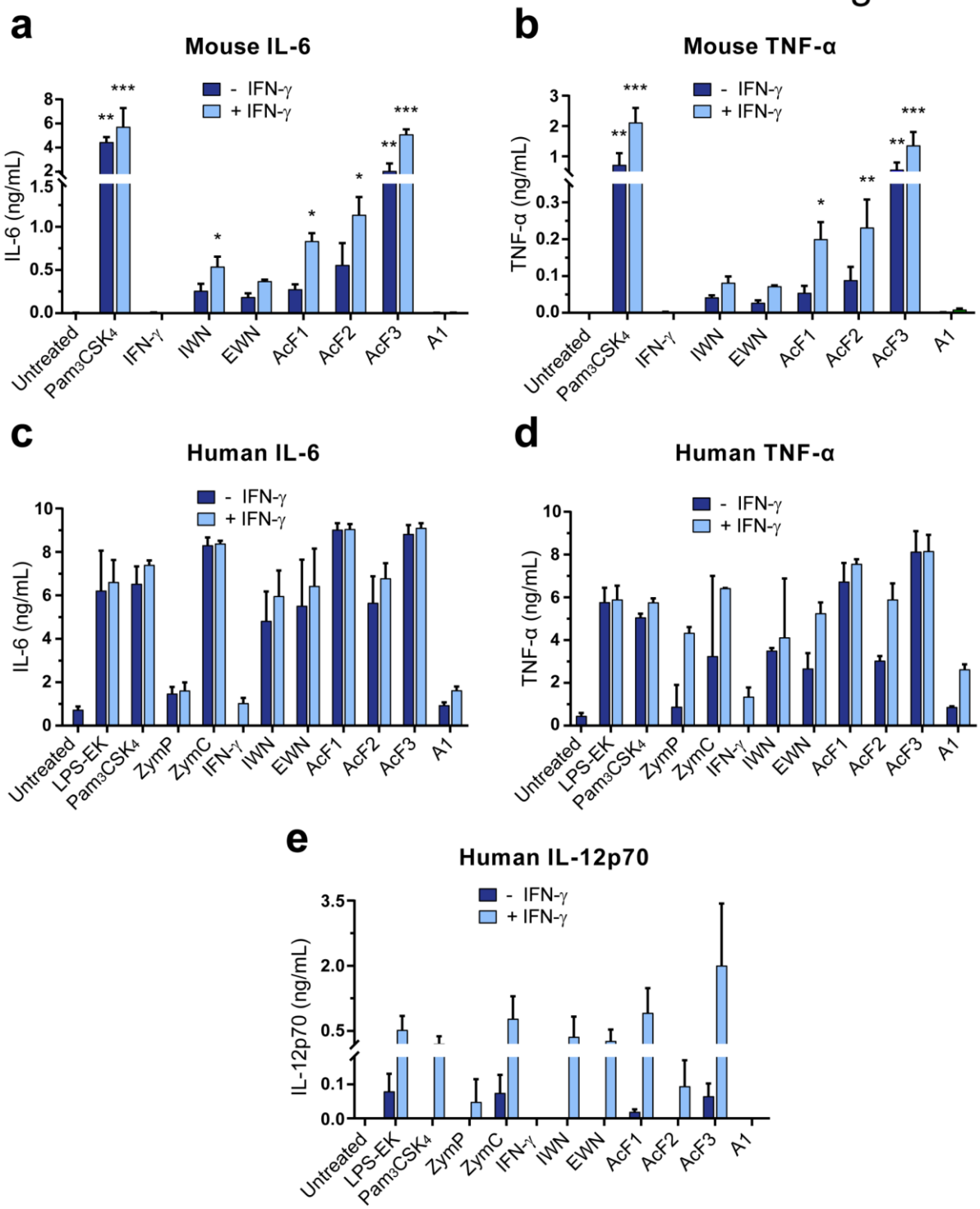

Figure 5. Polysaccharides from *I. obliquus* induce secretion of IL-6 and TNF-α by mouse and human macrophages, and IL12p70 from human macrophages. Macrophages were treated with polysaccharides (100 µg/mL) alone or in combination with IFN-γ (20 ng/mL) for 24 h, before cytokine concentrations in cell supernatants were quantified using Luminex technology. **a**) IL-6 and **b**) TNF-α quantified in supernatants of mouse BMDMs (2.5 x 10^5 cells/well

in 24-well plates). Before incubation with the *I. obliquus* polysaccharides in the presence or absence of IFN-γ, the macrophages were treated with mitomycin C for 2 h. Pam_3CSK_4 (100 ng/mL) with or without IFN-γ was used as a positive control. Three independent experiments were performed, and average values ± SD are shown. Statistical significance was calculated using one-way ANOVA followed by Dunn's multiple comparison test, with single comparisons against the untreated control *** = $p < 0.001$, ** = $p < 0.01$, * = $p < 0.05$. **c**) IL-6, **d**) TNF-α, and **e**) IL-12p70 quantified in supernatants of human monocyte-derived macrophages (1×10^5 cells/well in 48-well plates) treated with polysaccharides for 24 h in the presence or absence of IFN-γ (20 ng/mL). LPS-EK, Pam_3CSK_4 (both 100 ng/mL), zymosan crude (ZymC, 100 µg/mL) and zymosan purified (ZymP, 100 µg/mL) were used as controls. Two independent experiments were performed, and average values ± SD from one representative experiment are shown.

AcF1- and AcF3-activated macrophages prevent tumor development *in vivo* in mice

Due to the promising results when using AcF1 and AcF3 in the *in vitro* growth inhibition assay (Figure 3 and 4) we wanted to examine if a similar effect could be achieved *in vivo*. We activated mouse macrophages with AcF1 + IFN-γ, AcF3 + IFN-γ, IFN-γ only, or Pam_3CSK_4 + IFN-γ (positive control), before co-injecting the activated macrophages and LLC cells subcutaneously into C57BL/6 mice (Figure 6a). Co-activation of the macrophages caused a complete absence of tumor development in the majority of the mice (Figure 6b, c). This was in sharp contrast to the tumor development observed in mice that received untreated or IFN-γ-single-treated macrophages, where all mice except one developed tumors (Figure 6c). 48 days after the co-injection, only one or two mice in the groups receiving co-activated macrophages had developed tumors (Figure 6c). The results clearly demonstrate the capability of *I. obliquus* polysaccharides to induce a tumoricidal phenotype in macrophages, leading to *in vivo* clearance of LLC cells and a prevention of tumor establishment in mice.

Figure 6

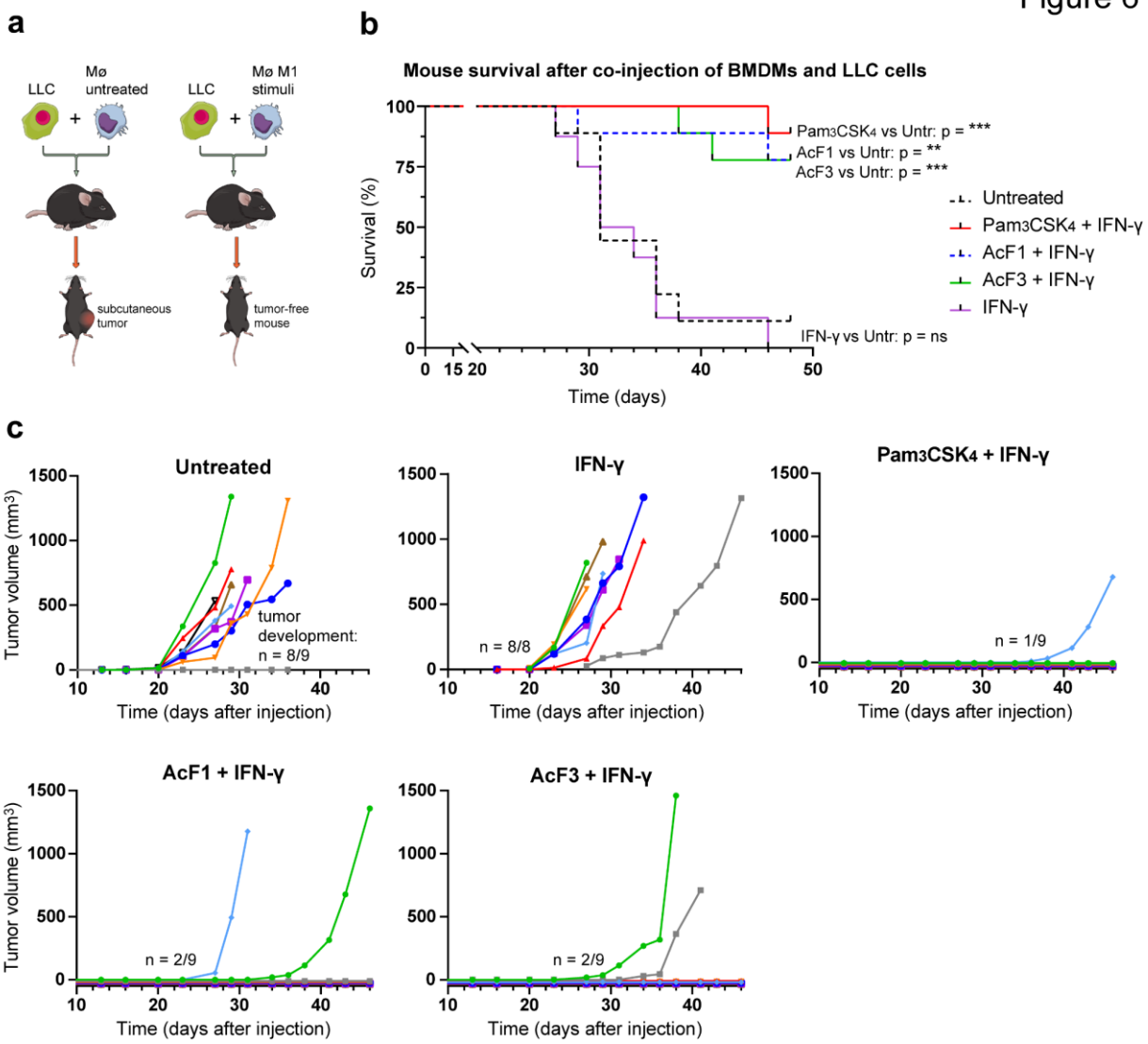

Figure 6. Polysaccharides from *I. obliquus* in combination with IFN-γ inhibit tumor growth *in vivo* by activating macrophages. **a**) Experimental setup: Macrophages (Mø, 7.5 x 10^5 cells/mouse) were treated with polysaccharides (100 µg/mL) and IFN-γ (20 ng/mL) for 24 h to induce an M1 macrophage phenotype. Macrophages treated with Pam_3CSK_4 (100 ng/mL) in combination with IFN-γ (20 ng/mL), IFN-γ (20 ng/mL) alone, and macrophages that were untreated were included as controls. The macrophages were mixed with LLC cells (5 x 10^4 cells/mouse) to a ratio of 15:1 in ice-cold PBS, and injected subcutaneously into 9 C57BL/6 mice per test condition. Tumor growth was monitored every second or third day. **b**) Kaplan-Meier plot showing survival curves for each group of mice. P-values were calculated by comparing each group to the "untreated" control group. *** = $p < 0.001$, ** = $p < 0.01$, * = $p < 0.05$, not significant (ns) = $p > 0.05$. **c**) Growth curves showing the tumor volume (mm^3) throughout the experimental period. Each line in the graphs indicates one single mouse.

The acidic *I. obliquus* polysaccharides activate several pattern-recognition receptors, including TLR2, TLR4, and Dectin-1a

Aiming to identify the macrophage receptors that are stimulated by fungal polysaccharides, reporter HEK-Blue™ cell lines transfected with specific PRRs were utilized. Interaction between a ligand and the transfected receptor causes activation of the transcription factors NF-κB and AP-1, and secretion of the reporter dye Secreted Embryonic Alkaline Phosphatase (SEAP). First, we investigated the interaction of *I. obliquus* polysaccharides with human TLR4. All samples were either pre-treated with the LPS inhibitor PMB or left untreated and as expected, the positive control, LPS, activated HEK TLR4 whereas PMB-pre-treated LPS gave no detectable activation of TLR4 (Figure 4a). Among the *I. obliquus* polysaccharides, AcF1 and AcF3 were the most potent TLR4 agonists, and the activity was retained after treatment with PMB (Figure 7a). Because the activity of AcF1 and AcF3 was similar in WT and TLR4 KO macrophages in the growth inhibition assay (Figure 4), this was an unexpected finding. EWN and AcF2 were also able to activate TLR4, although to a lower degree, and the activity disappeared at 10 µg/mL.

Next, we wanted to investigate if the polysaccharides activated TLR2, since several publications suggest that fungal and plant polysaccharides are able to activate macrophages through this receptor [27-29]. AcF1 and AcF3 strongly activated hTLR2 (Fig. 7b). EWN and A1 were inactive, whereas AcF2 and IWN were only active at the highest concentration tested (100 µg/mL). A crude formulation of zymosan containing various compounds including mannans, and lipoproteins was used as positive control. The crude zymosan formulation showed potent activity against TLR2. However, zymosan lost its TLR2-binding capability when used as the purified "β-glucan only" formulation, which is in agreement with previous findings [30].

Because β-glucans of various kinds are known to bind to the C-type lectin receptor Dectin-1 [13,31], we wanted to examine if the *I. obliquus* polysaccharides were agonists for this receptor as well. All six polysaccharides activated the hDectin-1a receptor, but to varying degrees (Fig. 7c). The activity of the polysaccharides was lower than that mediated by the particulate β-glucan zymosan (both purified and crude), but had comparable activity to the soluble β-glucan laminarin. Interestingly, IWN, EWN, and A1 were the most potent hDectin-1a ligands, but were the least active in the NO-, growth inhibition- and cytokine assays. The acidic polysaccharides AcF1, AcF2, and AcF3 gave detectable hDectin-1a activation only at the highest concentration tested (100 µg/mL). Finally, none of the polysaccharides activated the HEK-Blue™ null cells,

confirming that the results were specific to the specified transfected receptors (Figure 7d). Taken together, the results show that AcF1 and AcF3 are the most active PRR agonists of the isolated *I. obliquus* polysaccharides; they were able to bind to both TLR2 and TLR4 and to some extent Dectin-1a, although tumoricidal macrophage activation *in vitro* did not require activation of TLR4. An overview of the immunomodulating activities of the *I. obliquus* polysaccharides used in this study, as well as their interaction with TLR2, TLR4 and Dectin-1, is shown in Figure 8a. In addition, a figure showing how AcF3 likely interacts with macrophages to induce a tumoricidal phenotype by binding to multiple receptors is shown in Figure 8b, comparing this polysaccharide to the well-established PRR ligands LPS (TLR4), Pam_3CSK_4 (TRL2) and (1→3)/(1→6)-β-glucan (Dectin-1).

Figure 7

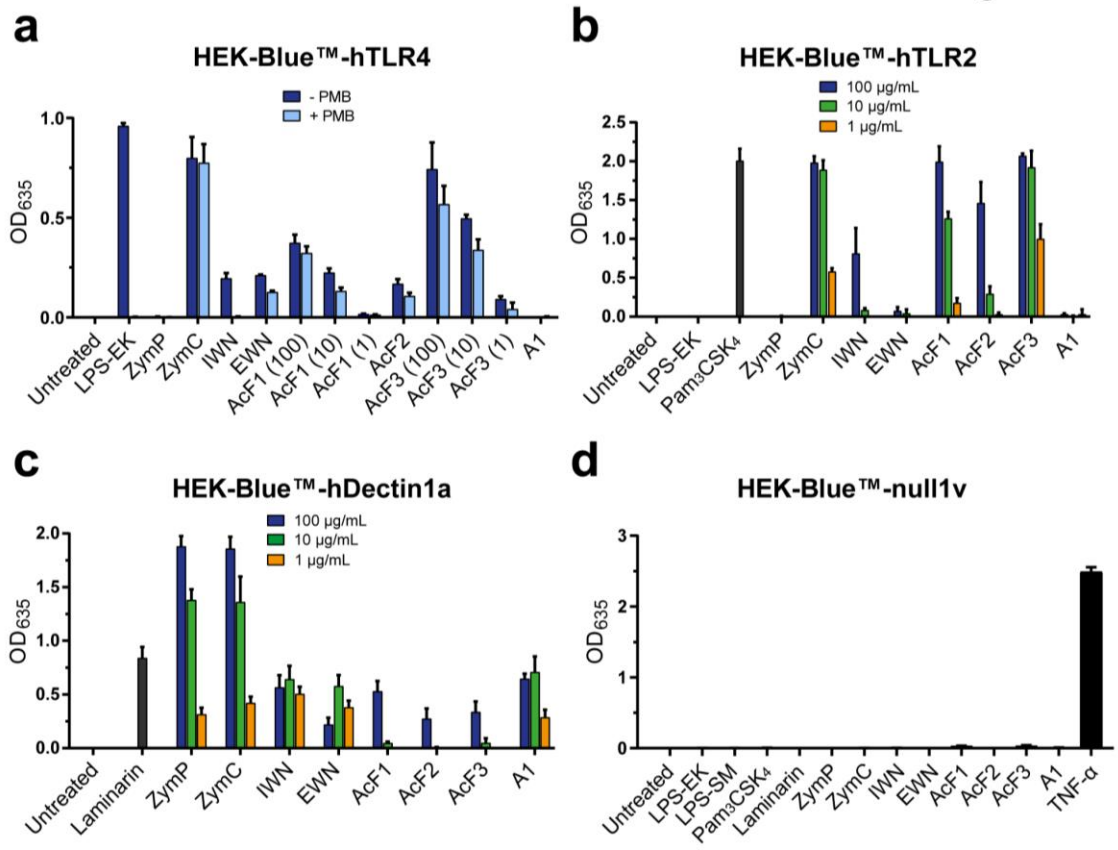

Figure 7. *I. obliquus* polysaccharides are agonists for the human immune receptors TLR4 (**a**), TLR2 (**b**) and Dectin-1a (**c**). HEK-Blue™ cells were incubated with polysaccharides or controls for 16 h. Then, OD_{635} was measured in order to detect Secreted Embryonic Alkaline Phosphatase (SEAP) in the supernatants. Polysaccharides were used at 1, 10 and 100 µg/mL; for the null cells, polysaccharides were used at concentration 100 µg/mL. LPS-EK (10 ng/mL), Pam_3CSK_4 (100 ng/mL), laminarin (100 µg/mL), zymosan crude (ZymC) and zymosan purified (ZymP) (both 1, 10 and 100 µg/mL) and TNF-α (10 ng/mL) were used as controls depending on which reporter cell line was used. PMB

concentration was 10 µg/mL for **a**. Three independent experiments were performed, and average values ± SD are shown.

Figure 8

a

	Macrophage activation				Receptor binding			
	Nitric oxide	LLC growth inhibition	IL-6, TNF-α	IL-12p70*	hDectin-1a	hTLR2	hTLR4	Suspected LPS contamination
IWN	+	+	+	(+)	++	+	-	(+)
EWN	+	+	+	(+)	++	-	(+)	(+)
AcF1	+++	+++^	++	++	+	+++	++	-
AcF2	++	++	++	-	+	++	(+)	(+)
AcF3	+++	+++^	+++	+++	+	+++	+++	-
A1	+	+	-	-	++	-	-	-
LPS-EK	+++	+++	+++*	+	-	-	+++	n.r.
Pam_3CSK_4	+++	+++^	+++	(+)	-	+++	-	-
ZymC	+++	+++	+++*	++	+++	+++	+++	+
ZymP	+	+	-*	n.t.	+++	-	-	-
Laminarin	-	-	-*	n.t.	-	-	--	-

(+) = very low activation; + = low activation; ++ = medium activation; +++ = high activation; - = not active. * = only tested in human macrophages; ^ = tested both *in vitro* and *in vivo*; n.r. = not relevant

b

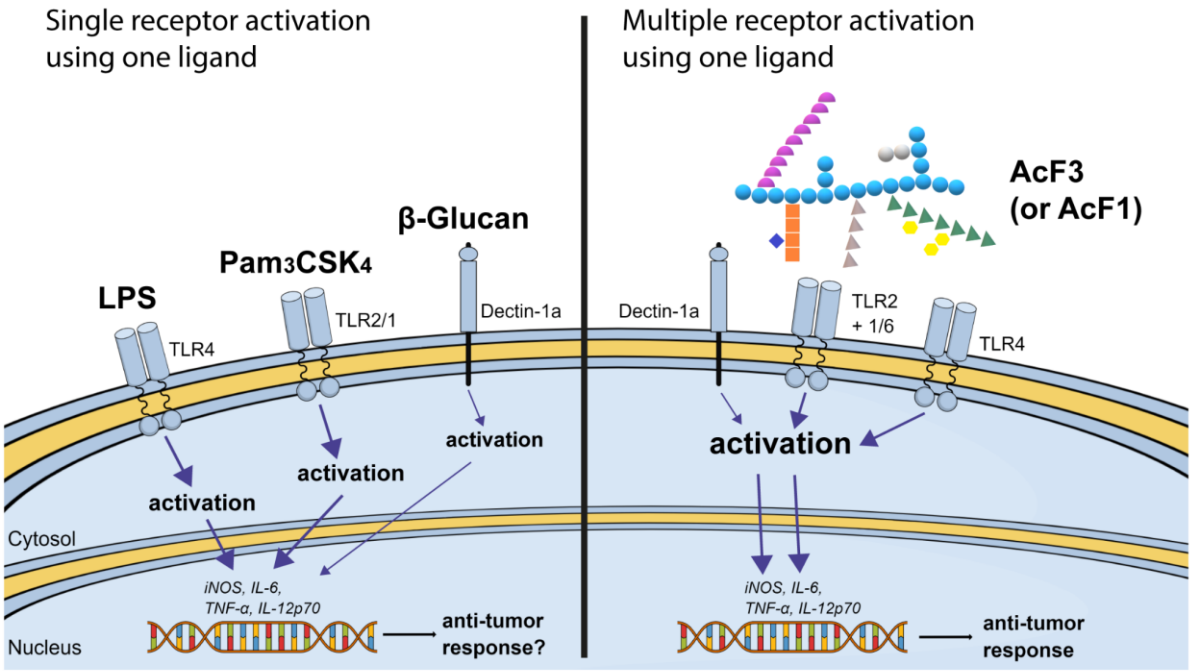

Figure 8. Macrophage activation by *I. obliquus* polysaccharides. **a**) Summary of the experiments carried out in this

study, giving each *I. obliquus* polysaccharide a grade ranging from – to +++ depending on its potency to activate macrophages in the indicated assay. The grading is based on synergy with IFN-γ, and comparison of the measured activity to a positive control such as LPS. Grading of suspected LPS contamination is based on a comparison between activities when the polysaccharides were pre-treated or not with the LPS antagonist polymyxin B. **b**) A schematic illustration on how AcF3 (or AcF1) could bind multiple receptors in the macrophage cell membrane and generate macrophages with an anti-tumor phenotype. This is in contrast to LPS, Pam_3CSK_4 and β-glucans, which predominantly are known to act as agonists for single receptors. It is unclear whether a single AcF3 molecule is able to bind all receptors simultaneously or if separate AcF3 molecules are needed to activate each receptor. For illustrative purposes, the former situation is depicted in this figure.

Discussion

In this paper, we investigated the potential of six polysaccharides isolated from the medicinal fungus *I. obliquus* to activate macrophages into a tumoricidal phenotype. Based on their structural motifs and molecular weight, the polysaccharides were allocated to three main structural types (Figure 1), defined as neutral and water-soluble (IWN and EWN), acidic and water-soluble (AcF1, AcF2 and AcF3) or neutral and particulate (A1). The acidic polysaccharides appeared to be more potent in activating macrophages compared to the neutral ones. In particular, AcF1 and AcF3 demonstrated a strong inhibition of tumor growth both *in vitro* and *in vivo*, through activation of macrophages. The *in vivo* growth inhibition assay demonstrated an almost complete prevention of tumor development in mice given macrophages treated with AcF1 or AcF3 in combination with IFN-γ, as opposed to single treatment with IFN-γ (Figure 6). These data demonstrate the potential of polysaccharides from *I. obliquus* for cancer immunotherapy by inducing an anti-tumorigenic phenotype in macrophages.

AcF1 and AcF3 were also able to induce secretion of the pro-inflammatory cytokines IL-6 and TNF-α by both mouse and human macrophages. In addition, AcF3 induced potent secretion of IL-12p70 by human macrophages when combined with IFN-γ. This result is of significance, since IL-12p70 is thought to be important for anti-tumor responses carried out by the immune system, likely by serving as a link between innate and adaptive immunity [32]. Therefore, further investigations into the functions of AcF3 on different parts of the immune system are warranted, for example investigating the effect AcF3 may exert *in vivo* on T cell maturation and differentiation subsequent of macrophage activation [33].

Compared to the neutral polysaccharides, the activities observed from AcF1 and AcF3 correlated with the ability to activate TLR2 and/or TLR4 in HEK-Blue™ reporter cell lines. The main difference between the acidic and neutral polysaccharides was the presence of 12-17 % (1→4)-α-galacturonic acid (GalA) in the acidic polysaccharides, suggesting that GalA might be crucial for the activity of AcF1 and AcF3. Citrus pectin containing mainly (1→4)-α-GalA has previously been reported to bind both TLR2 and TLR4 [34]. Another study found that citrus pectin containing de-esterified GalA was able to block Pam_3CSK_4-induced activation of the TLR2/1 heterodimer due to negative charges on the GalA polymer associating with positively charged areas of TLR2 [35]. These findings suggest that GalA is important for locating and binding the TLR2 receptor but is not necessarily responsible for its activation. Thus, it might be that other parts of the *I. obliquus* polysaccharides are important for TLR2 activation as well, requiring GalA in addition to other structural motifs present in the acidic polysaccharides, such as β-glucose-containing motifs. Further, it might be that the observed differences in activity are caused by variations in the three-dimensional structure of the polysaccharides, which could explain why AcF2 appeared less active than AcF1 and AcF3 [31]. According to GC-MS data, AcF2 exhibited a higher degree of side-chains than AcF1 and AcF3, which could affect the accessibility of the GalA towards TLR2.

AcF1 and AcF3 were able to induce NO production in mouse macrophages without co-treatment with IFN-γ (Figure 2). This might be explained by their ability to act through TLR4, and this hypothesis was confirmed by using the TLR4 reporter cell line (Figure 7a). Of the various extracellular TLRs, TLR4 is unique by its capability to induce iNOS in mouse macrophages without co-stimulation, possibly achieved by intracellular signaling through TRIF in addition to MyD88, leading to production of type I IFNs which ultimately function as autocrine co-stimulatory signals on the macrophages [36]. To rule out that the activation through TLR4 was due to LPS contamination in AcF1 and AcF3, several experiments were conducted. First, LPS detection by a GC-MS assay concluded that the fractions contained less than 1.4 ng/mL LPS [22]. Further, pre-treatment of 10 ng/mL LPS with PMB led to a complete inhibition of LPS-induced activity, while AcF1 and AcF3 were not affected by PMB treatment (Figure 7a and S1). Thus, it was concluded that the activity of the polysaccharide fractions against TLR4 was not due to LPS contamination.

In addition to TLR2 and TLR4, some of the *I. obliquus* polysaccharides were able to bind to hDectin-1a. Dectin-1 is the most well-characterized β-glucan receptor on macrophages, recognizing fungal β-glucans with high affinity [37]. Because all the *I. obliquus* polysaccharides

had a main structural motif resembling fungal β-glucans, their ability to bind Dectin-1 was not surprising. However, the acidic polysaccharides AcF1, AcF2 and AcF3 showed weak activation of Dectin-1a compared to the less active neutral fractions IWN, EWN and A1. Affinity for Dectin-1 is known to vary depending on the conformation of the β-glucan backbone [38]. Therefore, it is likely that the β-glucan parts of the polymers in IWN, EWN and A1 were more exposed to the outer environment compared to AcF1, AcF2 and AcF3, thus giving higher affinity for Dectin-1a. The Dectin-1a activity was weak for all *I. obliquus* polysaccharides compared to the particulate β-glucan zymosan, but had comparable activity to the soluble β-glucan laminarin. It has been reported that particulate, large-sized β-glucans like zymosan are able to induce immune responses upon activation of Dectin-1, while water-soluble β-glucans like laminarin have antagonistic effects on the same receptor [15]. However, it has recently been suggested that human Dectin-1 can be activated by soluble β-glucans, while mouse Dectin-1 requires particulate β-glucans to become activated [39]. The species-specific difference could also be due to different isoforms such as Dectin-1a or -1b being expressed, although this needs further verification [40]. Because the *I. obliquus* polysaccharides induced secretion of notably higher amounts of pro-inflammatory cytokines by the human macrophages compared to the mouse macrophages, adjusting for the positive control Pam_3CSK_4, this might be an indication of different isoforms of Dectin-1 being expressed between the species, and this should be explored further.

The capacity to bind more than one type of receptor is an interesting feature of AcF1 and AcF3. For example, Dectin-1 has been reported to collaborate with both TLR2 [41] and TLR4 [42] on the macrophage cell membrane upon recognition of fungal structures, and this co-activation may give synergistic effects [43,44]. Synergy between Dectin-1 and TLRs has been suggested to be caused by a combination of several distinct effector molecules in crude "β-glucan" formulations, such as mannoproteins, lipoproteins and β-glucans in crude zymosan [16], in agreement with our results. In contrast to zymosan, it appears that the complexity of the *I. obliquus* polysaccharides AcF1 and AcF3 could activate several receptors using just "one molecule". This would have interesting implications for the use of such molecules as immunomodulating drugs. In addition, the high water-solubility of the polysaccharides might be attractive for *in vivo* situations compared to the particulate β-glucan formulations most often used in the literature. For example, in addition to having local effects in the gastrointestinal tract, water-soluble polysaccharides of fungal origin may be internalized by gut epithelial cells and systemically distributed shortly after ingestion as opposed to larger, particulate polysaccharides that require phagocytic uptake by

macrophages [42]. The findings presented here should therefore be explored further in order to understand the full potential of *I. obliquus* polysaccharides as immunologically active agents.

In conclusion, we here report the immunological activity of several polysaccharides isolated from *I. obliquus*, with the acidic, water-soluble polysaccharides AcF1 and AcF3 being able to induce a potent tumoricidal macrophage phenotype both *in vitro* and *in vivo*. In addition, the polysaccharides were able to induce secretion of IL-6, TNF-α and IL-12p70 by human macrophages, and the activation was likely caused by a synergistic effect of TLR2, TLR4 and Dectin-1a. The tumoricidal activity of the polysaccharides through interaction with multiple receptors might provide interesting new opportunities for cancer immunotherapy.

Materials & methods

Isolation and characterization of polysaccharides from *I. obliquus*

Sclerotia (dense fungal conks) of *I. obliquus* were harvested from a birch tree in Oslo, Norway, and polysaccharides were isolated from the fungal material and characterized as previously described [22]. Briefly, dried material from the interior part of *I. obliquus* (IOI) or the exterior part of *I. obliquus* (IOE) was boiled in water or 1 M NaOH, before the extracts were precipitated using 70 % EtOH and dialyzed (cut-off 3.5 kDa). The extracts were then fractionated using column chromatography. The water-soluble extracts (W) were first applied to an ion-exchange column using a NaCl gradient to create neutral (N) as well as acidic (Ac) fractions. Two neutral, water-soluble extracts were isolated, one from the interior part (IOI-WN) and one from the exterior part (IOE-WN). The acidic fraction IOI-WAc was separated further using a size-exclusion column to yield IOI-WAcF1, IOI-WAcF2 and IOI-WAcF3. The alkali extract was applied to a size-exclusion column to yield IOI-A1. The fractions were characterized using several different methods, including gas chromatography (monosaccharide composition), gas chromatography-mass spectrometry (GC-MS, linkage analysis), 2D NMR spectroscopy (anomeric configuration), size exclusion chromatography – multiple-angle laser light scattering (SEC-MALLS, for molecular weights) and Smith degradation (relationship between parts of the polymer).

Mice

C57BL/6NRj mice were purchased from Janvier Labs (Le Genest-Saint-Isle, France) and bred at the Department of Comparative Medicine, Oslo University Hospital, Rikshospitalet (Oslo, Norway) in specific pathogen free (SPF) conditions. Bone marrow cells from C57BL/6NRj mice deficient in TLR4 ($Tlr4^{-/-}$) were kindly provided by Maykel Arias, University of Zaragoza.

Isolation and differentiation of bone marrow-derived macrophages

Conditioned medium (CM) containing macrophage colony-stimulating factor (M-CSF) was generated by culturing L929 cells in RPMI 1640 medium with L-Glutamine (Thermo Fisher Scientific) containing 10 % fetal bovine serum (FBS, Biochrom GmbH) and 1 % penicillin-streptomycin (P/S, Sigma-Aldrich). After 10 days, CM was collected, centrifuged, filtered and stored at −20°C, and was used for the differentiation and maintenance of bone marrow-derived macrophages (BMDMs). For isolation of the macrophages, femurs and tibiae of the hind legs from 8- to 12-week-old C57BL/6NRj mice and C57BL/10ScN $TLR4^{(-/-)}$ knockout (KO) mice were harvested and flushed with RPMI 1640 medium containing 10 % FBS under sterile conditions. The bone marrow was passed through a cell strainer with 70 μm pores (Sigma-Aldrich) and cultured in non-tissue culture treated dishes (10 cm, VWR) in RPMI medium with L-Glutamine containing 10 % FBS, 1 % P/S and 30 % L929-derived CM. The cells were cultured for 5 days, after which non-adherent cells were washed off using phosphate buffered saline (PBS, with $MgCl_2$ and $CaCl_2$, Sigma-Aldrich) and the adherent macrophages were cultured for 2 more days. Macrophages were then harvested by incubation (20 min at 4°C) with cold PBS (without $CaCl_2$ and $MgCl_2$, Sigma-Aldrich). Macrophages were then flushed off the plate, collected, counted and kept frozen in aliquots at −150°C in FBS with 10 % dimethyl sulfoxide (DMSO, VWR) for future experiments. The purity of the cells was 99 % as analyzed by flow cytometry using the macrophage markers CD11b (M1/70, BioLegend) and F4/80 (BM8, BioLegend).

Isolation and differentiation of human monocyte-derived macrophages

Buffy coats were obtained from the Blood bank at Oslo University Hospital and approved for use by the Norwegian Regional Committee for Medical and Health Research Ethics, REK no. 2019/113. The buffy coats were mixed with an equal volume of PBS containing 2 % FBS, before gently added on to Lymphoprep™ in 50 mL tubes in volumes recommended by the provider

(Progen, #1114545; Heidelberg, DE). The tubes were centrifuged at 800 g for 20 min at room temperature (RT), before the middle, buffy layer containing peripheral blood mononuclear cells was collected and washed twice in PBS by centrifugation (400 g, 7 min, RT). Next, the cells were filtered through a 30 µm filter to remove cell clumps and debris, before the monocytes were positively selected by magnetic-activated cell sorting (MACS) technology using CD14 MicroBeads (Miltenyi) according to the manufacturer's instructions. Briefly, magnetic beads conjugated to an anti-human CD14 antibody (CD14 MicroBeads) were added to the peripheral blood mononuclear cells and incubated for 15 min at 4 °C. Unbound, excess beads were washed away, and the cell suspension was applied to a column placed in a MACS magnetic separator. Unlabeled cells were washed out before the column was removed from the magnet field and the magnetically labeled cells were flushed out with a plunger. Staining with APC/Cy7-conjugated anti-human CD14 antibody (clone HCD14, BioLegend) followed by flow cytometry, showed that > 95% of the positively selected cells were monocytes. APC/Cy7-conjugated mouse IgG1k (clone MOPC-21, BioLegend) was used as an isotype-matched control antibody.

The positively selected $CD14^+$ monocytes were differentiated into macrophages by cultivation for 6 days in medium with macrophage colony-stimulating factor (M-CSF, Peprotech). More specifically, 3 x 10^6 cells were seeded out in 10 mL RPMI 1640 containing 10 % FBS, 1 % P/S, and 50 ng/mL M-CSF per 10 cm non-tissue culture treated dish (VWR). At day 3, half of the medium was replenished with fresh medium containing 50 ng/mL M-CSF. On day 6, macrophages were harvested by first collecting culture medium into polypropylene falcon tubes (50 mL, SARSTEDT), pre-coated with FBS and placed on ice. Then 10 mL of detachment buffer made in-house, containing PBS-/- + 2.5 mM EDTA + 1% FBS, was added to each culture plate and incubated at 37°C for 30 min. Next, dislodged cells were collected by pipetting up and down several times. A cell scraper was used to detach the remaining macrophages.

Pattern recognition receptor agonists and cytokines

The following PRR agonists were used as controls in various experiments: $Pam_3CysSerLys_4$ (Pam_3CSK_4, TLR1/TLR2 agonist, InvivoGen); Lipopolysaccharide (LPS) from *Escherichia coli* and *Salmonella minnesota* (both ultrapure TLR4 agonists, InvivoGen); Lipoteichoic acid (LTA) from *Staphylococcus aureus* (TLR2/TLR6 agonist, Sigma-Aldrich); CL264 (TLR7 agonist,

InvivoGen), zymosan from *Saccharomyces cerevisiae* (zymosan crude/ZymC, TLR2 and Dectin-1 agonist, Sigma-Aldrich), zymosan depleted from *S. cerevisiae* (zymosan purified/ZymP, InvivoGen), laminarin from *Laminaria digitata* (Dectin-1 ligand, Sigma-Aldrich). The PRR agonists were used alone or in combination with 20 ng/mL mouse recombinant IFN-γ (Peprotech).

Quantification of nitric oxide

NO production by activated macrophages was measured using the Griess reagent system as previously described with some modifications [22]. Cells were seeded out in a flat bottom 96-well plate (Costar) at cell density 6×10^4 cells to a final volume of 200 µL/well. Cell medium was RPMI 1640 with L-Glutamine containing 10 % FBS and 10 % CM. After 24 h treatment with *I. obliquus* polysaccharides or other activation factors, cell media (100 µL) were collected and centrifuged (400 *g*, 2 min), and 50 µL supernatant was then mixed with equal parts Griess reagents A (dH_2O with 1 % sulphanilamide [Sigma-Aldrich] and 5 % phosphoric acid [Sigma-Aldrich]). The mixture was incubated in the dark for 10 min at room temperature (RT), before 50 µL of Griess reagent B (0.1 % *N*-(1-napthyl) ethylenediamine [Sigma-Aldrich] in dH_2O) was added in order to convert NO into nitrite (NO_2^-), which was quantified colorimetrically at A_{540} using $NaNO_2$ (1.56 – 100 µM) as a standard curve. Samples were set up in duplicates or triplicates depending on the experimental setup. For experiments using the LPS inhibitor polymyxin B (PMB, Polymyxin B sulfate salt, Sigma-Aldrich), the samples were mixed with PMB and incubated for 30 min at RT before being added to the cultivated cells. The experiments were carried out at least three times.

***In vitro* Growth Inhibition Assay**

Wild-type (WT) and TLR4 KO mouse BMDMs were thawed and cultured for 3 days in non-tissue culture treated dishes (VWR) in RPMI 1640 medium with L-Glutamine containing 10 % FBS and 10 % CM (= complete medium). The macrophages were harvested by scraping, incubated for 2 h at 37°C with mitomycin C (10 mg/mL, Sigma-Aldrich) to inhibit proliferation, and then washed twice with PBS. Next, the macrophages were resuspended in the same type of medium and seeded out in triplicates in flat bottom 96-well plates (Costar) at three densities: 6 ×

10^4, 3×10^4, and 3×10^3 cells/well in a final volume of 200 µL/well. After 20 h, half of the medium was replaced with complete medium containing *I. obliquus* polysaccharides with or without IFN-γ, and incubated for 24 h. Next, half of the cell supernatants (100 µL) were removed and used for quantification of NO2−. Lewis lung carcinoma (LLC) cells (CLS Cell Line Service, 3×10^3 cells/well) were then added to the macrophages, resulting in varying ratios of effector to target cells: 20:1, 10:1 and 1:1. After 20 h of co-culture, ^{3}H-thymidine (10 µL, 0.2 µCi/well, Hartmann Analytic) was added and the cells were harvested 24 h later after a freeze- and thaw cycle. The amount of radiolabeled DNA was measured on a 1450 MicroBeta Trilux Microplate Scintillation counter (Perkin Elmer). The experiments were carried out at least three times.

In vivo Growth Inhibition Assay

C57/BL-6 mice from Janvier Labs (Le Genest-Saint-Isle, France) were in-house bred at the Department of Comparative Medicine, Oslo University Hospital, Rikshospitalet (Oslo, Norway). The study was approved by the Norwegian Food Safety Authority (approval number 20/102031) and all the performed experiment conform to the national regulations and the EU directive 2010/63/EU. For the co-injection experiments (Winn assay), 7.5×10^5 pre-activated macrophages with the indicated stimuli for 24 h were mixed and co-injected with 5×10^4 LLC cells (15:1) subcutaneously in mice. Tumor growth was monitored using a caliper every other or every third day until humane end points were reached (15mm length) using the formula: Tumor volume (mm^3) = [width^2 x length] x 0.4 [45]. For the re-challenge experiments, 1.25×10^4 LLC cells were injected subcutaneously in opposite flanks.

Determination of iNOS mRNA Levels by Real-Time Quantitative PCR

Mouse macrophages were seeded in 12-well plates (Sigma-Aldrich) at a density of 6×10^5 cells/well in 1 mL RPMI medium with L-Glutamine supplemented with 10 % FBS and 10 % CM. The cells were incubated for 2 h, before 0.5 mL of the medium was removed and replaced with 0.5 mL medium containing *I. obliquus* polysaccharides with or without IFN-γ (20 ng/mL). After 24 h, cell culture media were removed and total RNA was extracted from the cells by using 300 µL/well of TRI Reagent (Merck) and Direct-zol RNA minipreps (Zymo Research) according to manufacturer's instructions. Next, mRNA concentrations were measured using Nanodrop

One/One (Thermo Fisher), and 250 ng RNA of each sample was reverse transcribed to cDNA using the Primescript RT kit (Takara Bio) according to the manufacturer's instructions. Real-time quantitative PCR (qPCR) was performed with 50 ng of the obtained cDNA, using a Kapa SYBR fast qPCR kit (Kapa Biosystems) and 0.2 µM of mRNA specific primers for the mouse gene *Nos2* which encodes iNOS (forward primer: TTCACCCAGTTGTGCATC GACCTA, reverse primer: TCCATGGTCACCTCCAACACA AGA) and with primers for 18s rRNA (forward primer: CGCTTCCTTACCTGGTTGAT, reverse primer: GAGCGACCAAAGGAACCATA) as the endogenous control, at temperature cycling conditions: 95°C for 3min, then 95°C for 3 s and 60°C for 30 s for 40 cycles. All samples were run in duplicates and the final values were averaged. Following melting curve analysis, the relative differences in iNOS mRNA levels were expressed using the - ΔCq values (Cq 18s rRNA – Cq iNOS), where a more negative value means lower relative expression of iNOS mRNA compared to the housekeeping gene 18S rRNA. One unit increase in the negative ΔCq value corresponded to a doubling of iNOS mRNA. The experiment was carried out three times.

Quantification of pro-inflammatory cytokines using Luminex technology

Mouse macrophages, 2.5 x 10^5 cells in 0.5 mL medium per well in 24-well plates (Costar) were cultured in RPMI 1640 supplemented with 10 % FBS (Biochrom) and 10 % CM. Human monocyte-derived macrophages, 1 x 10^5 cells in 0.3 mL medium per well in 48-well plates (Costar) were cultured in RPMI 1640 supplemented with 10 % FBS (Biowest) and stimulated for 24 h with polysaccharides with or without IFN-γ. Cell culture media were collected and centrifuged (1000g for 15 min at 4°C). Next, the supernatants were moved to new Eppendorf tubes and centrifuged again (1000g for 15 min at 4°C) to remove cells and debris before storage at −80°C until analysis. The concentrations of mouse and human IL-6 and TNF-α were determined by a multiplex Bio-Plex assay (Bio-Rad) according to the manufacturer's instructions. Samples were analyzed in duplicates, using a Bio-Plex MAGPIX Multiplex Reader and Bio-Plex Manager 6.1 software (Bio-Rad Laboratories). The experiment was carried out three times.

Reporter cell lines

HEK-Blue™ reporter cell lines (Invivogen) transfected with human TLR2, human Dectin1a, human TLR4/CD14/MD2 or non-transfected (null-1) were cultured and maintained using

DMEM GlutaMAX™ containing 10 % FBS (Sigma-Aldrich), 1 % P/S, Normocin (100 µg/mL) and HEK-Blue™ selection antibiotics. Experiments were carried out according to the manufacturer's instructions. Briefly, *I. obliquus* polysaccharides (20 µL) at various concentrations were added to wells in 96-well plates (Costar). Then, cells were gently washed with warm PBS before suspended in HEK-Blue™ SEAP detection medium. Finally, the cells were seeded out in a density of 5 x 10^4 cells/well to the wells containing samples and detection medium. After 16 h incubation (37 °C, 5 % CO_2), Secreted Embryonic Alkaline Phosphatase (SEAP) was detected colorimetrically at A_{635}. The experiments were carried out at least three times.

Statistical analysis

Statistical analysis was conducted by using the GraphPad Prism 8 software (GraphPad). Values from control samples were used as a reference to each individual value, unless otherwise stated. The data were analyzed using one-way ANOVA test, followed by Dunn's multiple comparison test, or using two-way ANOVA followed by Sidak's multiple comparison test. The values were compared either across the data set or individually against the controls depending on the experiment (stated specifically below each experiment figure).

Acknowledgements

This study was financially supported by funding grants from the Norwegian Cancer Society (grant no. 198040), The Research Council of Norway (grant no. 262814) and the South-Eastern Norway Regional Health Authority (grant no. 2018046).

References

1 Corthay, A. Does the immune system naturally protect against cancer? *Front Immunol* **5**, 197, doi:10.3389/fimmu.2014.00197 (2014).

2 Waldman, A. D., Fritz, J. M. & Lenardo, M. J. A guide to cancer immunotherapy: from T cell basic science to clinical practice. *Nat Rev Immunol* **20**, 651-668, doi:10.1038/s41577-020-0306-5 (2020).

3 Gajewski, T. F., Schreiber, H. & Fu, Y. X. Innate and adaptive immune cells in the tumor microenvironment. *Nat Immunol* **14**, 1014-1022, doi:10.1038/ni.2703 (2013).

4 Pathria, P., Louis, T. L. & Varner, J. A. Targeting tumor-associated macrophages in cancer. *Trends Immunol* **40**, 310-327, doi:10.1016/j.it.2019.02.003 (2019).

5 Takeya, M. & Komohara, Y. Role of tumor-associated macrophages in human malignancies: friend or foe? *Pathol Int* **66**, 491-505, doi:10.1111/pin.12440 (2016).

6 Riabov, V. *et al.* Role of tumor associated macrophages in tumor angiogenesis and lymphangiogenesis. *Front Physiol* **5**, 75, doi:10.3389/fphys.2014.00075 (2014).

7 Mills, C. D., Lenz, L. L. & Harris, R. A. A breakthrough: Macrophage-directed cancer immunotherapy. *Cancer Res* **76**, 513-516, doi:10.1158/0008-5472.CAN-15-1737 (2016).

8 Muller, E. *et al.* Toll-like receptor ligands and interferon-gamma synergize for induction of antitumor M1 macrophages. *Front Immunol* **8**, 1383, doi:10.3389/fimmu.2017.01383 (2017).

9 House, I. G. *et al.* Macrophage-Derived CXCL9 and CXCL10 Are Required for Antitumor Immune Responses Following Immune Checkpoint Blockade. *Clin Cancer Res* **26**, 487-504, doi:10.1158/1078-0432.Ccr-19-1868 (2020).

10 Haabeth, O. A. *et al.* Inflammation driven by tumour-specific Th1 cells protects against B-cell cancer. *Nat Commun* **2**, 240, doi:10.1038/ncomms1239 (2011).

11 Corthay, A. *et al.* Primary antitumor immune response mediated by CD4+ T cells. *Immunity* **22**, 371-383, doi:10.1016/j.immuni.2005.02.003 (2005).

12 Erwig, L. P. & Gow, N. A. Interactions of fungal pathogens with phagocytes. *Nat Rev Microbiol* **14**, 163-176, doi:10.1038/nrmicro.2015.21 (2016).

13 Liu, M. *et al.* Dectin-1 activation by a natural product beta-glucan converts immunosuppressive macrophages into an M1-like phenotype. *J Immunol* **195**, 5055-5065, doi:10.4049/jimmunol.1501158 (2015).

14 Batbayar, S., Lee, D. H. & Kim, H. W. Immunomodulation of fungal beta-glucan in host defense signaling by Dectin-1. *Biomol Ther (Seoul)* **20**, 433-445, doi:10.4062/biomolther.2012.20.5.433 (2012).

15 Goodridge, H. S. *et al.* Activation of the innate immune receptor Dectin-1 upon formation of a 'phagocytic synapse'. *Nature* **472**, 471-475, doi:10.1038/nature10071 (2011).

16 Ikeda, Y. *et al.* Dissociation of toll-like receptor 2-mediated innate immune response to zymosan by organic solvent-treatment without loss of Dectin-1 reactivity. *Biol. Pharm. Bull.* **31**, 13-18 (2008).

17 Bourgeois, C. & Kuchler, K. Fungal pathogens-a sweet and sour treat for toll-like receptors. *Front Cell Infect Microbiol* **2**, 142, doi:10.3389/fcimb.2012.00142 (2012).

18 Feng, Y. *et al.* A toll-like receptor agonist mimicking microbial signal to generate tumor-suppressive macrophages. *Nat Commun* **10**, 2272, doi:10.1038/s41467-019-10354-2 (2019).

19 Chen, Y., Huang, Y., Cui, Z. & Liu, J. Purification, characterization and biological activity of a novel polysaccharide from *Inonotus obliquus*. *Int J Biol Macromol* **79**, 587-594, doi:10.1016/j.ijbiomac.2015.05.016 (2015).

20 Kim, Y. O. *et al.* Immuno-stimulating effect of the endo-polysaccharide produced by submerged culture of *Inonotus obliquus*. *Life Sci* **77**, 2438-2456, doi:10.1016/j.lfs.2005.02.023 (2005).

21 Won, D. P. *et al.* Immunostimulating activity by polysaccharides isolated from fruiting body of *Inonotus obliquus*. *Mol Cells* **31**, 165-173, doi:10.1007/s10059-011-0022-x (2011).
22 Wold, C. W. *et al.* Structural characterization of bioactive heteropolysaccharides from the medicinal fungus *Inonotus obliquus* (Chaga). *Carbohydr Polym* **185**, 27-40, doi:10.1016/j.carbpol.2017.12.041 (2018).
23 Bogdan, C. Nitric oxide synthase in innate and adaptive immunity: an update. *Trends Immunol* **36**, 161-178, doi:10.1016/j.it.2015.01.003 (2015).
24 Lieder, R., Petersen, P. H. & Sigurjonsson, O. E. Endotoxins-the invisible companion in biomaterials research. *Tissue Eng Part B Rev* **19**, 391-402, doi:10.1089/ten.TEB.2012.0636 (2013).
25 Duff, G. W. & Atkins, E. The inhibitory effect of polymyxin B on endotoxin-induced endogenous pyroggen production. *J Immunol Methods* **52**, 333-340 (1982).
26 Poltorak, A. *et al.* Defective LPS signaling in C3H/HeJ and C57BL/10ScCr mice: mutations in Tlr4 gene. *Science* **282**, 2085-2088 (1998).
27 Lee, S. G. *et al.* Immunostimulatory polysaccharide isolated from the leaves of *Diospyros kaki* Thumb modulate macrophage via TLR2. *Int J Biol Macromol* **79**, 971-982, doi:10.1016/j.ijbiomac.2015.06.023 (2015).
28 Yang, G. *et al.* A novel linear 3-O-methylated galactan isolated from *Cantharellus cibarius* activates macrophages. *Carbohydr Polym* **214**, 34-43, doi:10.1016/j.carbpol.2019.03.002 (2019).
29 Zhang, J. *et al.* Macrophage activation by edible mushrooms is due to the collaborative interaction of toll-like receptor agonists and dectin-1b activating beta glucans derived from colonizing microorganisms. *Food Funct* **10**, 8208-8217, doi:10.1039/c9fo01707k (2019).
30 Walachowski, S., Tabouret, G. & Foucras, G. Triggering Dectin-1-pathway alone is not sufficient to induce cytokine production by murine macrophages. *PLoS One* **11**, e0148464, doi:10.1371/journal.pone.0148464 (2016).
31 Camilli, G., Tabouret, G. & Quintin, J. The complexity of fungal beta-glucan in health and disease: effects on the mononuclear phagocyte system. *Front Immunol* **9**, 673, doi:10.3389/fimmu.2018.00673 (2018).
32 Tugues, S. *et al.* New insights into IL-12-mediated tumor suppression. *Cell Death Differ* **22**, 237-246, doi:10.1038/cdd.2014.134 (2014).
33 Schoenborn, J. R. & Wilson, C. B. Regulation of Interferon-γ During Innate and Adaptive Immune Responses. *Adv Immunology* **96**, 41-101, doi:10.1016/s0065-2776(07)96002-2 (2007).
34 Vogt, L. M. *et al.* The impact of lemon pectin characteristics on TLR activation and T84 intestinal epithelial cell barrier function. *J Funct Foods* **22**, 398-407, doi:10.1016/j.jff.2016.02.002 (2016).
35 Sahasrabudhe, N. M. *et al.* Dietary fiber pectin directly blocks toll-like receptor 2–1 and prevents doxorubicin-induced ileitis. *Front Immunol* **9**, doi:10.3389/fimmu.2018.00383 (2018).
36 Muller, E. *et al.* Both type I and type II interferons can activate antitumor M1 macrophages when combined with TLR stimulation. *Front Immunol* **9**, 2520, doi:10.3389/fimmu.2018.02520 (2018).
37 Brown, G. D. *et al.* Dectin-1 is a major beta-glucan receptor on macrophages. *J Exp Med* **196**, 407-412, doi:10.1084/jem.20020470 (2002).
38 Goodridge, H. S., Andrea J. Wolf, A. J. & Underhill, D. M. beta-Glucan recognition by the innate immune system. *Immunol Rev* **230**, 38-50 (2009).
39 Takano, T. *et al.* Dectin-1 intracellular domain determines species-specific ligand spectrum by modulating receptor sensitivity. *J Biol Chem* **292**, 16933-16941, doi:10.1074/jbc.M117.800847 (2017).
40 Heinsbroek, S. E. M. *et al.* Expression of Functionally Different Dectin-1 Isoforms by Murine Macrophages. *J Immunol* **176**, 5513-5518, doi:10.4049/jimmunol.176.9.5513 (2006).

41 Yadav, M. & Schorey, J. S. The beta-glucan receptor dectin-1 functions together with TLR2 to mediate macrophage activation by mycobacteria. *Blood* **108**, 3168-3175, doi:10.1182/blood-2006-05-024406 (2006).
42 Sahasrabudhe, N. M., Dokter-Fokkens, J. & de Vos, P. Particulate beta-glucans synergistically activate TLR4 and Dectin-1 in human dendritic cells. *Mol Nutr Food Res* **60**, 2514-2522, doi:10.1002/mnfr.201600356 (2016).
43 Ferwerda, G., Meyer-Wentrup, F., Kullberg, B. J., Netea, M. G. & Adema, G. J. Dectin-1 synergizes with TLR2 and TLR4 for cytokine production in human primary monocytes and macrophages. *Cell Microbiol* **10**, 2058-2066, doi:10.1111/j.1462-5822.2008.01188.x (2008).
44 Li, W., Yan, J. & Yu, Y. Geometrical reorganization of Dectin-1 and TLR2 on single phagosomes alters their synergistic immune signaling. *Proc Natl Acad Sci U S A* **116**, 25106-25114, doi:10.1073/pnas.1909870116 (2019).
45 Tomayoko, M. M. & Reynolds, C. P. Determination of subcutaneous tumor size in athymic (nude) mice. *Cancer Chemother Pharmacol* **24**, 148-154 (1989).